Timmins, Anna Louise (1990) ***A phosphate and fluorine bearing aluminous assemblage developed in the lower palaeozoic deformed volcanics of the Balcooma - dry river region.*** **Honours Thesis, James Cook University of North Queensland.**

https://doi.org/10.25903/b460%2Dqr76

A PHOSPHATE AND FLUORINE BEARING ALUMINOUS ASSEMBLAGE DEVELOPED IN THE LOWER PALAEOZOIC DEFORMED VOLCANICS OF THE BALCOOMA - DRY RIVER REGION

Thesis submitted by
Anna Louise Timmins BSc (UQ)

In partial fulfilment of the requirements for the degree of Bachelor of Science with Honours in the Department of Geology of the James Cook University of North Queensland.

January 1990

Ursula on Quartzite Ridge

STATEMENT OF ACCESS:

I the undersigned, the author of this thesis, understand that the James Cook University of North Queensland will make it available for use within the University Library and, by microfilm or other photographic means, allow access to users in other approved libraries. All users consulting this thesis will have to sign the following statement:

" In consulting with this thesis I agree not to copy or closely paraphrase it in whole or in part without the written consent of the author; and to make proper written aknowledgement for any assistance which I have obtained from it. "

Beyond this I do not wish to place any restriction of access to this thesis.

A. L. Timmins

16/1/1990

STATEMENT OF SOURCES:

I declare that this thesis is my own work and has not been submitted in any form for another degree or diploma at any other university or institute of tertiary education. Information derived from the published or unpublished works of others has been aknowledged in the text and a list of references is given.

A. L. Timmins

16/1/1990

AKNOWLEDGEMENTS

I would like to thank everybody at JCU Geology Department for their friendly and helpful attitude that has made my stay here worthwhile.

In particular I would like to thank Mike Rubenach for his invaluable advice and continued enthusiasm throughout the year. I also thank Roger Taylor for finding me such an interesting project and being supportive in general.

Ken Harvey of CEC first thought of Quartzite Ridge for an Honours project and followed it through in extending logistical support. John Jackson, Ken Scott and Glenn Horne were excellent company at Balcooma as well as being extremely helpful and tolerant.

I have sought and received advice and assistance from many people during the project, especially nocturnal PhD. students. Fop Van der Hor's assistance included many constructive discussions on the geological nature of Quartzite Ridge, and he thoughtfully reviewed much of this text, the input of which I was extremely grateful for. Thanks to Doug Haywick for expert assistance in all aspects of thesis production and wine appreciation.

Most importantly I would like to thank the other Honours students for freely offered friendship, support, commiserations, alcoholic beverages, and toast. David A-Izzedan and Sev Simeone are completely responsible for my partial computer literacy. Thanks also to Kirsty and Dave for their companionship during the drastic dismemberment of circadian rythyms of the last desperate dash.

ABSTRACT

Quartzite Ridge is an extensive, linear zone of siliceous and high alumina alteration within the Cambrian - Ordovician Balcooma Metavolcanics. These acid to intermediate metavolcanics and lesser metasedimentary host rocks are metamorphosed to greenschist facies and steeply dipping. A regional submylonitic foliation was developed during the early Silurian, when the rocks formed the axial zone of a major orogeny. This foliation is subparellel to stratigraphy and coeval and parallel with the Balcooma mylonite zone 1km to the west.

The alteration occurs along a high strain zone of the main foliation and cuts the stratigraphy at a low angle. It consists of an elongate, fine grained, mylonitic siliceous body in which widespread kyanite and andalusite occur along foliation planes and in crosscutting veins. It also contains elongate pods up to 8m across of structureless kyanite or andalusite, with lesser corundum, diaspore, muscovite, topaz and apatite. Aluminium phosphates scorzalite, lazulite, goyazite and svanbergite occur abundantly with apatite and andalusite in a restricted area.

Topaz occurs also as extremely fine grained irregular aggregates and veins within fine grained quartz and angular or finely milled quartz - topaz breccias. Topaz and abundant foliated muscovite are present in some areas within the foliated quartz. Apatite, pyrite and fluorite are common in topaz rich rocks. Fine grained rutile is present ubiquitously in the alteration zone. Pyrophyllite and kaolinite extensively vein and replace aluminosilicates throughout the zone.

The paragenesis of the above assemblage can be divided into four stages: (1) silicification of host rocks (2) aluminous alteration (3)topaz/muscovite alteration (4) clay alteration. All phases of

alteration were part of a continuous evolving hydrothermal event with gradually waning temperature and increasing μHF. The physio-chemical conditions during formation of the alteration assemblage can be inferred by a study of the system F_2O_{-1}-K_2O-Al_2O_3-SiO_2-H_2O and mineral reactions infered from textures.

Silicification probably occured in conjunction with hydrolytic cation leaching of the host rocks producing a residual enrichment of silica, aluminium, TiO_2 and possibly phosphate. Aluminium was mobilized and extensively veined and replaced the silicification. Increasing temperature and low aSiO_2 causes nonstochiometric disolution of SiO_2 over Al_2O_3. Low aSiO_2 within aluminous veins formed corundum and diaspore in high fluid flow areas. Muscovite formed as K^+/H^+ increased. μHF can increase due to cooling, thus topaz usurped Al_2SiO_5 as the stable aluminosilicate, and fluorite formed. Kaolinite and pyrophyllite alteration occured as the low aSiO_2 fluid cooled futher.

Widespread apatite shows the fluid was high in H_3PO_4. Scorzalite/lazulite (Mg/Fe bearing aluminium phosphates) formed from H3PO4 alteration of andalusite. Sulphate bearing aluminium phophates (goyazite and svanbergite) are isostructural with alunite and formed from in response to increased H_2SO_4 and Sr.

P/T considerations of the assemblage andalusite-kyanite-corundum indicate the assemblage was not the product of prograde regional metamorphism and that it probably formed between 2.5 - 3.0 Kb and over a range of 435-220°C. This suggests the event was of Silurian age. This is consistant with foliation developement within the alteration suggesting it developed in the closing stages of the mylonitic event A possible source for an acidic F rich fluid of appropriate age is the Ringwood Park Microgranite.

High alumina alteration zones of extremely analogous mineral assemblages and similar styles occur in other Palaeozoic felsic metavolcanic belts in the world, particularly the Carolina Slate Belt. These high alumina zones are sometimes associated with Au and sulphide mineralization however a drilling program at Quartzite Ridge failed to detect significant mineralization. These zones represent a distinctive alteration style characterised by high F and PO_4 and having genetic affinities with both porphyry Cu-Mo systems and greisens.

CONTENTS

CHAPTER 1 INTRODUCTION

CHAPTER 2 REGIONAL GEOLOGY

CHAPTER 3 GEOLOGY AND MINERALOGY OF QUARTZITE RIDGE

CHAPTER 4 GEOCHEMISTRY

CHAPTER 5 MINERAL REACTIONS AND STABILITY FIELDS

CHAPTER 6 DISCUSSION AND CONCLUSIONS

LIST OF TABLES

LIST OF FIGURES

CHAPTER 1 - INTRODUCTION

1.1 INTRODUCTION

Quartzite Ridge is a 2km linear zone of aluminous alteration hosted by the Palaeozoic Balcooma Metavolcanics. It is located on the western margin of the Greenvale Subprovince, 250km west of Townsville, North Queensland. The alteration is a dominantly aluminosilicate assemblage: kaolinite, pyrophyllite, andalusite, kyanite, diaspore. Muscovite and F- and PO_4- bearing minerals and rutile are common associate phases. The zone is closely related and partially hosted by a fine grained mylonitic siliceous body.

The alteration suite at Quartzite Ridge is particularly distinctive. It has correlatives both internationally (e.g. Brewer Mine, Carolina Slate Belt, USA; Schmidt, 1985) and locally (e.g. Truncheon Prospect, Mt Windsor Volcanics, Australia; Beams et al., 1989). This alteration style is sometimes associated with gold or sulphide mineralisation and is typically mesothermal. Its genetic relationship to magmatic processes is generally unclear, but is characterised by formation from a high fluid flow of strongly acidic F bearing solutions.

Advanced argillic alteration assemblages found associated with acid sulphate epithermal ores and high levels of porphyry style deposits have important differences from the high alumina suites mentioned above. These latter have been largely overlooked in the literature and are unknown as distinct alteration style in Australia, compared with the veritable flood of information on epithermal and porphry systems from 1980 to the present.

1.2 AIMS

It is the aim of this study to document the alteration assemblage at Quartzite Ridge and propose a paragenesis by means of the following approaches:

(1) identification of mineral phases and their associations.

(2) determining temporal and spatial relationships of mineral associations to each other.

(3) determining the approximate conditions of formation of different mineral associations, and of the alteration suite in general with respect to fluid composition, temperature and pressure.

(4) investigating the timing of the alteration with regard to the major mylonitic deformational event.

This approach was desigened to allow comment on the origin of the fluid and the age of the alteration event.

Due to the time constraints of a Honours thesis it is not within the scope of this study to futher define the structural and stratigraphic geology of the area.

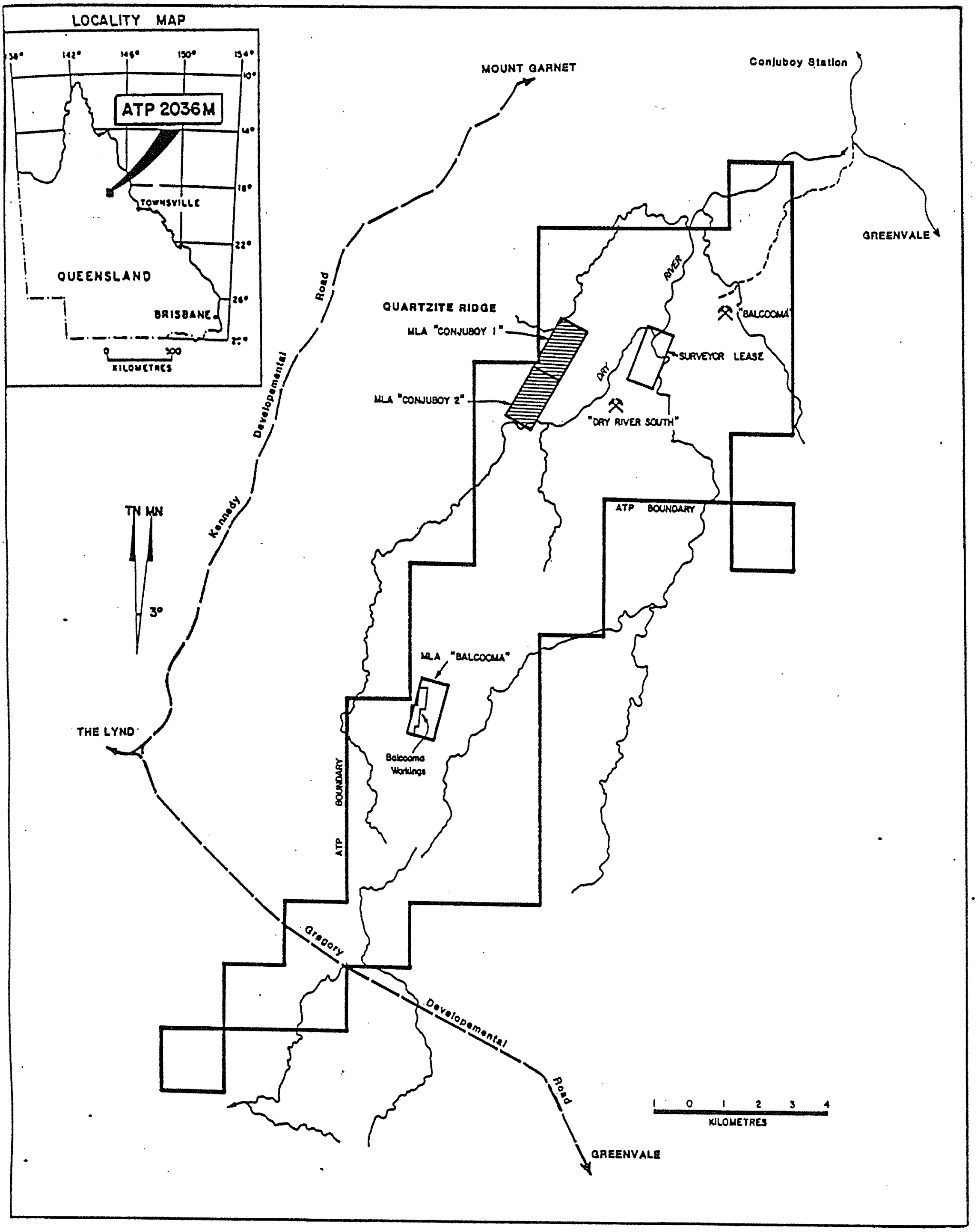

Figure 1 - Location map for Quartzite Ridge ML's (after Jackson, 1988).

1.3 METHODS

The alteration zone was extensively sampled and mapped at 1:2000 during 4 weeks in the field, and 700m of drill core was logged and sampled.

A petrological study included preparation and examination of 80 thin sections, use of the SEM probe on 10 polished thin sections, and XRD analysis of clay and mineral phases.

1.4 EXPLORATION AND MINING HISTORY

The unusual alteration was first noticed by Chevron Exploration Corporation and Carpentaria Exploration Company (CEC) geologists during a regional exploration programme of ATP2036M 'Balcooma' in 198?. Anomalous gold values detected in associated drainages during regional stream sediment sampling and initial identification of pyrophyllite led to futher investigation by CEC and suggestions of a possible acid-sulphate epithermal origin.

Quartzite Ridge is within M.L.'s 1451 and 1452 held by Carpentaria Exploration Company and joint venture partner Metallgeschellshaft of Australia Pty Ltd (fig 1). Testing for possible mineralisation was carried out in 1988-89 by CEC, and provided assistance for this project, access to drillcore and geochemical analyses. No significant mineralisation was detected.

Several massive sulphide prospects (Cu-Pb-Zn) 'Surveyor' (ML805 Geopeko Limited), 'Balcooma' (Harvey, 1984) and 'Dry River South' (Withnall, 1989) (fig 1), are all within five kilometres of Quartzite Ridge. They are hosted by the Balcooma Metavolcanics and are of presumed syngenetic/volcanogenic origin (Withnall, 1989).

Ten kilometers to the south are several old workings which were included in the Balcooma Goldfield. Shallow mining of small but rich reefs resulted in total production to the order of around 30kg (records are incomplete) (Anon.? 1984).

1.5 LOCATION AND GEOGRAPHY

Quartzite Ridge is located approximately 40km NW of the mining town of Greenvale. It is accessed via the Kennedy Developemental Road and approximately 15km of 4WD track from Conjuboy Homestead (fig 1). Several crossings of the Dry River are impassable after heavy rain.

The topography is characterised by low irregular ridges trending NW, and eroded plateaus of tertiary laterites and basalts.
Vegetation is open savanah of dry sclerophyll with areas of wattle scrub and prolific speargrass with occaisional spinifex on hilltops.

CHAPTER 2 - REGIONAL GEOLOGY

2.1 GENERAL SETTING

The Balcooma - Dry River area is within the Greenvale subprovince, which is the easternmost region of the Proterozoic Georgetown Province (Withnall, 1982) (fig 2.1).

The Greenvale subprovince is an elongate fault bounded belt trending NW, of dominantly Lower Palaeozoic rocks. The Balcooma Mylonite Zone (BMZ) forms the western margin of the subprovince with the Georgetown Province, represented here by the Precambrian Einasleigh Metamorphics. The Broken River Fault seperates the Greenvale subprovince from the Palaeozoic Broken River Province in the east. Both the NW and SE extensions of the region are obscured. An extensive intrusion of the Silurian - Devonian Dido Tonalite truncates the subprovince in the south, and Cainozoic sediments and basalts cover the northern end.

The Lower Palaeozoic rocks west to east, comprise the Balcooma Metavolcanics and the Lucky Creek Metamorphic Group (Withnall, 1989). The contact between the two is concealed by the Dido Tonalite. Contacts of units within the Lucky Creek Metamorphic Group are typically faulted parallel to the NW trend and are most probably thrust faults (Withnall, 1989). Pervasive steeply dipping schistose to mylonitic foliations are a feature.

A narrow fault bounded band of Proterozoic rocks (the Halls Reward Metamorphics) occurs on the easternmost margin.

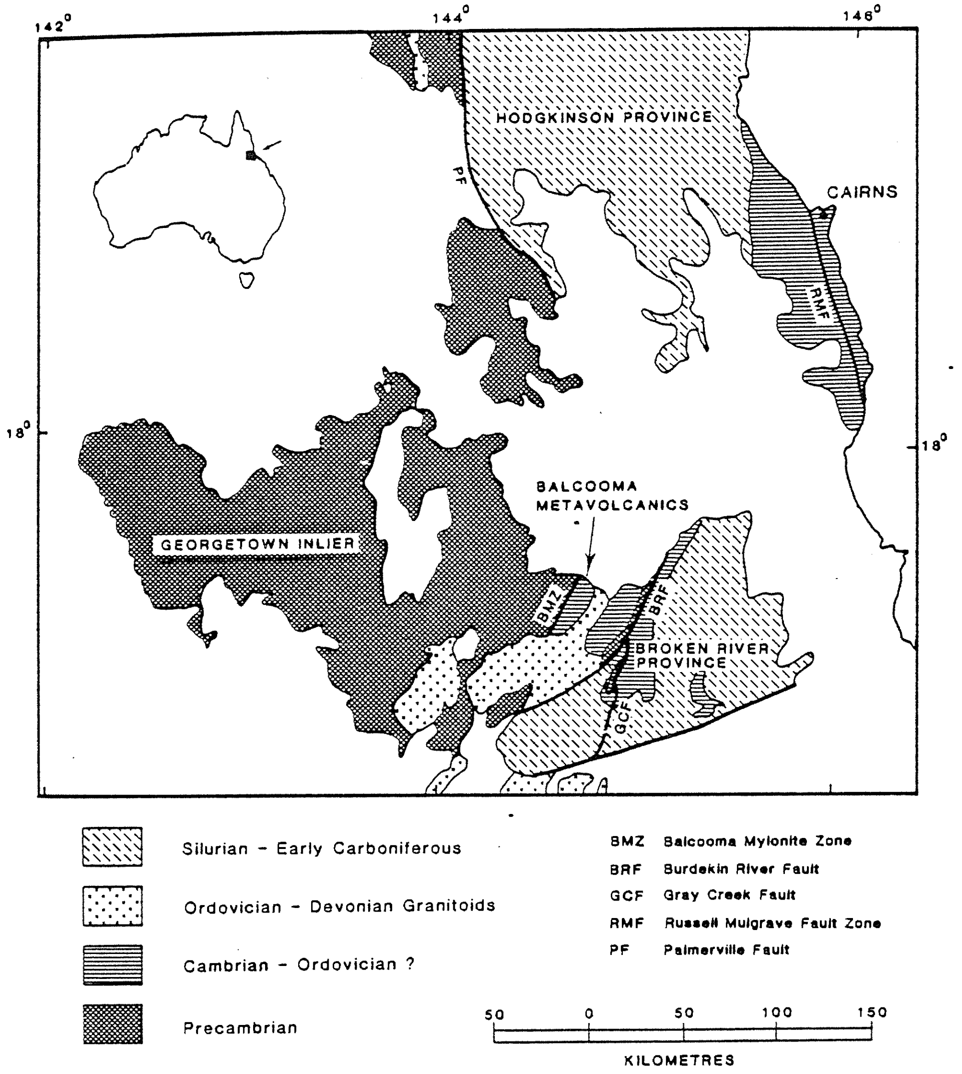

Figure 2.1 - Regional tectonic setting of the Balcooma Metavolcanics (Van der Hor, 1989).

Rare patches of later Palaeozoic sediments are unconformable to the lower sequence, and small isolated outcrops of Carboniferous volcanics.

2.2 PREVIOUS WORK

2.2.1 Regional

The Georgetown Province and Broken River Province were mapped by the Bureau of Mineral Resources (BMR) and the Geological Survey of Queensland in the 1950's (White 1962a, b, 1965). Later work by the BMR, GSQ, and university geologists on the Georgetown Province was reviewed by Withnall and Mackenzie (1980), and Withnall (1982).

Bell and Rubenach (1976) discovered the BMZ, and Arnold and Rubenach reappraised the geology of the Greenvale area with particular reference to the origin and emplacement of the Proterozoic mafic and ultramafic complexes.

Additional mapping and investigations of the Georgetown Province were carried out during exploration activities by they CEC geologists led to the discovery of the Balcooma base metal deposit in 1978 (Harvey, 1984), and identified deformed and metamorphosed acid to intermediate volcanics in the Balcooma and Lucky Creek areas.

The Greenvale Subprovince and the Broken River Province were studied as part of the BMR-GSQ Georgetown Project between 1980 and 1983, and are presented by Withnall (1989). Most of the following lithological information on the Greenvale subprovince has been summarized from this source.

Deformation and metamorphism of the Balcooma area were the subject of a PhD study by Van der Hor (1989).

2.2.3 Quartzite Ridge

The alteration at Quartzite Ridge has not been previously studied. A similar kyanite assemblage has been observed by Withnall within siliceous rock in the Lucky Creek Formation 25km to the ESE.

2.3 LATE PALAEOZOIC - Conjuboy Formation

The early Devonian Conjuboy Formation unconformably overlies the Balcooma Metavolcanics and Einasligh Metamorphics in the BMZ. Its main occurence is as a narrow northeast trending belt about 9km long and 1.5 -2.0 km wide, and dips 30° to the NE.

Lithologies are thickbedded and commonly trough bedded medium to coarse grained quartzose sandstones, mudstones and shales and sporadic lenses of bioclastic calcirudites. Faunas have not been studied in detail.

2.4 EARLY PALAEOZOIC

2.4.1 Balcooma Metavolcanics

The Balcooma Metavolcanics form a belt 30 km long and 7 km wide and represent the remnnants of an extensive northerly trending metamorphic belt that developed in the Ordovician-earliest Silurian during compression and uplift of a Cambrian-Ordovician sedimentary basin (Van der Hor, 1989).

Acid metavolcanics, rhyolitic to dacitic in composition, volcanoclastic rocks and intercalated schist are the dominant lithologies. Andesites, mafic andesites and andesitic tuffs form a minor proportion and are found in the western region with rare metadolerite (Withnall, 1989; Van der Hor, 1989) (fig 2.2).

The metasediments occur mainly in the eastern area of the formation and comprise thick bedded greywackes, sandstones, mica schists, quartzites, and minor calcsilicates. Graded bedding and cross bedding can be seen in the northern area near the Balcooma massive sulphide deposit (Van der Hor, 1989).

Primary lithologies inferred for the Balcooma Metavolcanics are similar to the Seventy Mile Range Group of the Southern Charters Towers Province and the two units are probably correlative (Withnall, 1982; Henderson, 1986).

Metamorphic grade increases from greenschist facies in the western part of the formation to amphibolite facies in the east, and mineral assemblages indicate a temperature increase towards the north (Van der Hor, 1989).

A lower Palaeozoic Cambrian-Ordovician age has been inferred by Harvey (1984), Withnall (1982) and Oversby et al (1983) on the basis of limited isotropic evidence (Gulson and Vaajofi, 1978). Withnall

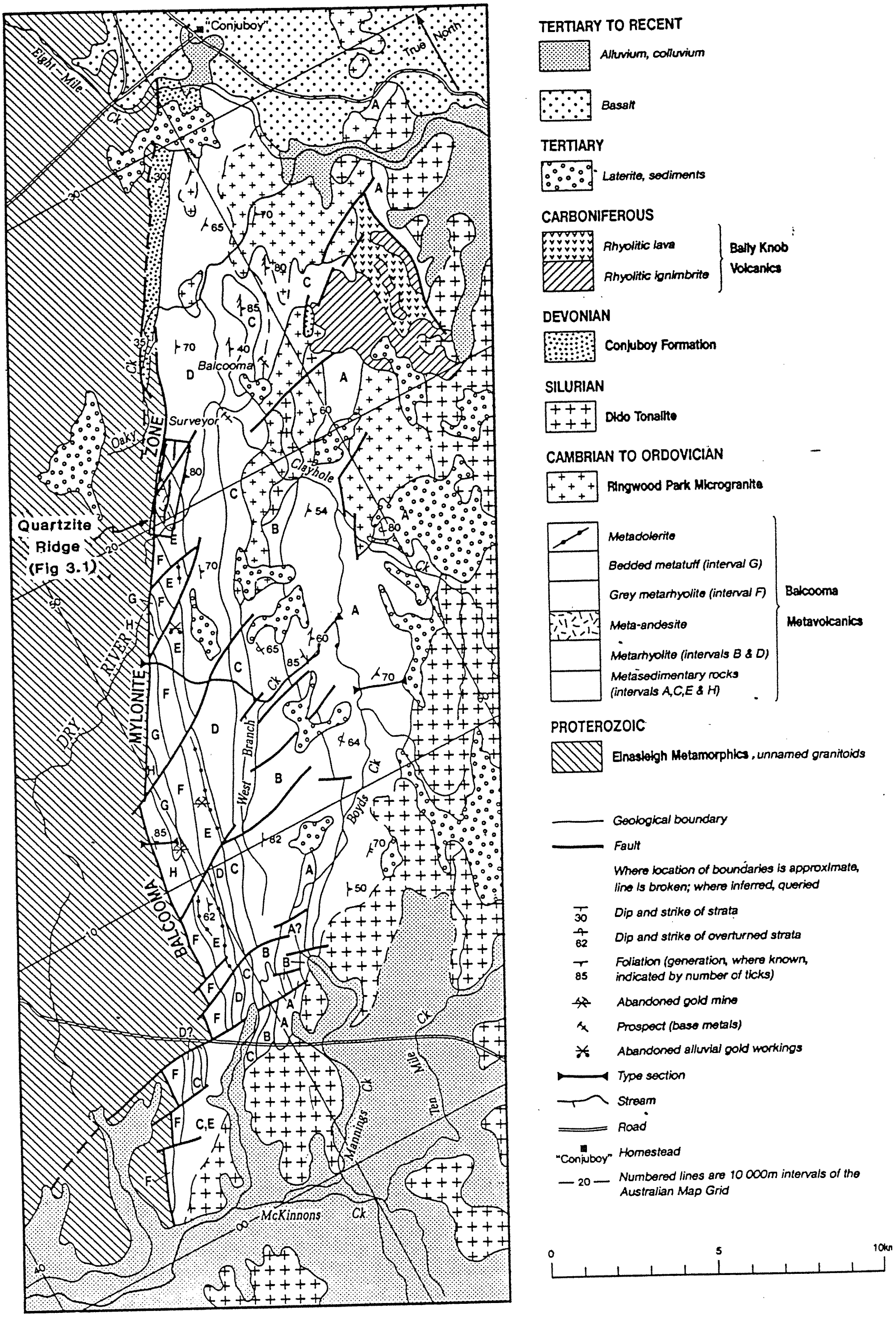

Figure 2.2 - Geology of the Balcooma Metavolcanics (Withnall, 1989).

(in prep) has determined ages of 471±4 Ma (^{206}Pb / ^{238}U) and 507±22 Ma (^{207}Pb / ^{206}Pb) obtained from zircons using an ion microprobe, placing them as middle Ordovician.

Structure

Metasedimentary rocks are generally well foliated, and acid felsic volcanics variably foliated. The foliation is sub-parallel to bedding in some outcrops particularly towards the BMZ, but commonly it cuts across bedding at low to moderate angles. Both bedding and cleavage dip predominantly to the east to southeast (Withnall, 1989). Withnall takes the dominant foliation to be S1 and describes a locally occuring partially differentiated S2 crenulation. Withnall proposes the lack of repetition and vergences suggest that the sequence is the western limb of a major anticline.

The structure of the area was the subject of a PhD study by Van der Hor (1989). Van der Hor recognizes 6 deformation events. The complex structural and metamorphic features of the Balcooma metavolcanics are interpreted in terms of an orogen with several stages of orthogonal cleavage developement, culminating in D5. D1-3 were detected by study of porphyroblast microstructures. Evidence for these events in the matrix are destroyed by younger folding events.

Balcooma Mylonite Zone

The BMZ was discovered by Bell and Rubenach (1976). It is a diffuse zone 1-2 km wide in the Einasleigh metamorphics adjacent to the Balcooma Metavolcanics. The western margin is not well defined (Withnall, 1989).

Withnall (1989) describes the deformation effects in the Balcooma Metavolcanics as somewhat heterogeneous with more strongly deformed and less deformed zones commonly interspersed. The Balcooma Metavolcanics do show some increase in deformation visible up to 700m from the contact, but the mylonitic effects may be less visible in the finer grained rocks.

Van der Hor (1989) proposes dextral strike slip movement along the fault zone. Evidence for strike slip movement are shallowly dipping to subhorizontal stretching lineations. Dextral sense is infered from microstructural studies and by correlation with overall dextral transcurrent movements on the Tasman Fold Belt.

The Einasleigh Metamorphics have been much more strongly affected however, with intensely ribboned and laminated rocks of probable granitoid origin showing the most intense deformation in a subvertical zone 30-100 wide (Van der Hor, 1989).

Synkinematic mineral assemblages in ampphibolites indicate transitional amphibolite facies metamorphic conditions during mylonite formation. (Van der Hor, 1989).

A syntectonic or post D5 age is suggested by Van der Hor (1989) for the BMZ. Dating of D5 is on the basis of the Silurian metasedimentary rocks of the Graveyard Creek subprovince showing no evidence of a major folding event that could be correlated with D5. Thus suggests a maximum earliest Silurian age is inferred for the BMZ. The BMZ is overlain unconformably by the Devonian Conjuboy Formation. This sets a minimum age for the BMZ as pre Devonian.

2.4.2 Lucky Creek Metamorphic Group

The Lucky Creek Metamorphic Group includes from west to east , the Lungano Metamorphics, the Eland Metavocanics and the Paddys Creek Metamorphics (Withnall, 1989). These occur to the east of the Balcooma Metavolcanics in a northeasterly trending zone, and are generally of greenschist facies, and locally amphibolite facies where intruded by the Dido Tonalite.

Lungano Metamorphics

The Lungano Metamorphics include abundant massive to well layered amphibolite; feldspathic schist and gneiss, mica schist, quartzite and minor marble. Their origin is uncertain but they are thought to be derived from coarse grained, very thick bedded arenites and siltstones, shale, and minor tuff with submarine basaltic lavas, volcanoclastics and minor limestone.

A distinctive ridge forming quartzite occurs near Galah Dam that appears similar to Quartzite Ridge. It occurs in a synform and is intelayered with quartz-mica schist. It contains abundant radiating kyanite prisms on foliation planes, in places replaced by kaolinite and minor muscovite with acessory rutile. Other acessory minerals occuring at Quartzite Ridge have not been reported, but chemical analyses show a similar anomalous Sr values.

The Lungano Metamorphics are generally well foliated and metamorphosed mainly in greenschist facies.

Eland Metavolcanics

These occur east of the Lungano Metamorphics and predominately consist of chlorite and actinolite schists containing relict plagioclase phenocrysts. Basaltic to andesitic volcanoclastics were probably the original rocks. Less strained volcanogenic sedimentary rocks, metacherts and tuffs also occur to a lesser extent.

They are very strongly foliated and locally mylonitic. The rocks are of greenschist facies and are thought to be of early Ordovician age by correlation with the lithologically similar Troopers Creek Formation of the Seventy Mile Range Group (Henderson 1982, 1986).

Paddys Creek Phyllite

This unit consists mainly of quartz-muscovite phyllites with minor chlorite grading into quartz phyllite or quartzite. The rocks are strongly foliated and show a layer differentiated crenulation cleavage. They are thought to be derived from an original mudstone and quartz arenite sequence and are now probably metamorphosed to greenschist facies.

A probable early Palaeozoic age is suggested by correlation with the Judea Beds of the Graveyard Creek subprovince.

2.5 PROTEROZOIC ROCKS - Halls Reward Metamorphics

These rocks outcrop as a narrow belt 5 km wide and 90 km long east of the Lucky Creek Metamorphic Group, and together with the mafic and ultramafic Boiler Gully Complex form a sliver of fault bounded proterozoic rocks of indeterminate origin.

2.6 INTRUSIVES

2.6.1 Ringwood Park Microgranite

The early Palaeozoic Ringwood Park Microgranite intrudes the Balcooma Metavolcanics in the northern region and Withnall (1989) proposes it is coeval with them. However increasing metamorphic grade towards the north of the Balcooma Metavolcanics suggests a correlation between metamorphism and granite emplacement and that emplacement was syntectonic (Van der Hor, 1989).

Composition is of variably porphyritic microgranite and microgranodiorite with local biotite granite. The fine crystal texture and granophyric textures indicate high level emplacement.

The rocks are generally at least weakly foliated and were probably metamorphosed with the Balcooma Metavolcanics. They are dated as Middle Ordovician by Withnall (1989) on the assumption that they are contemperaneous with the Balcooma Metavolcanics.

2.6.2 Dido Tonalite

The Silurian - Early Devonian Dido Tonalite forms a large NNE trending batholith at least 90 km long and 30 km wide and intrudes the Balcooma Metavolcanics, the Einasliegh Metamorphics and the Lucky Creek Metamorphics.

It forms a composite batholith and includes tonalite, quartz diorite, diorite and gabbro and this is more mafic than other pre Carboniferous granitic rocks of the Georgetown Province. The Dido tonalite generally shows a foliation. Muscovite pegmatite dykes and veins probably generated by partial melting of the country rocks intrude the tonalite near the contact in places. The Dido Tonalite is petrologically similar to the Craigie Granodiorite and the Ravenswood Granodiorite in the Ravenswood - Lolworth block (Wyatt and others 1971, Clarke 1971, McLennan 1986). The Ravenswood Granodiorite has lower Sr and Y values, however and was generated at shallower depths (D. Wybon p. comm to Withnall 1989).

Dating by Black and Mc Culloch (in prep.) U-Pb, and Richards and others (1966), K-Ar; indicate an Early Silurian or older age for the Dido Tonalite.

2.6.3 Carboniferous volcanics. and related intrusives

The Carboniferous Bally Knob Volcanics are relatively flat lying and unmetamorphosed. An irregular belt 5 by 20 km outcrops in the northeast of the area (fig.2.2), and a smaller area occurs a few kilometers to the northeast of the Balcooma Base Metals prospect. The volcanics overlie or are faulted against the Balcooma Metavolcanics , Lucky Creek Metamorphics, Halls Reward Metamorphics and Dido Tonalite.

They are an acid assemblage of crystal plagioclase rich lithic tuff, rhyolite ignimbrite, aphyritic dacite (weakly flow banded) and flow banded rhyolite.

Intrusive felsic and mafic Carboniferous rocks are mainly associated with the Bally Knob Volcanics. These include sparsely porphyritic small rhyolite plugs and dykes, microgranite, porphyritic microdiorite or dolerite intrusions 4 by 2 km's wide and a small dyke like body of gabbro.

A few rhyolite dykes were observed by Withnall(1989) locally along some of the major faults.

The Bally Knob Volcanics's have not been dated radiometrically, but are correlated with lithologically similar units of the Cairns-Townsville hinterland (the Coastal Igneous Province) which have Carboniferous ages.

2.7 TECTONIC HISTORY

The Palaeozoic geological history of the Greenvale subprovince is dominated by large scale strike slip faulting, parallel the general trend occuring in the Tasman Orogenic Zone at that time; and periodic episodes of crustal compression and extension. Both of these were controlling factors in basin developement. Interpretation of the Palaeozoic history of the area discussed below is a brief summary of van der Hor (1989).

The Balcooma Metavolcanics and Lucky Creek Metamorphic Group, probably formed during a Cambrian - rifting of the eastern margin of the Proterozoic craton. Scarcity of basaltic assemblages suggests that rifting would not have been so extensive as to generate the formation of oceanic crust (van der Hor 1989).

The Cambrian - Ordovician basin was closed during E-W compression and orogenesis in the Late Ordovician - Early Silurian. The Balcooma Metavolcanics represent the axial core of the hinge, and gravitational collapse produced low angle thrusts emplacing a Lower Palaeozoic Paddys Creek and Eland Metavolcanics over the Halls Reward Metamorphics.

Crustal thinning due to possible lithospheric root detatchment and accompanying emplacement of the Dido Tonalite may have occurred late in the orogenis. Heated crust would have facilitated the developement of ductile mylonite zones.

Developement of the Balcooma Mylonite Zone and other N associated trending dextral strike slip faults (Palmerville, Clarke River and Graveyard Creek Faults) occured during the Early Silurian, following the northerly structural trend of the fold belt. The first phase of crustal extension produced the Greenvale Subprovince as a pull apart basin.

Futher extension resulted in the formation of the Hodgkinson and Camel Creek basins and later Palaeozoic sedimentation to occur. Rapid subsidence of parts of the axial zone of the fold belt during wrench faulting covered it in later Palaeozoic sediments. Closing and folding occured of these basins in the Late Devonian. Variations of the above model are also proposed and discussed by Fawkner (1981).

Henderson (1987) interprets the formation of the later Palaeozoic rocks differently. An active Andean style subduction zone with forearc basin and accretionary prism is used to explain the Graveyard Creek subprovince and Camel Creek - Hodgkinson provinces respectively.

CHAPTER 3 - QUARTZITE RIDGE GEOLOGY AND MINERALOGY

3.1 GENERAL SETTING

The alteration zone that defines Quartzite Ridge, (fig 3.1) is very extensive being some 2km long and a maximum of 70m wide, and extends to a depth of at least 210m. It strikes NNE and is steeply dipping concordant with the dominant foliation. It crosscuts the stratigraphy of the Balcooma Metavolcanics at a low angle. To the north the zone narrows slightly and is less intense where it disappears under tertiary lateritic cover. At its southern end the zone is obscured by Cainozoic sediment cover of the Dry River and was not observed to outcrop south of the river.

The alteration zone forms a narrow prominent ridge, slightly sinuous and trending NNE, parelleling the Balcooma Mylonite Zone. The ridge is displaced by two sets of crosscutting brittle faults, trending NE and E, the displacement of which are visible on the summary map (fig 3.1).

A prominently outcroping fine grained mylonitic silicic zone (the quartz tectonite) forms the backbone of the ridge along much of its extent. Mylonitic quartz andalusite/kyanite rocks form the main body of the ridge. Irregular patches of medium to coarse grained andalusite/kyanite structureless rock (Al_2SiO_5 rock) outcrop along its length. Significant replacement of andalusite rock by Al phosphates and apatite occurs but is restricted to a confined area (map - appendix 5).

Sub-angular breccias of very fine grained topaz - quartz rock are

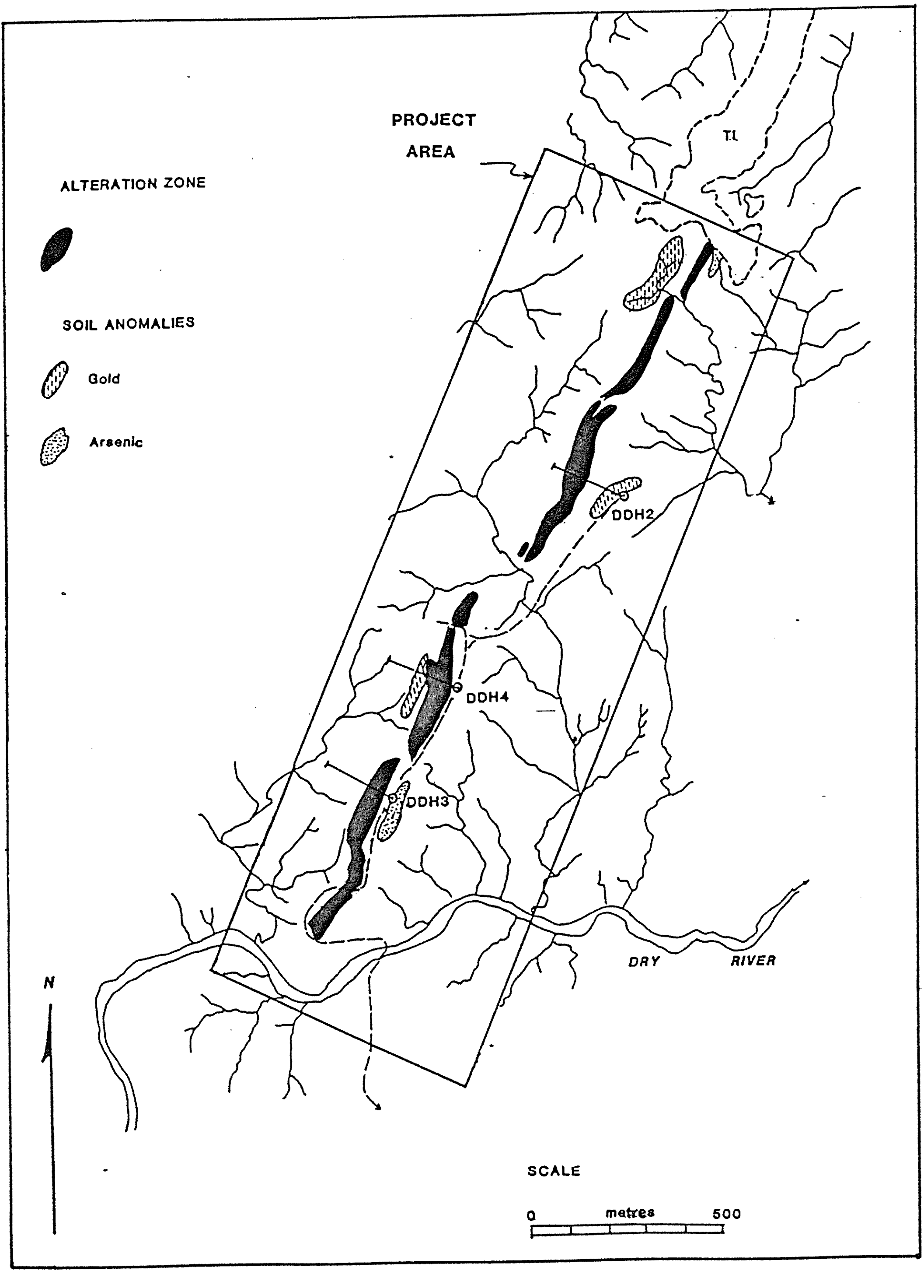

Figure 3.1 - Summary map of Quartzite Ridge. (Appendix is a map at 1:2000 of alteration geology within the project area).

peripheral to outcrops of Al_2SiO_5 rock, and topaz - muscovite veining and alteration overprints the purely aluminous assemblage extensively in some areas.

Alteration to, and veining by a clay assemblage of dominantly kaolinite and pyrophyllite, is widespread and pervasive. Al_2SiO_5 rock is commonly almost entirely replaced.

3.2 COUNTRY ROCKS

At Quartzite Ridge the Balcooma Metavolcanics units trend NNW and consist of interbedded metasedimentary rocks and basic to intermeadiate metavolcanics; and acidic volcanics in the northern most area. They are generally well foliated and may have three or more additional subparallel crenulations present. They are metamorphosed to greenschist facies. They have been affected by several apparently previous metasomatic episodes of alteration and veining and have been extensively silicified in areas.

Lithologies which are probably of metasedimentary origin include:

- fine grained quartz - biotite schists,

- fine grained dark grey quartz - mica - chlorite schist (with variable epidote and sericitic alteration),interbedded with minor fine grained calcsilicate schist,

- fine grained quartz feldspathic schists with chlorite and sericite,

- very fine grained sericitic quartzite.

The basic to intermeadiate metavolcanics in the area are:

- Metadolerite consisting of augite, olivine, plagioclase, serpentitised and displaying ophitic texture.

- Albite - tremolite - quartz - chlorite - epidote schist with magnetite (Coxford, 1989).

- Actinolite - albite - quartz schist, with oligoclase, chlorite, sphene, and illmenite.

More acidic metavolcanic rocks were obsreved at the northern end of the alteration zone. These were not sampled and were classified in the field as quartz porphyry rhyolites. Samples submitted by CEC to Rocko Pty Ltd (Mineralogical Services) for petrological analyses included :

- Quartzofeldspathic schist of acid volcanic origin, with quartz phenocrysts.

- Quartzofeldspathic, blastoporphyritic schist of probably derived from an acidic tuffaceous rock.

- Biotitic, quartzofeldspathic blastporphyritric schist probably derived from a dacite.
  (Coxford, 1988).

Veining of the country rocks is by:

(1) Quartz - carbonate
(2) Quartz - carbonate - chlorite - epidote - pyrite (up to 10cm wide)
(3) Carbonate (approx. 1mm)

3.3 ALTERATION PETROGRAPHY AND PARAGENESIS

3.3.1 Aspects of paragenesis

Paragenesis of the alteration assemblage can be broadly divided into four major phases (table 3). A detailed paragenesis of individual mineral phase relationships can be postulated on the basis of microtextures.

Overprinting of later phases is prevalent throughout the alteration zone. This caused some difficulty in interpretation of some individual mineral phase replacement textures. Distinguishing replacement from infill textures is problematic in a system under moderate pressure (lithostatic pressure equal to hydrostatic pressure) as both can promote euhedral crystal growth. Infill would not be expected to constitute a major process in this type of enviroment.

Identification of some individual mineral phases in hand specimen (e.g. fine grained topaz) caused problems in interpretation of macrotextures. Identification of clay minerals and fine grained aluminosilicates was very difficult optically, and electron microprobe and XRD methods were used.

Broadscale alteration types in pargenetic sequence were determined to be:

I. Silicification of country rocks.

II. The formation of large (15m x 8m) pods of Al_2SiO_5 rock within the silicified rock (also containing corundum and diaspore), a finer network of Al_2SiO_5 veins and Al_2SiO_5 along foliation planes within the silicified rock.

TABLE 3.1 - MINERAL PARAGENESIS

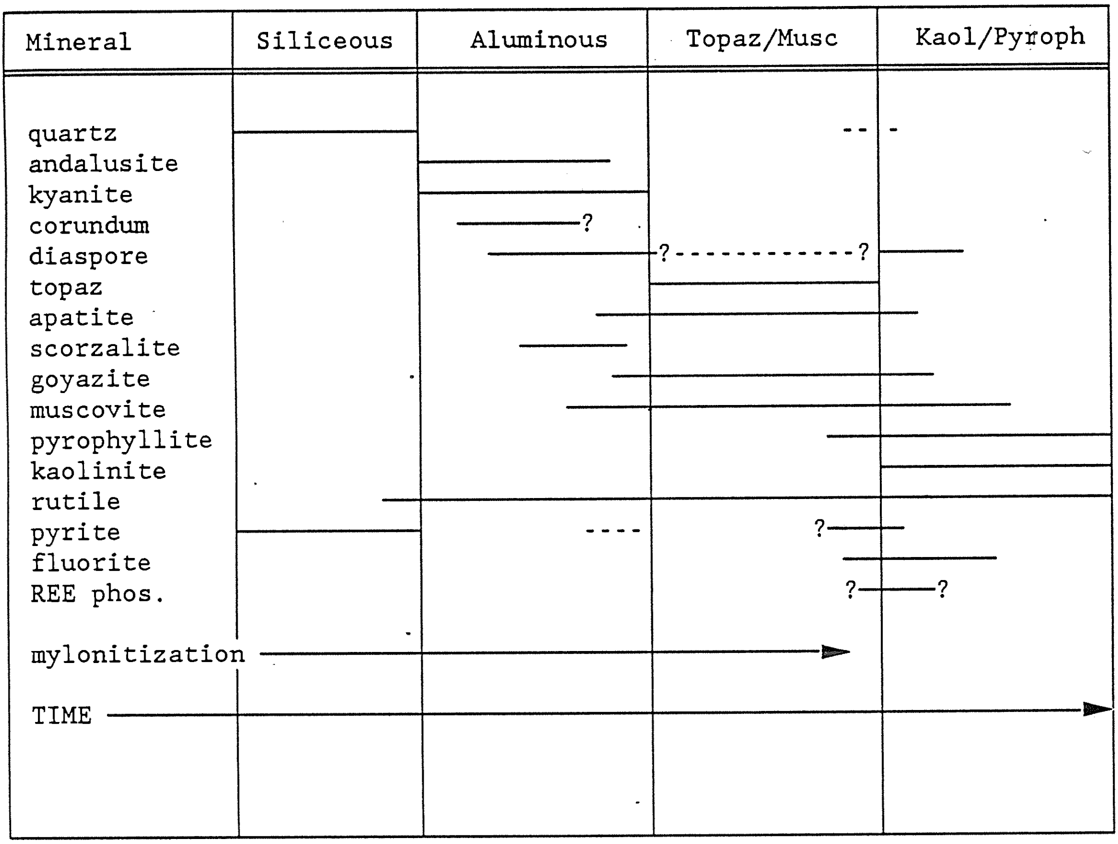

III. Alteration of silicification and other assemblages of II by muscovite, topaz and apatite (± quartz). In one locality of limited extent apatite alteration of andalusite rock is associated aluminium phosphate minerals including distinctive blue - green scorzalite.

IV. Widespread pervasive alteration of both I and II by veining and brecciation to fine grained pyrophyllite and kaolinite with small amounts of muscovite and ubiquitous rutile. Fluorite occurs in some topaz rich rocks.

3.3.2 Alteration assemblages and textural relationships

Vein and rock types of the three groups outlined above and their interrelationships and processes of formation are described in more detail in this section and are summarized in table x. Overprinting of these groups on prexisting alterations results in mineral assemblages listed in the table, the textural relationships of which are discussed below.

ALUMINOUS AND SILICEOUS ALTERATION:

Silicification

This consists of replacement of prexisting country rocks by a very fine grained mylonitic quartz tectonite with quartz veins from 1 -20 cm wide (fig 3.2). A large massif of this fine grained quartz rock forms an extensive outcropping unit that is largely unaffected by later alteration with the exception of a marginal zone of <1m. Drilling directly below this pure quartz rock did not intersect it at depth (drilling summary - appendix 3).

Quartz veins remaining in altered silicified rock are usually irregularly folded, the nature of which may be obscured by later brecciation. Casts after pyrite up to 12mm were observed in some larger veins. Vein quartz crystals are up to 8mm in size, highly strained and with sutured boundaries. They are sometimes recrystalized to a finer grained equigranular texture.

Country rocks not proximate to the main alteration zone contain quartz veins of a similar nature that may be related to this silicification.

Andalusite/Kyanite Alteration

Al_2SiO_5 polymorphs andalusite and kyanite occur as vein material within silicified rock. The aluminosilicates are found in three general styles:

(i) Veins commonly one crystal wide, are developed in fine grained quartz tectonites parallel to foliation planes, and are continuous with occaisional larger crosscutting veins.

(ii) Larger sized veins are found concordant with, and of a similar proportion to prexisting deformed quartz veins in the altered quartz tectonite.

(iii) Brecciation and/or replacement of the coarsley quartz veined silicous rock by the larger Al_2SiO_5 veins produces extensive areas of medium to coarsely crystalline Al_2SiO_5 rock.

Andalusite and kyanite occur in fine grained quartz schists along foliation planes, as strings of single crystals 240μm - 1.2mm (fig 3.3). These can be seen forming as 10μm grains which nucleated along quartz foliation planes in optical continuity in fig 3.4. Crosscutting the foliation are wider $AlSi2_05$ veins in optical continuity with the Al_2SiO_5 extending along foliation planes (thus the Al_2SiO_5 are of vein origin and not the result of regional metamorphism) (fig 3.5).

Deformed vein quartz encloses proportionally sized areas of randomly orientated medium grained Al_2SiO_5 laths. Andalusite frequently displays an equigranular texture. These apparently initially vein concordant with the prexisting quartz veins. Al_2SiO_5 vein thickness is (approximately) in direct proportion to the grainsize of the silicous rock.

In areas of intense alteration of prexisting deformed quartz veins, these are replaced and possibly brecciated by Al_2SiO_5 minerals (fig 3.6). This has produced a medium to coarse grained rock composed dominantly of Al_2SiO_5 (fig 3.7) occuring in pods up to 10m wide (map - appendix 5, fig 3.8). Vein quartz relicts or fragments are commonly enclosed in this rock at vein margins (fig 3.7, 3.6).

Kyanite occurs as masses of interlocking laths from 150μm to 15mm long. Andalusite is more commonly equigranular with sutured boundaries, but may occur as stubby prisms. Crystals range from 30μm to 2.4mm and patches of finer grained crystals may show triple point junctions. Andalusite equigranular rock in one locality has a banded texture. Gradational bands up to a few milimeters wide are of coarser (1mm) crystals alternating with finer ones (250μm) (fig 3.14). Rutile trails along these bands suggests they may represent an original foliation texture.

The Al_2SiO_5 polymorph mineral present is generally either 100% andalusite or kyanite, but also found are mixtures of both, apparently coexisting stably. However kyanite appears to replace andalusite in some instances (fig 3.9). The two polymorphs are indistinguishable in hand specimen and their is insufficient information from thin sections to speculate on gross spatial relationships.

In rock consisting almost completely of Al_2SiO_5 corundum and diaspore are commonly present as alteration products.

FIG 3.2 - Outcrop of unaltered silicification with quartz veins on the mainridge area.

FIG. 3.3 - Quartz tectonite with single crystals of both andalusite and kyanite along foliation planes and crosscutting foliation planes. Andalusite and kyanite are the very pale crystals indicated by the arrow up to several millimetres long (field specimen 32).

FIG. 3.2

FIG. 3.3

FIG. 3.4 - Quartz tectonite with fine grained andalusite nucleated along foliation planes in plane light (A), and crossed polars with gypsum plate inserted (B). (B) displays the optical continuity of the crystals. Field of view is 5.4mm (sample field specimen 32, TS 162).

FIG. 3.5 - Recrystalized quartz tectonite with andalusite developed along foliation planes in optical continuity with andalusite from a crosscutting vein. The middle of the vein is replaced by clays and fine grained muscovite. Field of view is 5.4mm (TS 122 from DDH2, 193.3m).

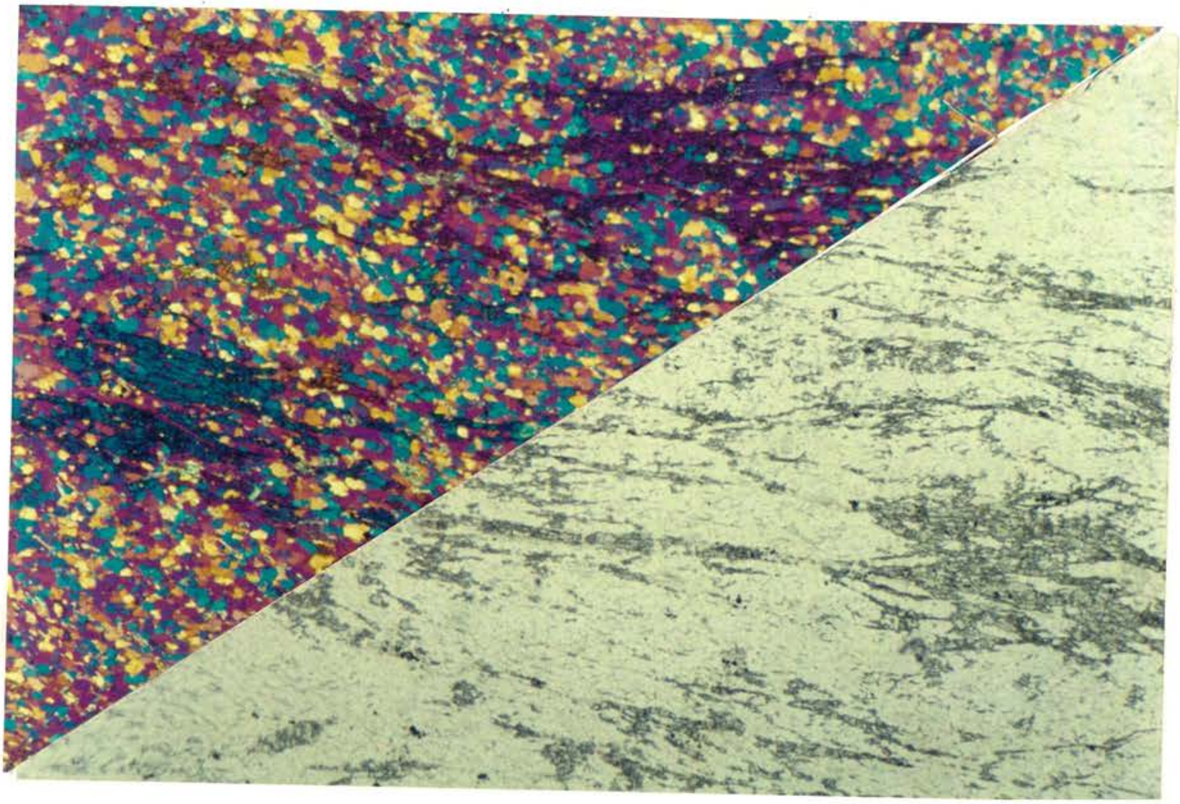

FIG. 3.4 A & B

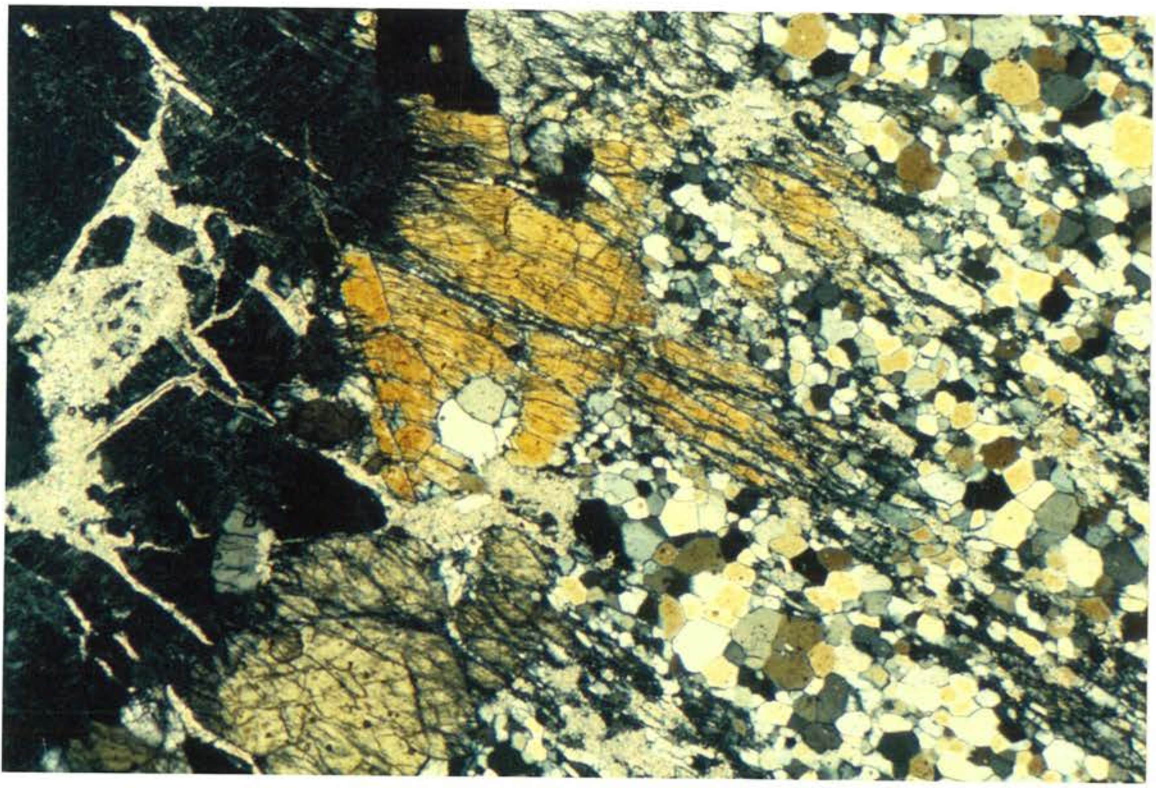

FIG. 3.5

FIG. 3.6 - Structureless medium grained kyanite occurs as veins within quartz and enclosing quartz fragments. Fine brown veins in the middle sample are are later clay (samples are a selection of drillcore from DDH4, 46-51.4m).

FIG. 3.7 - Andalusite rock with both medium and fine grained equigranular texture. A relict quartz crystal in the left of the frame is veined and replaced by pyrophyllite and kaolinite. Field of view is 5.4mm (field sample 34D, TS 151).

FIG. 3.6

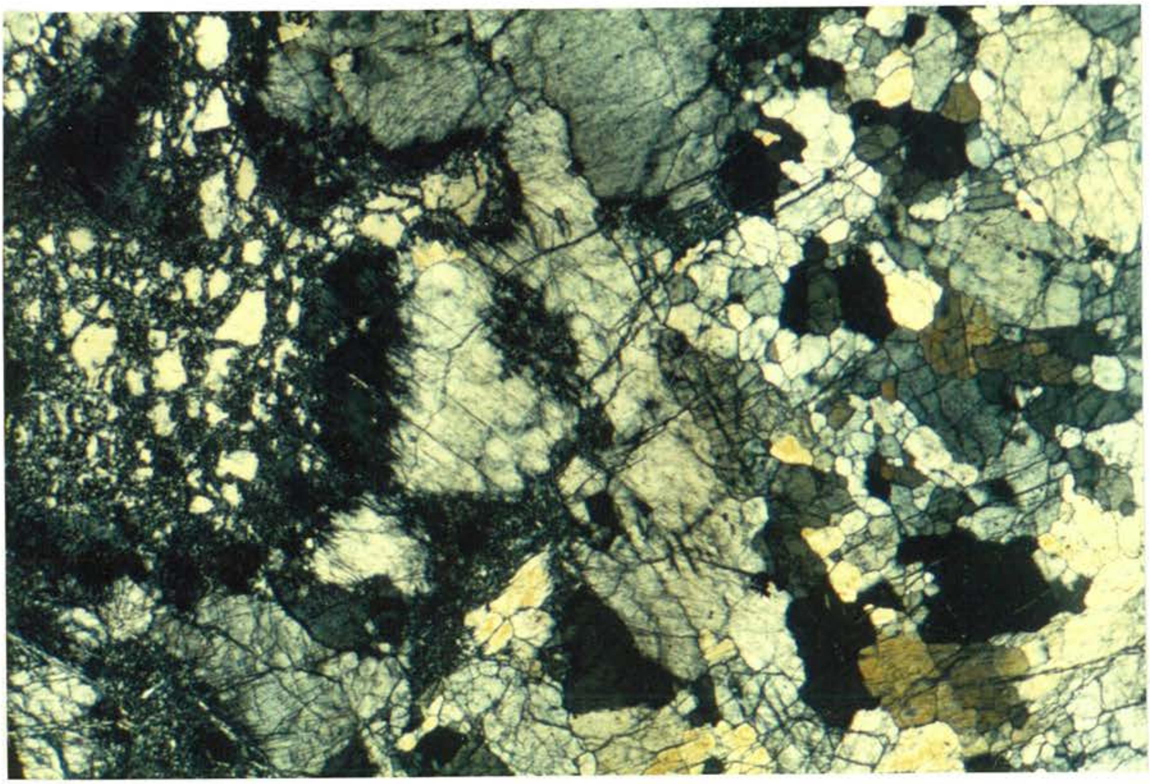

FIG. 3.7

FIG. 3.8 - Outcrop of an andalusite pod on the main ridge area with abundant aluminium phosphate alteration (20m SW of DDH4). Some of the boulders have a banded texture.

FIG. 3.9 - Al_2SiO_5 rock with both andalusite and kyanite. The kyanite laths formed after the equigranular andalusite. Field of view is 5.4mm (field sample 36F, TS 145).

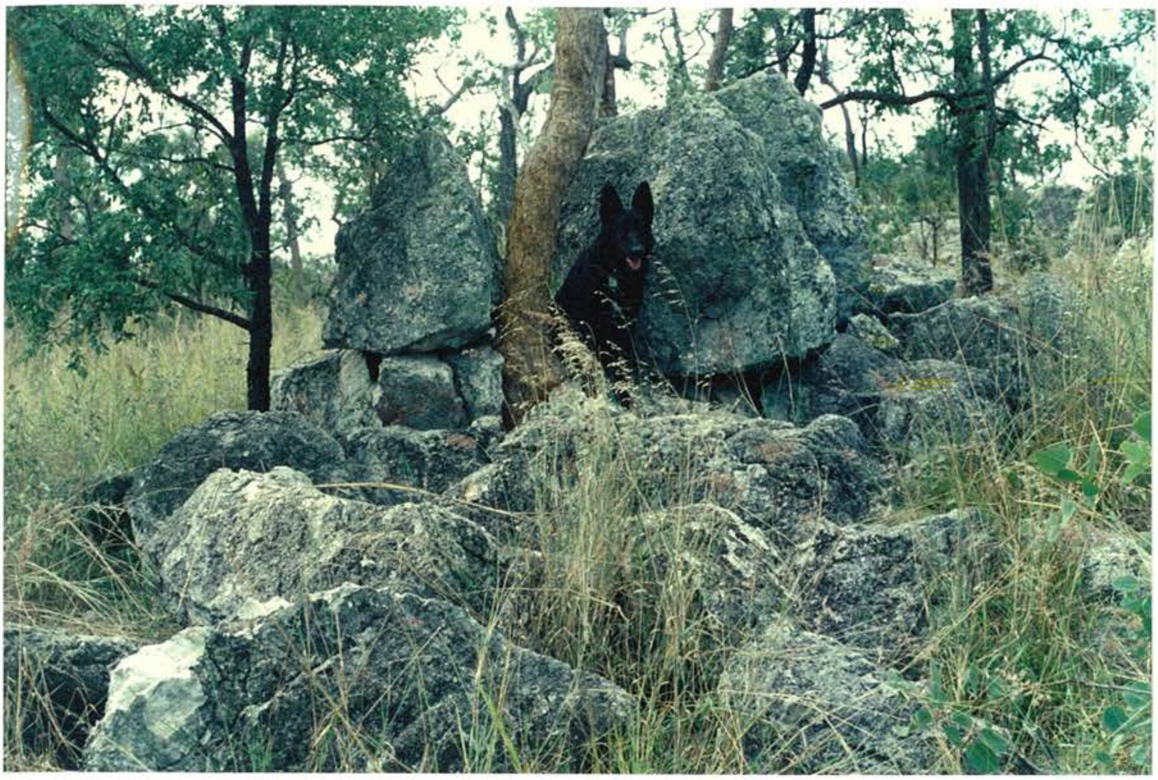

FIG. 3.8

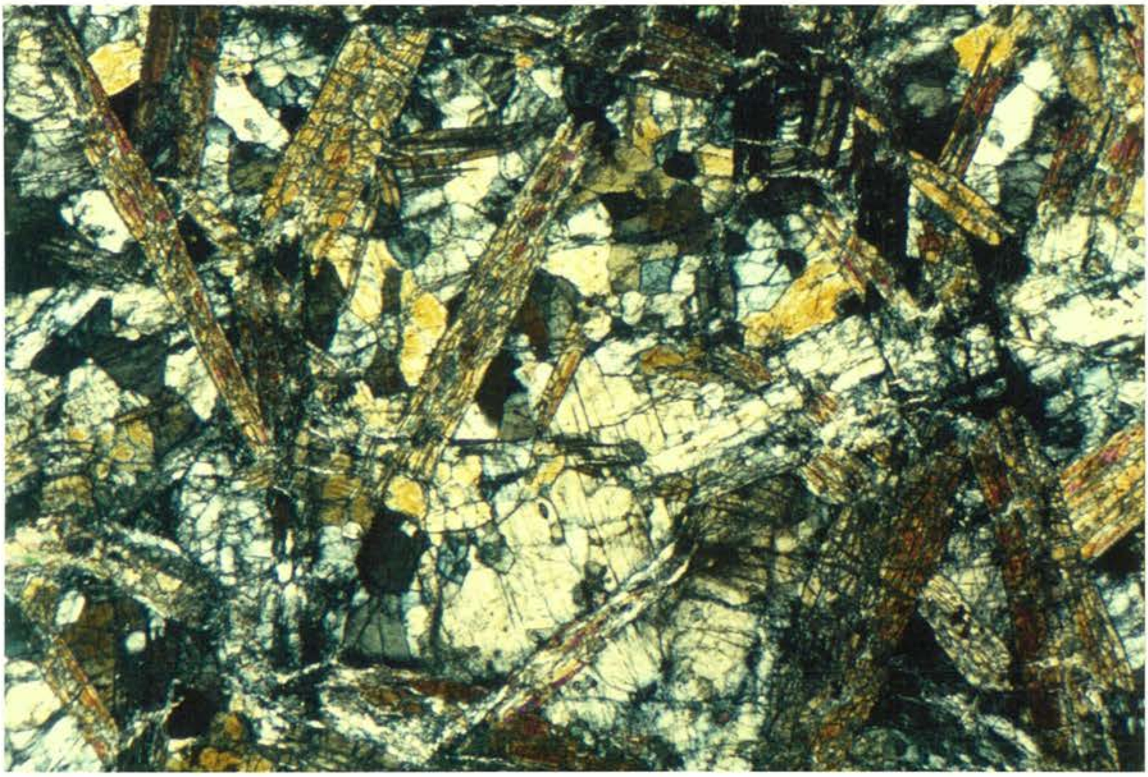

FIG. 3.9

Corundum

Corundum occurs as oikocrysts which are 10μm to 250μm hexagonal plates or stubby prisms within andalusite or kyanite crystals. In some areas it is found as single crystals studding margarite veins in the same rock (fig 3.10). Complete replacement results in irregular pea sized aggregates of corundum crystals veined and brecciated by muscovite (fig 3.11). This latter rock is a dark grey-blue colour in hand specimen and rocks with partial corrundum replacement show patchy areas of the same colouration.

The physical processes of corundum replacement are not clear, as replacement tends to be pervasive, and veining and brecciation textures are ambiguous. The formation of pervasive oikocrysts of corundum is possibly from diffusive alteration of irregular Al_2SiO_5 breccia fragments by veins of the same. Corundum may occur as irregular rings around both fine and coarser grained andalusite (fig 3.13). Rock with complete corundum replacement occurs as irregular rounded breccia fragments of up to 30cm in size in a Al_2SiO_5 matrix (This matrix is altered and veined by later muscovite and clay alteration) (fig 3.12).

Diaspore

Diaspore is present in three different textural forms within Al_2SiO_5 rock. These are:

(i) Sparse prismatic needles up to 25mm long randomly orientated to radiating, and crosscuting all other textures (fig 3.14, 3.15).

(ii) Interlocking bladed prisms within subspherical vugs 3 to 15mm across, displaying coarsening of crystal size towards the centre (fig 3.15) (and more rarely filling interstitial spaces and as small veins).

(iii) Fine grained masses associated with kaolinite, replacing

FIG. 3.10 - Andalusite (An) rock with corundum (C) replacement, and corundum within margarite (Ma). An apatite (Ap) vein replaces the other minerals. Field of view is 5.4mm (field sample 31, TS 154).

FIG. 3.11 - Rounded aggregates of corundum are veined by muscovite. The corundum has replaced andalusite (An) which is now completely altered to a fine grained diaspore - kaolinite mixture. Field of view is 5.4mm (field sample 39 - indicated by arrow in fig 3.12, TS 160).

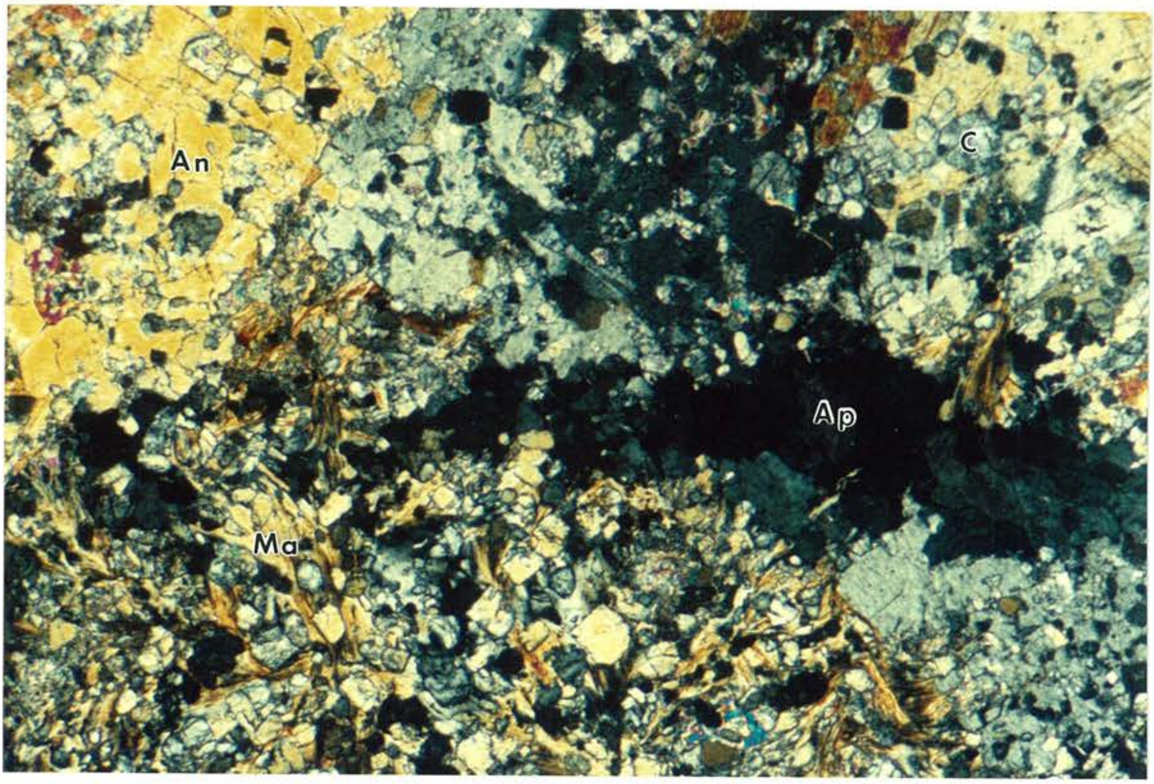

FIG. 3.10

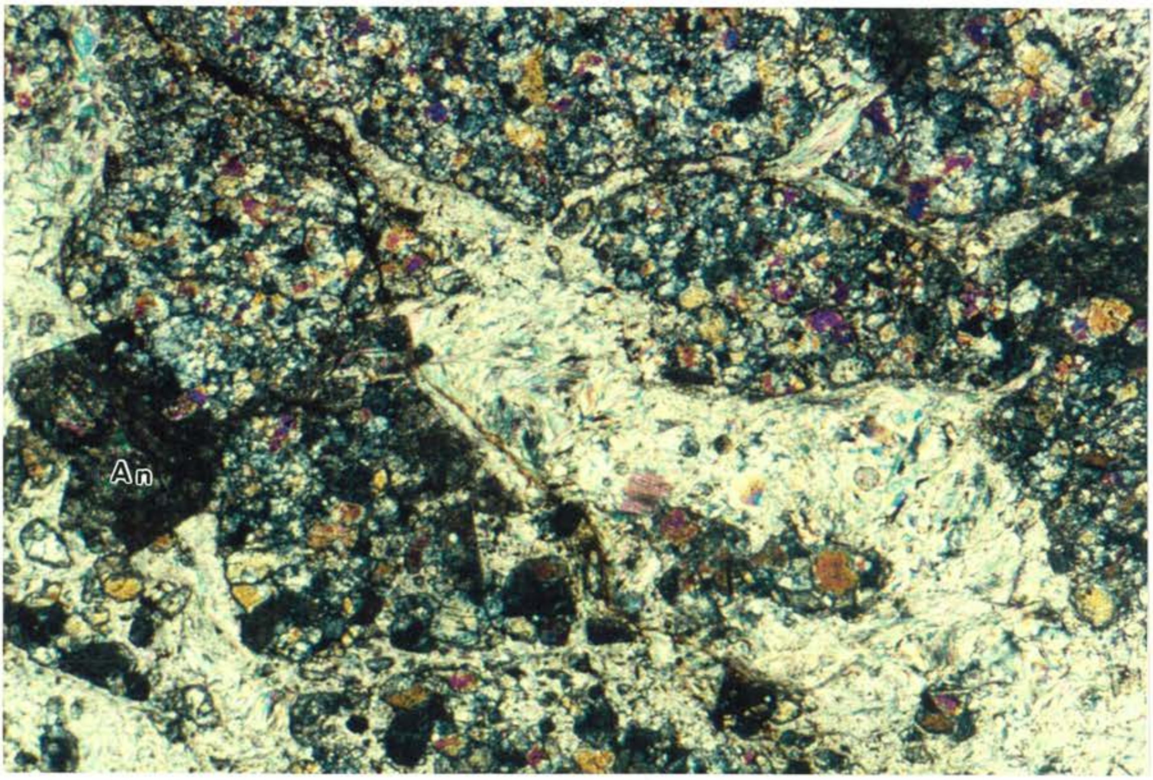

FIG. 3.11

FIG. 3.12 - Kyanite rock enclosing irregular fragments of corrundum rock. Both are veined by muscovite. The arrow indicates the location of figure 3.11 (field sample 39).

FIG. 3.13 - Andalusite rock with fine grained corrundum (C) in irregular trails. A fracture controlled clay vein (P) with fine grained diaspore alteration cuts the rock. Field of view is 5.4mm (field sample 28D, TS 159).

FIG. 3.12

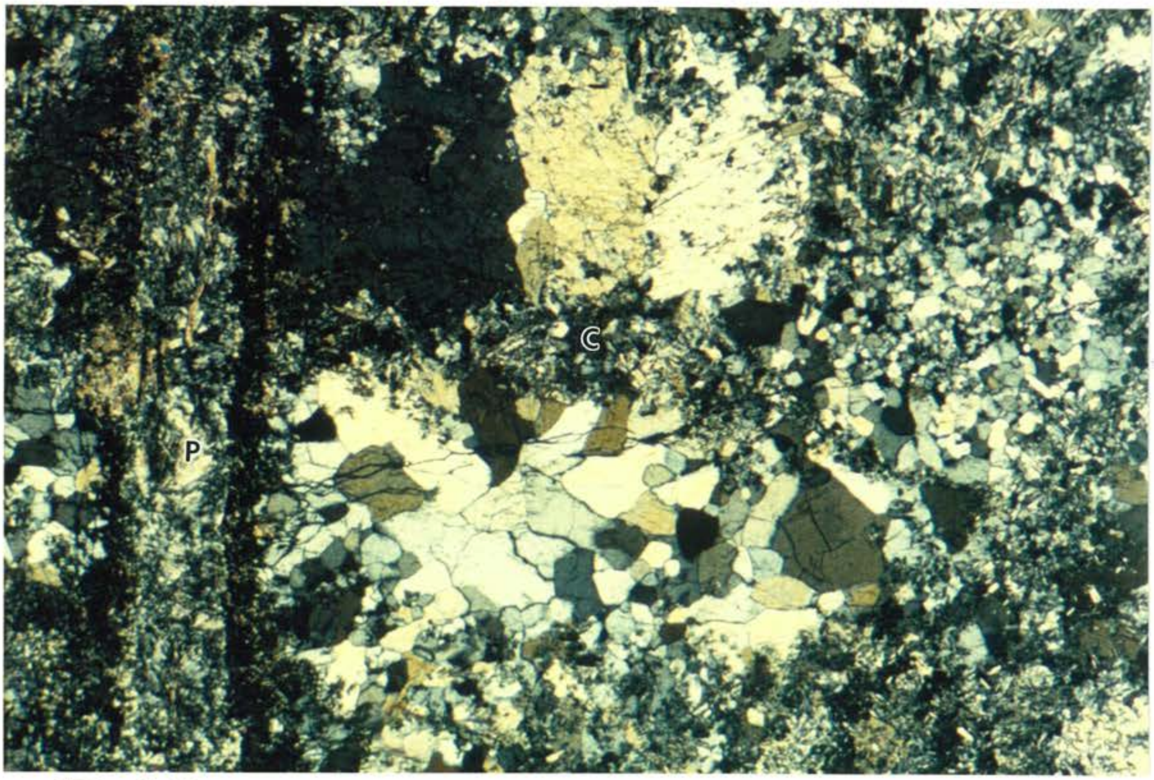

FIG. 3.13

FIG. 3.14 - (A) Coarse grained kyanite rock veined by orange muscovite (field sample 7).

(B) Banded andalusite rock with large prismatic crosscutting diaspore crystals. The dark bands are rutile rich (field specimen 28I).

FIG. 3.15 - Andalusite rock with large prismatic crosscutting diaspore crystals. The diaspore crystals have fine grained pyrophyllite alteration rims. Field of view is 5.4mm (field sample 28D, TS 160).

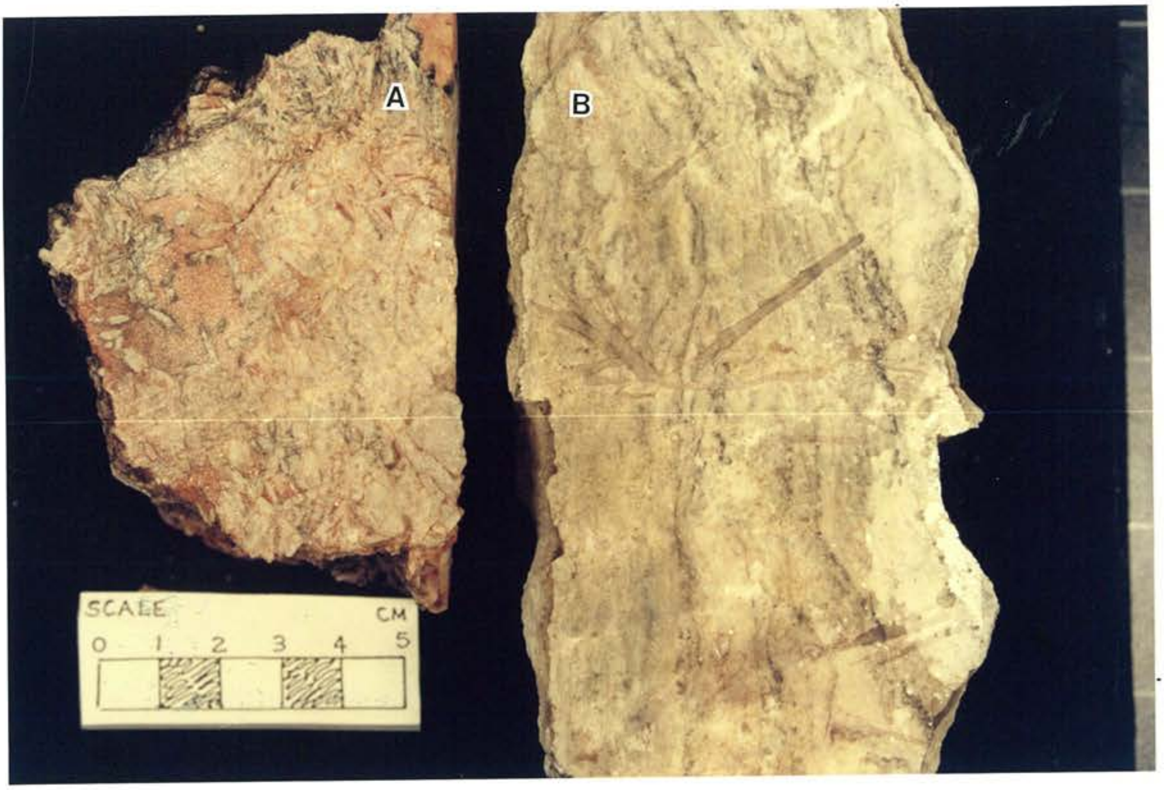

FIG. 3.14

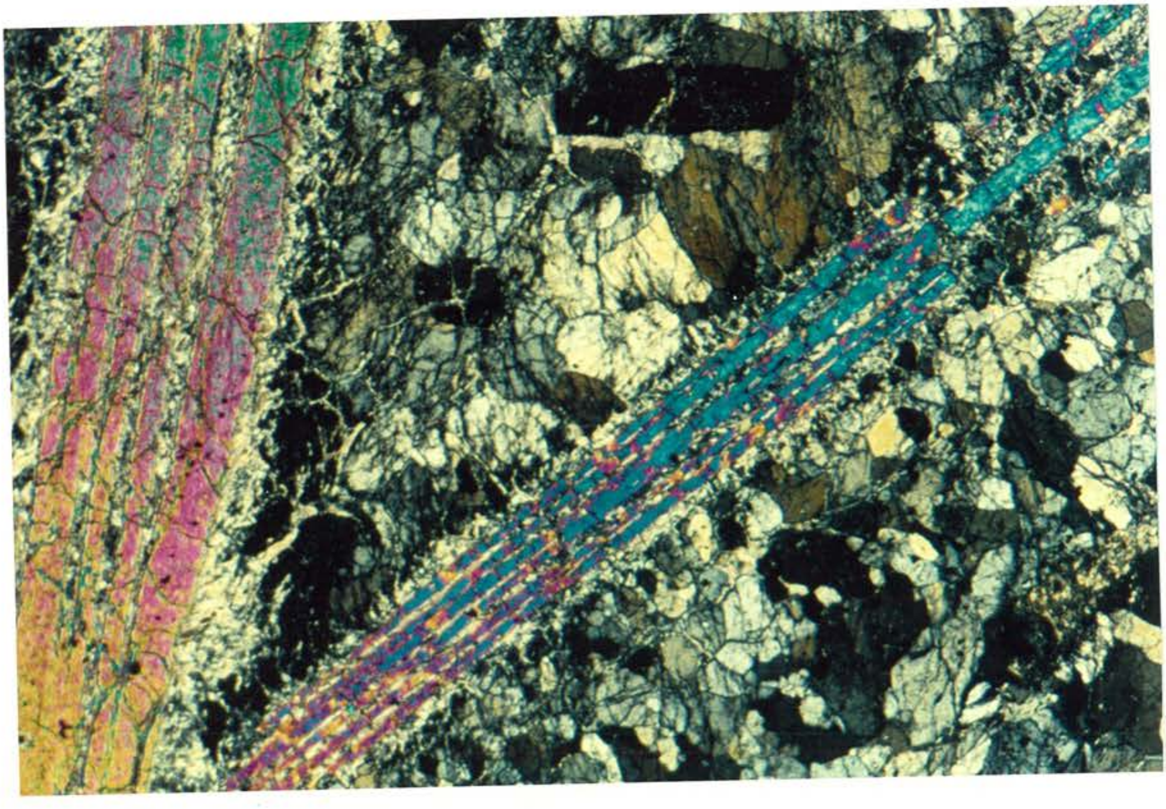

FIG. 3.15

Al_2SiO_5 or corundum (fig 3.27). Diaspore occuring as (i) does not appear to be associated with any vein formation and is probably a direct replacement. Interpretation of type (ii) as vug infill is not certain as actual margins with Al_2SiO_5 minerals show replacement and are usually associated with kaolinite/pyrophyllite alteration of the same. This alteration is most likely associated with later clay alteration overprinting, but small amounts of pyrophyllite also occur interstially with diaspore.

Type (iii) is associated with later clay alteration of aluminous minerals.

PHOSPHATIC ALTERATION OF ALUMINOSILICATES

Medium grained equigranular andalusite rocks in an area approximately 8m by 15m shown on the map are extensively replaced and veined by apatite and aluminium phosphate minerals. These include blue green scorzalite/lazulite series (magnesium - iron aluminium phosphates) and goyazite/svanbergite (strontium aluminium phosphate with sulphate substitution). In intensley altered rocks of this type veining relationships are commonly obscure. Aluminium phosphates were not observed associated with kyanite.

The two main aluminium phosphate minerals and fluorapatite, were identified initially by XRD at the University of Queensland, during initial petrological investigations by Rockco Pty. Ltd. for CEC. These identifications were confirmed by electron microprobe (microprobe analyses - appendix 1) during this study. Several other aluminium phosphates containing Ca and variable silica were analysed but did not correspond to any available analyses in the literature. However these did not appear to be present in any significant quantity.

Apatite is present as small diffusive veinlets in Al_2SiO_5 rocks, but is not widespread and is more common in those with partial corrundum replacement (fig 3.10). It is present as a major constituent in alumino phosphate bearing rocks as veins and large hexagonal plates up to 4.5mm across in the more goyazite rich rock (fig 3.21).

Scorzalite extensively veins and replaces andalusite pervasively imparting an intense blue green colouration to the rock in hand specimen and displaying characteristic polysynthetic twinning in thin section (fig 3.17). Late veins of andalusite (white) up to 8mm wide, sometimes vein the scorzalite - andalusite rock along breakages. These may also contain apatite (fig 3.18, 3.19). Andalusite and scorzalite is often veined and replaced by apatite-goyazite veins which are white - cream in hand specimen. These occur both as breakages and more diffuse replacive channelways (fig 3.20).

Goyazite occurs interstitially within apatite veins and pervasively within apatite altered andalusite rock with or without scorzalite. Goyazite has remarkably similar optical properties to quartz, but has a slightly higher relief.

TOPAZ MUSCOVITE ALTERATION

Topaz muscovite alteration of quartz tectonite

Topaz muscovite alteration and replacement occurs in quartz tectonites and Al_2SiO_5 rocks i.e. it overprints siliceous and aluminous alteration. Within quartz tectonites the alteration is multiphase and may be:

(1) Very fine grained (10μm) nodular crystals of topaz replacing quartz along foliation planes with small amounts of accompanying muscovite (± pyrite) .

(2) Brecciation and intense alteration and discordant veining by fine grained nodular topaz. These are frequently brecciated and

FIG. 3.16 - Kyanite rock with part of a subspherical diaspore nodule. At the margin of the nodule, pyrophyllite alteration of kyanite occurs, and a thin kaolinite vein cuts the nodule. Field of view is 5.4mm (field sample 36D, TS 153).

FIG. 3.17 - Andalusite (An) rock extensively replaced by scorzalite (Sc). A thin apatite vein replaces both. Field of view is 5.4mm (field sample 28I, TS 158).

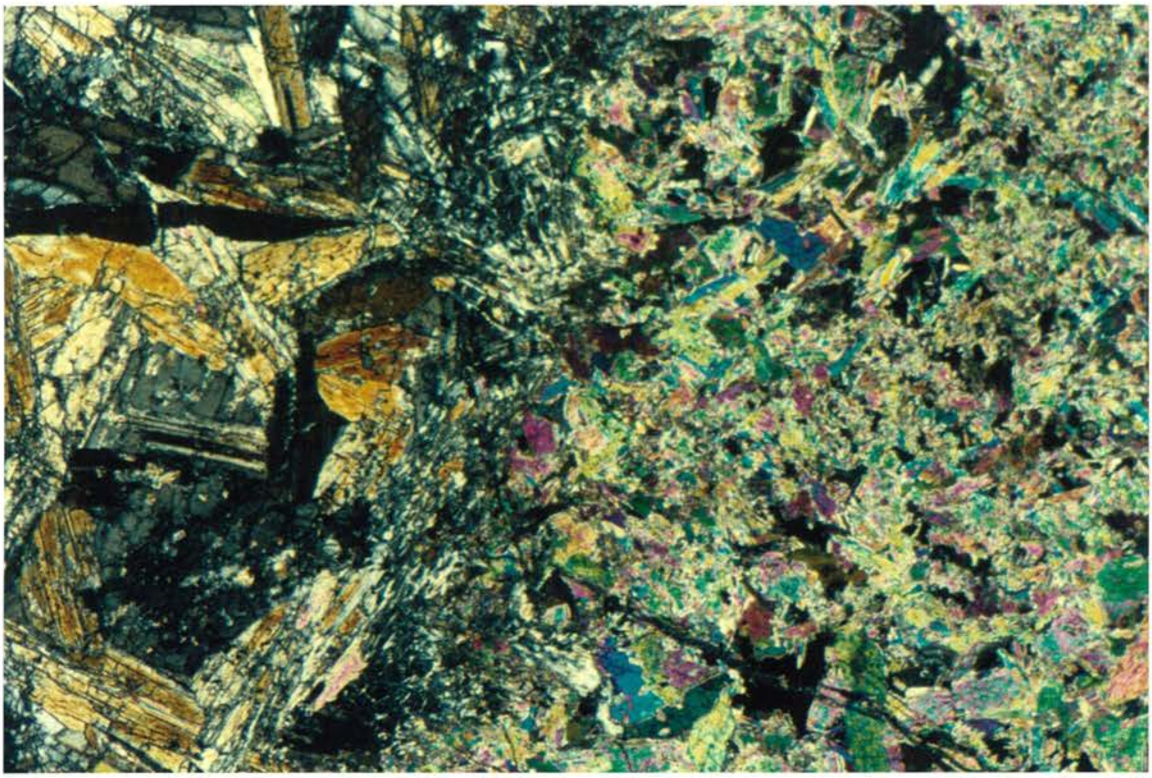

FIG. 3.16

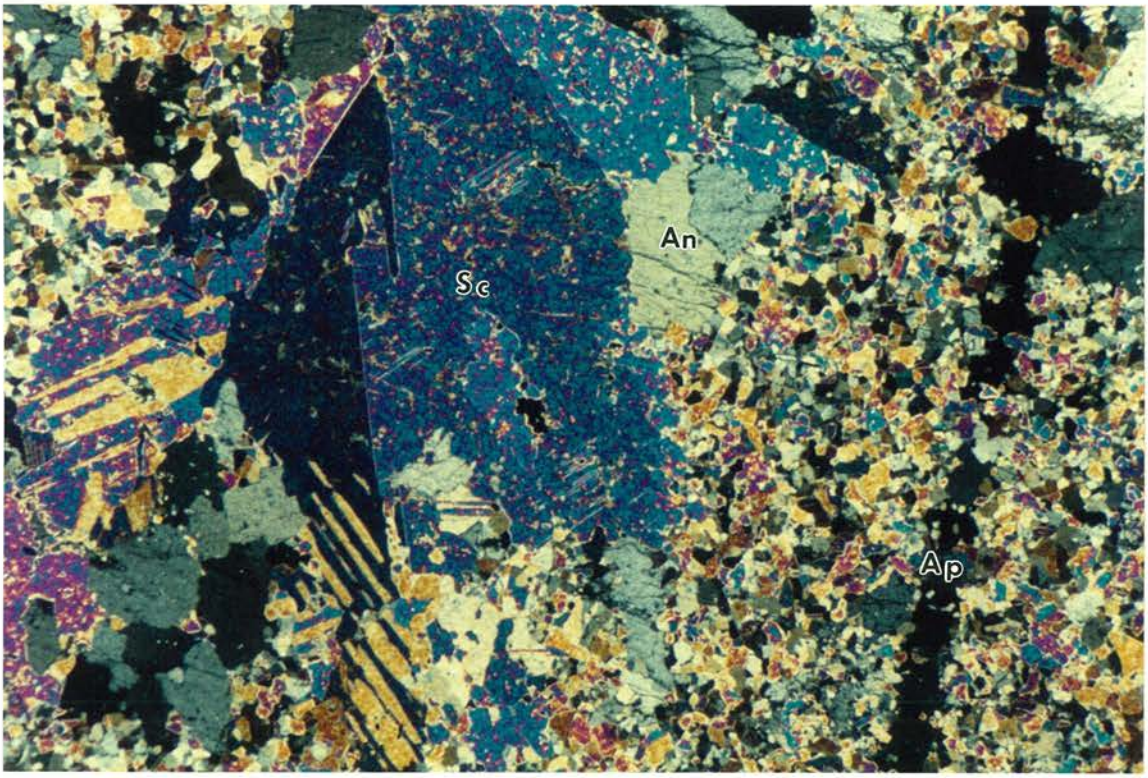

FIG. 3.17

FIG. 3.18 - Scorzalite/lazulite - andalusite rock veined by later andalusite and apatite (pale yellow). The thin white crosscutting veins are kaolinite. Field of view 5.4mm (field sample 28J).

FIG. 3.19 - Scorzalite/lazulite (Sc) - andalusite (An) rock with fracture controlled andalusite vein (shown in figure 3.18). The andalusite vein contains apatite (Ap) in the centre, and has fine grained edges, and extends along a fine fracture in the phosphatic rock shown by the arrow in the bottom right of the frame. Field of view is 5.4mm (field sample 28J, TS 166).

FIG. 3.18

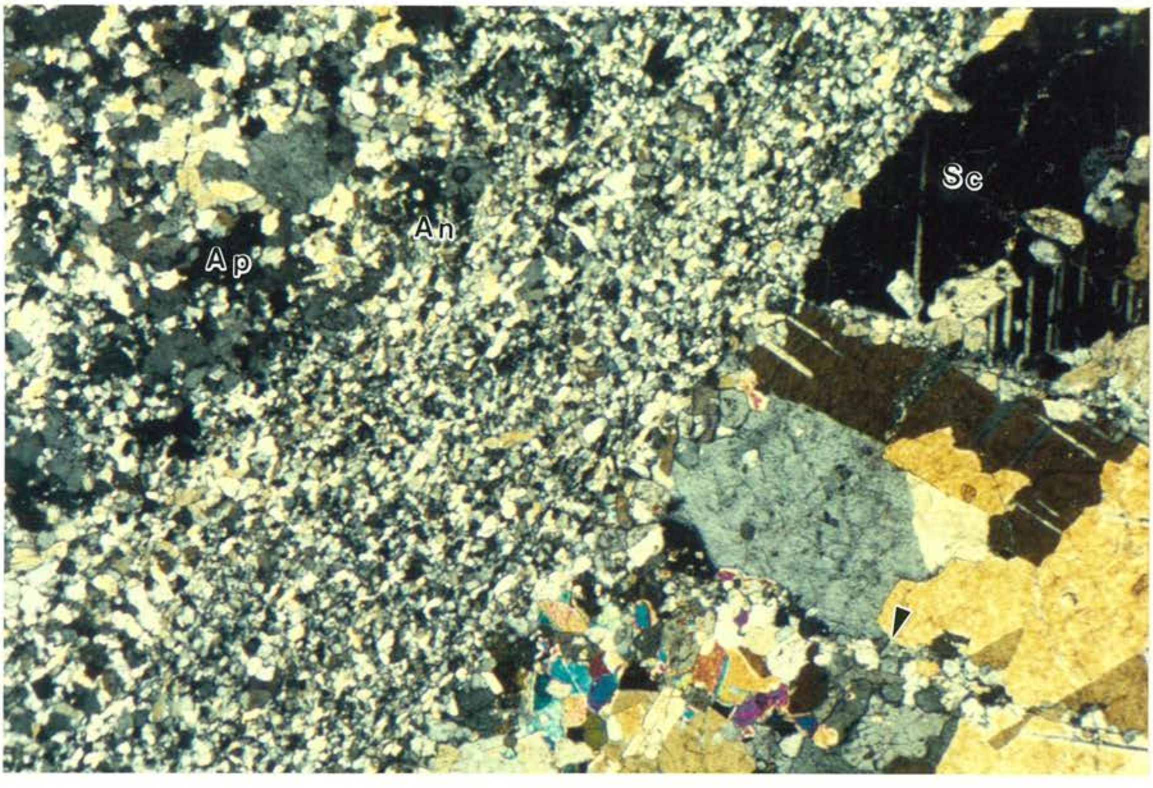

FIG. 3.19

FIG. 3.20 - Andalusite (An) - scorzalite (Sc) rock is replaced extensively by apatite (Ap) and goyazite (Go). Diaspore (Di) replaces scorzalite, but is replaced by apatite and goyazite. Field of view 5.4mm (field sample 28D, TS 147).

FIG. 3.21 - Andalusite (An) rock replaced by diaspore, both of which are replaced by apatite (Ap) and goyazite (Go). Diaspore (Di) has a pyrophyllite alteration rim and clay alteration (KP) extensively replaces andalusite. Field of view is 5.4mm(field sample 28D, TS 148).

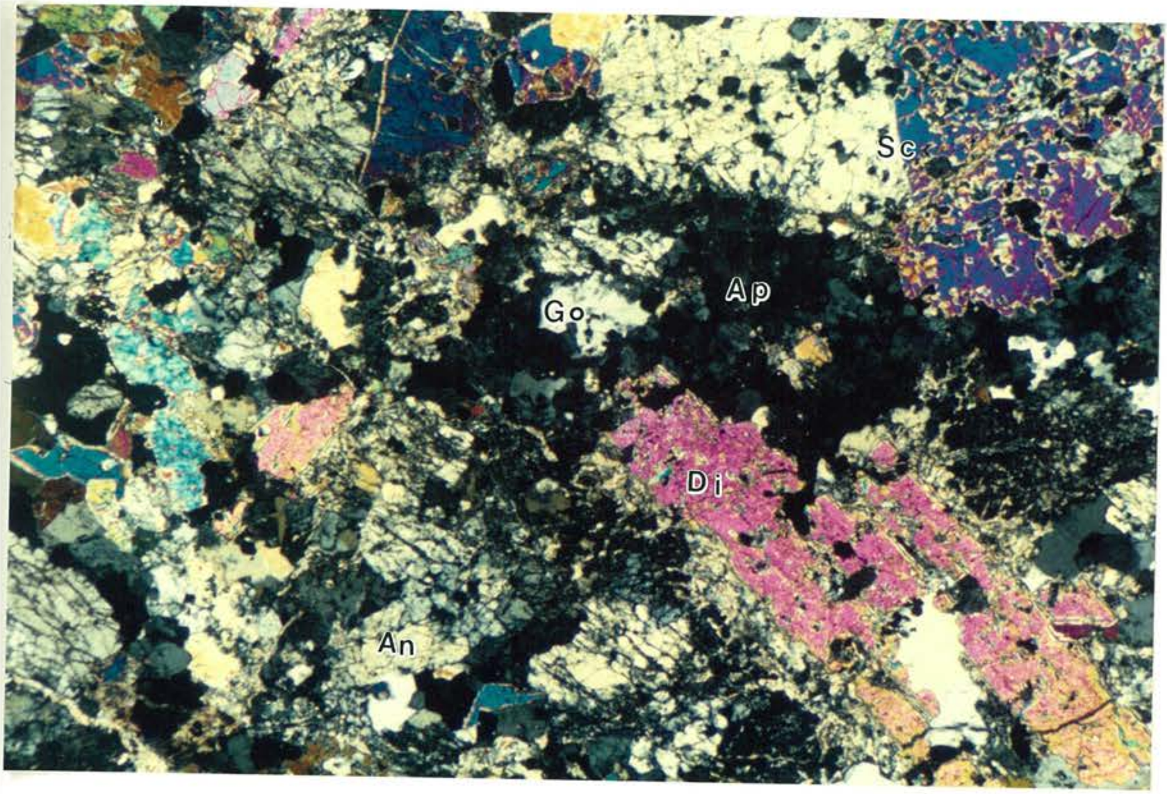

FIG. 3.20

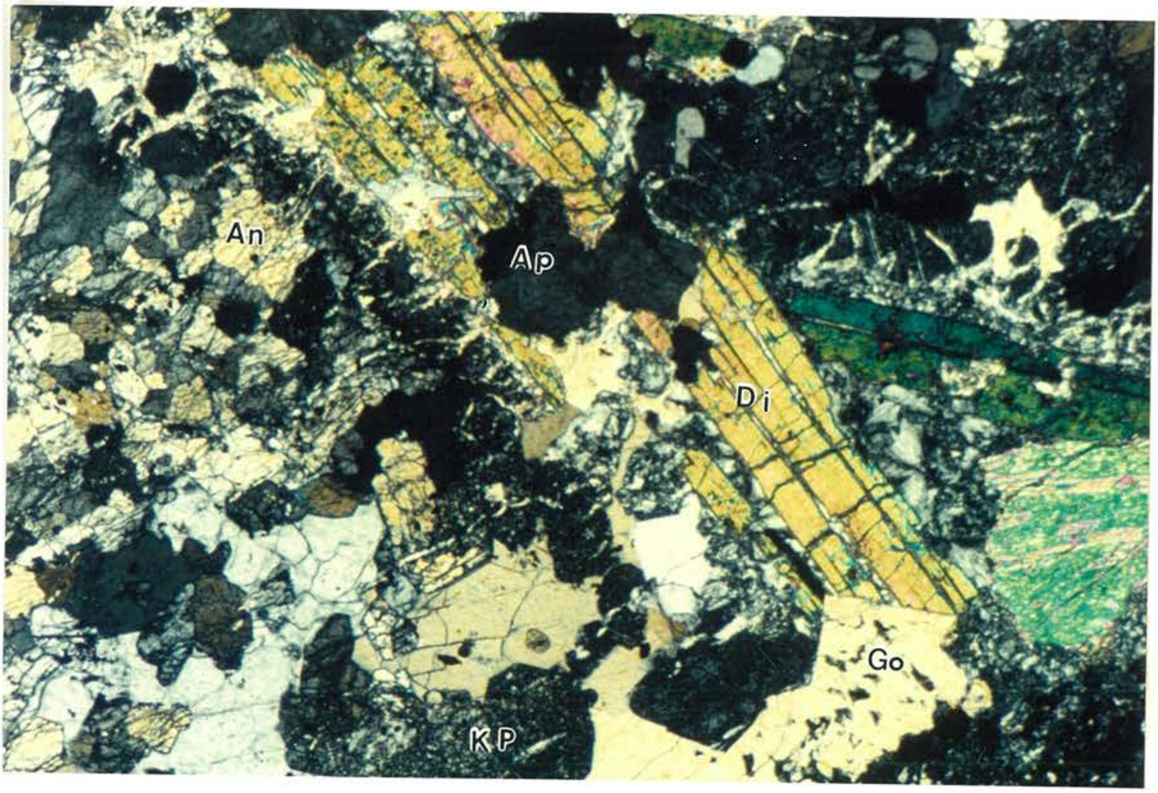

FIG. 3.21

crystals of topaz, and also commonly contain abundant apatite, and less commonly pyrite. These may follow the quartz foliation or be discordant, and commonly vein and brecciate (2) (fig 3.23).

All of the above phases are usually accompanied by small amounts of 5 - 30μm globular rutile grains in clusters.

Topaz appears to form in a similar manner to Al_2SiO_5 on foliation planes in silicified rock. In some cases small andalusites are present and are seen to be replaced by topaz. Euhedral cubes of pyrite may be widely distributed in the same veins. In the strain shadow of the pyrite crystals topaz crystals may grow up to 200μm.

Topaz replacement also occurs as discordant veins and irregular replacment patches. Topaz altered quartz tectonites are frequently brecciated by futher very fine grained topaz veins (fig 3.22, 3.24) These veins may contain angular to subangular fragments of vein quartz and quartz tectonite and topaz altered quartz tectonite. Muscovite topaz apatite (± pyrite) veins may also brecciate and vein these very fine grained topaz breccias (fig 3.23). 100μm apatite veins may be present, apatite also occurs as vug infill in some late topaz veins. These veins consisting of topaz and flourapatite are up to 30mm wide and have replacive margins.

Muscovite topaz veining also occurs of silicous rock. These may follow foliation planes forming a greenish quartz - muscovite-topaz schist (fig 3.34) or are fracture controlled. Typically larger (up to 150μm) euhedral prism and diamond shaped crystals stud a fine grained muscovite matrix.

All these phases of topaz and topaz - muscovite veining are intimately associated in intensley brecciated zones up to 1.5m wide in drillcore. Breccia fragments are generally angular to slightly rounded and vary from 50μm to 4cm. Larger fragments are commonly previously brecciated rock. Fragments of older quartz veins are often present.

Late quartz veins occuring in these topaz altered and brecciated rocks (originally siliceous) may represent local silica remobilization. Late quartz veins do not occur in any other rock type. These veins are characterised by their less deformed nature, crystals are less strained and sutured; and more euhedral crystal growth representing infill. The veins may also contain coarse grained (2 - 3mm cubes) aggregates of pyrite, 100μm euhedral apatite, and vugs containing flourite (fig 3.25). These veins are sometimes dominantly either apatite or quartz at different areas along their length.

Topaz muscovite alteration of aluminous assemblages

Topaz - muscovite alteration also overprints aluminous alteration zones as:

(1) Muscovite - topaz veining, replacement and brecciation of Al_2SiO_5 rock (fig 3.26, 3.14)

(2) Topaz - muscovite alteration of apatite veins in Al phosphate bearing rocks.

Coarse to medium grained muscovite commonly veins corundum and diaspore altered Al_2SiO_5 rock, and Al_2SiO_5 rock (fig 3.14). Small (20-100μm) rounded crystals of topaz often line vein margins and replace Al_2SiO_5 mineral, and diaspore (fig 3.26). It may occur also as sparse 200-800μm euhedral oblong or diamond crystals in a fine grained muscovite matrix (fig 3.27). Al_2SiO_5 is sometimes altered to very fine grained kaolinite /pyrophylite/diaspore psuedomorphs during this process, or is less commonly directly replaced by topaz. The muscovite veins appear also to replace the altered product occasionally and relicts or fragements of altered Al_2SiO_5 minerals. Small amounts of interstitial muscovite is sometimes observed in Al_2SiO_5 rock, and muscovite without topaz also veins Al_2SiO_5 rock.

Topaz occasionally is found as tiny (up to 100μm) oikocysts within apatite and goyazite in in phosphatically altered rocks associated

FIG. 3.22 - Quartz (Q) - topaz (T) breccia, with fragments of quartz vein, quartz tectonite and quartz tectonite with fine grained topaz alteration. The high relief matrix is fine grained topaz. Field of view is 5.4mm (TS 140 from DDH4, 91.7m).

FIG. 3.23 - Quartz - topaz rock with fine grained muscovite and muscovite - apatite veins. The muscovite - apatite vein is is veined by later clay, fine grained topaz and fluorite. field of veiw is 5.4mm (TS 142 from DDH3, 99.0m).

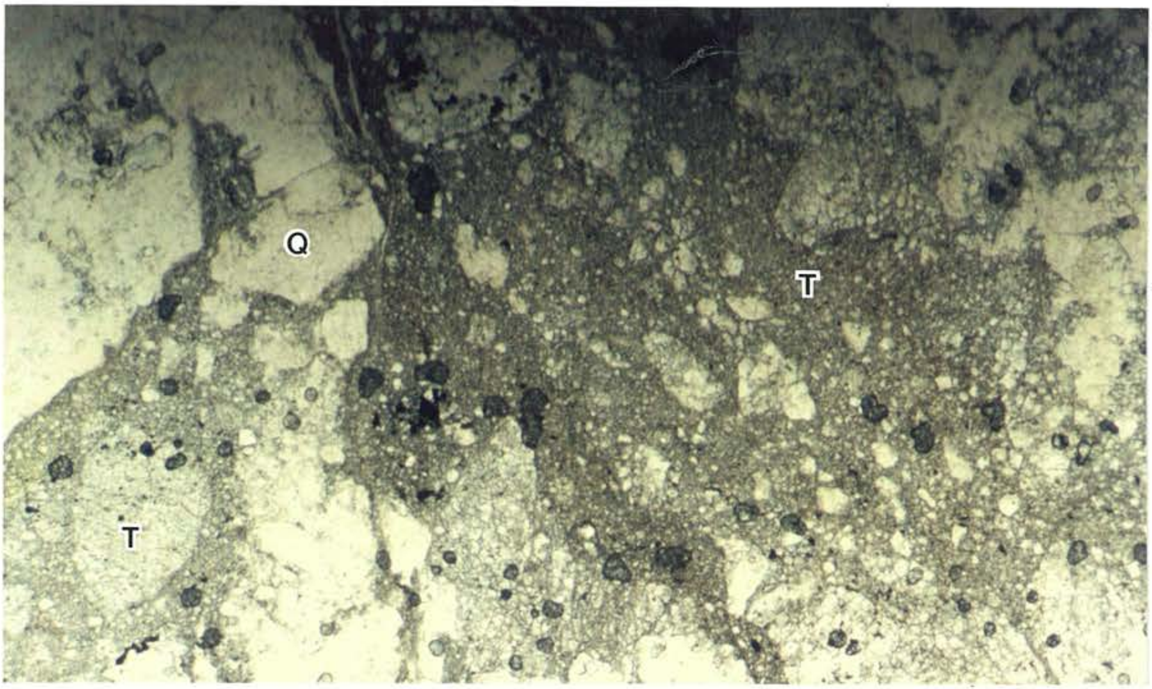

FIG. 3.22

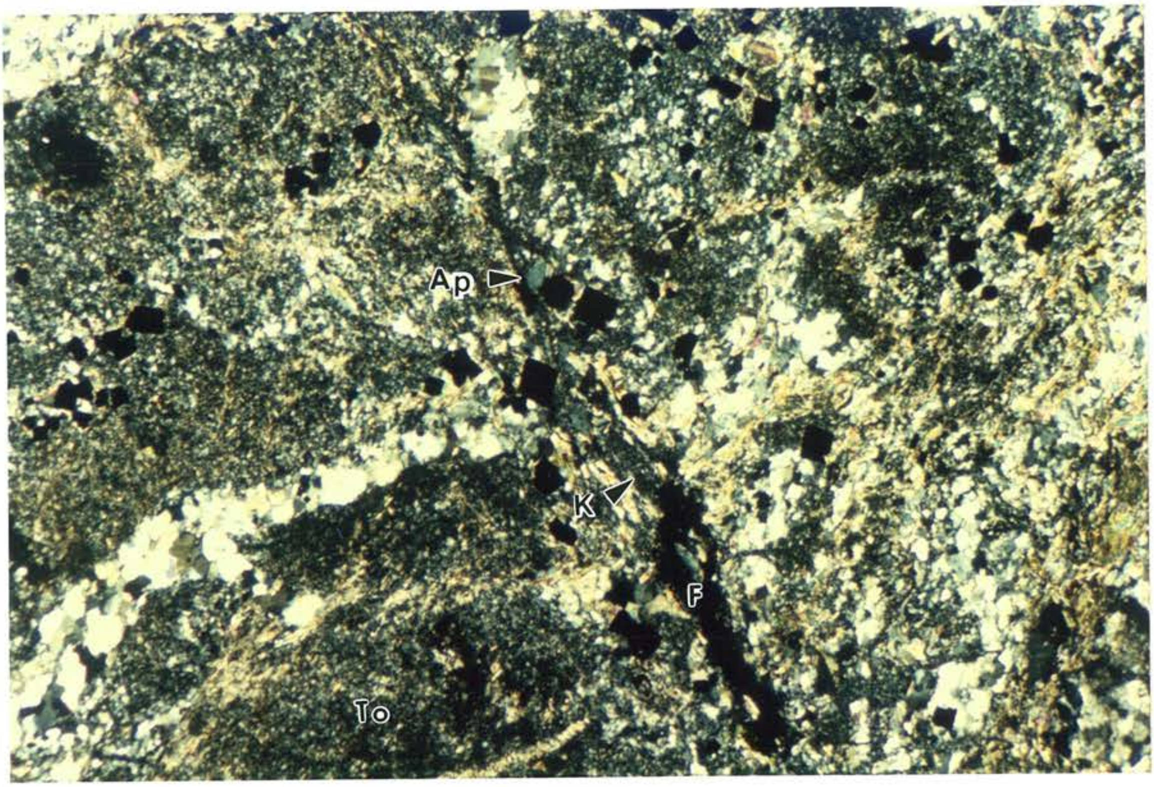

FIG. 3.23

FIG. 3.24 - Quartz topaz breccias. The paler material is very fine grained topaz, and pale green areas are muscovite rich. The sample on the right is cut by later quartz fluorite veins (A selection of drillcore from DDH2).

FIG. 3.25 - Fine grained topaz alteration (To) of quartz tectonite is veined by muscovite (Mu) - topaz - apatite (Ap), quartz-fluorite (F) and clay - fluorite veins with quartz fragments. Field of view is 5.4mm (TS 142 from DDH3, 99.0m).

FIG. 3.24

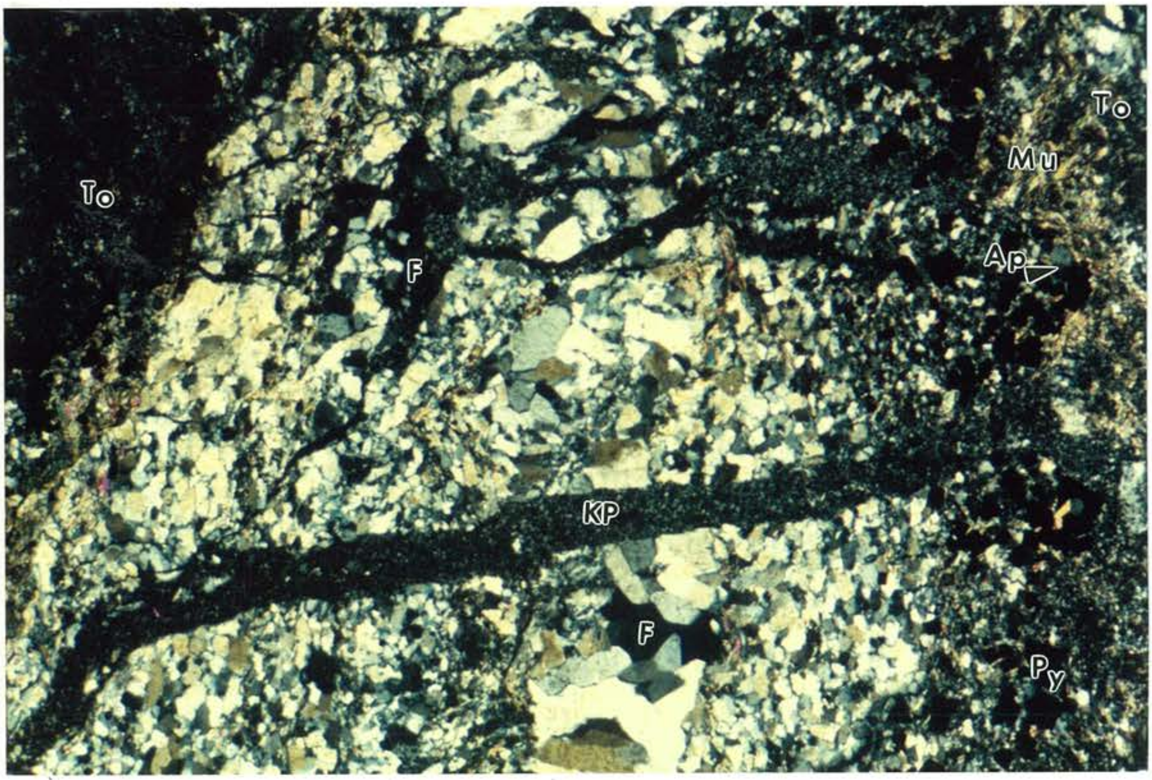

FIG. 3.25

FIG. 3.26 - Kyanite rock is veined and replaced by topaz (To) and muscovite (Mu). Field of view is 5.4mm (field sample 36F, TS 152)

FIG. 3.27 - Kyanite rock is altered to clays and fine grained dispore (Di), and is extensively veined by muscovite with large euhedral topaz crystals, and sometimes partly replaced. Field of view is 5.4mm (field sample 31 II, TS 149).

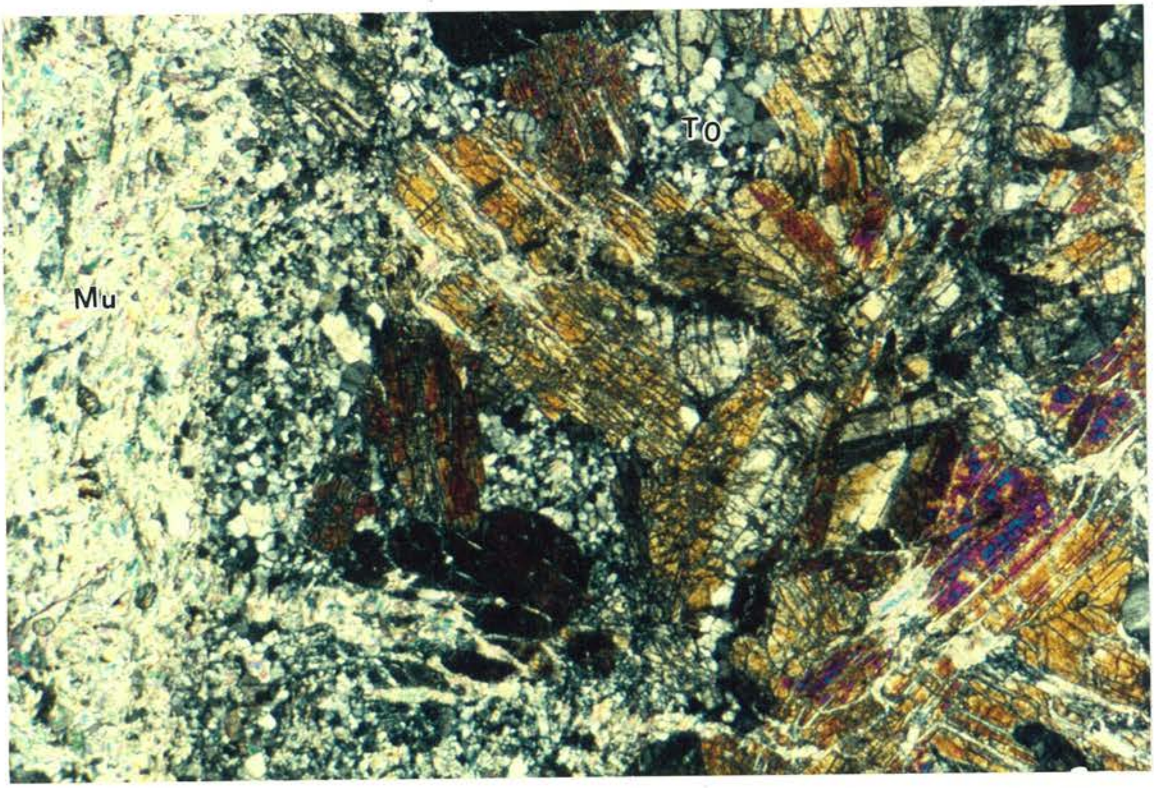

FIG. 3.26

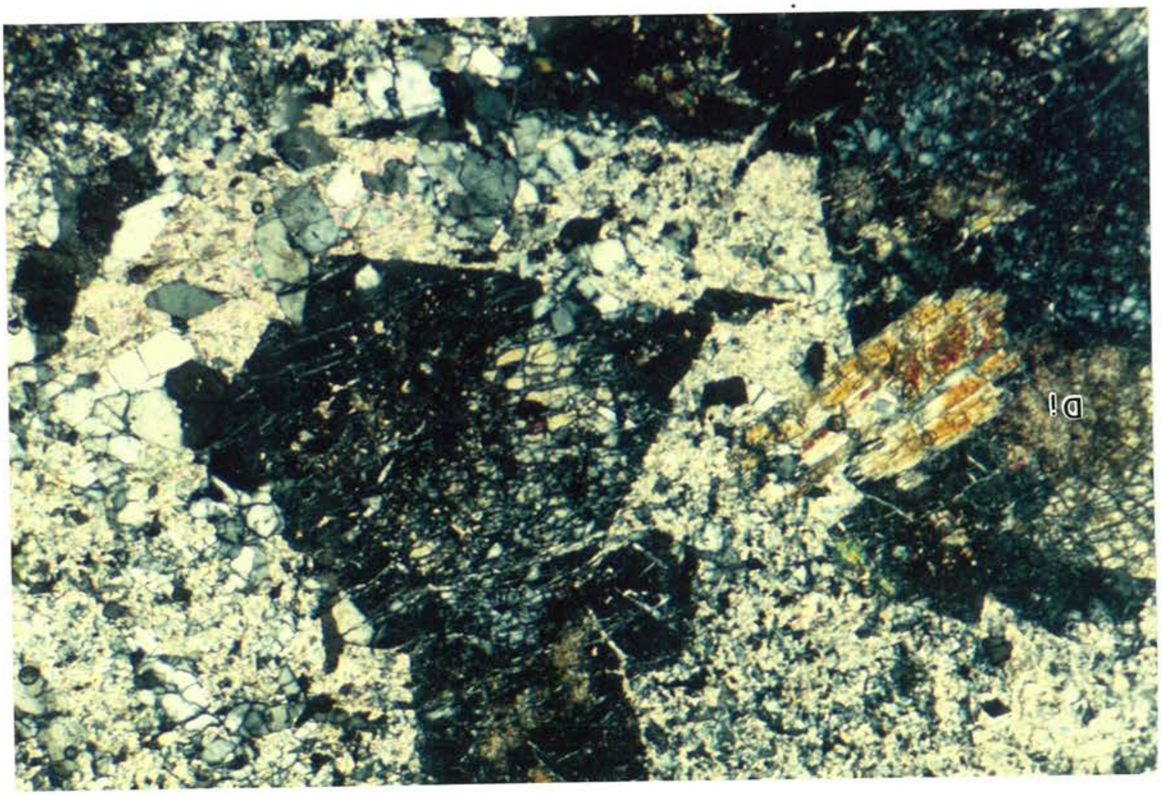

FIG. 3.27

with muscovite and pyrophyllite veins.

Muscovite alteration of host rocks

A peripheral muscovite alteration zone 5-1m wide, of host rocks is seen in the drillcore at both margins of the alteration zone. Muscovite completely replaces albite, chlorite, and biotite through the 1.5m transistion zone from the meta andesite resulting in muscovite - quartz schist. This zone is often highly altered to kaolinite. The possible identification of a topaz within this muscovite suggests that this alteration is associated with topaz-muscovite overprinting of the previous margins rather than an earlier muscovite alteration associated with the silicification.

CLAY ALTERATION

Widespread, pervasive multiphase veining and replacement by pyrophyllite and kaolinite has occured. Al_2SiO_5 rock is often almost compltely replaced. Quartz and other mineral phases such as topaz, muscovite, apatite and goyazite; are less affected by the clays to the same degree. Fracture controlled clay veins up to 1mm wide are ubiquitous throughout the alteration.

Late stage pervasive alteration of prexisting Al_2SiO_5 phases to a very fine grained pyrophyllite kaolinite mixture is extensive. This overprints all other texture. It is usually accompanied by small amounts of fine grained nodular rutile.

Pyrophyllite and kaolinite are extremely difficult to distinguish optically. Electron microprobe investigations suggest that most clay veins are a kaolinite pyrophyllite mixture, but that areas of higher birefringence (first order white) are pyrophyllite rich and vice versa.

Clay alteration of silicous and aluminous rocks

Al_2SiO_5 veins are replaced almost completely by clays, which also vein the quartz discordantly. Al_2SiO_5 rock is highly altered in large areas to a pale grey to grey green translucent rock with pale opaque irregular rounded patches of less altered Al_2SiO_5 mineral (fig 3.28,3.29). Fine grained pyrophyllite along Al_2SiO_5 cleavgae traces outlines the completely psuedomorphed minerals. Relicts of the andalusite or kyanite commonly remain. (fig 3.29). Quartz is veined and altered by pyrophyllite discordantly. It is sometimes replaced more completely than the Al_2SiO_5 (fig 3.7), but is usually only slightly replaced along grain boundaries and is preserved as large relicts with 'cloudy' margins in pervasively altered rocks (fig 3.31, 3.30).

Diaspore large prisms and subspherical aggregates are commonly rimmed and replaced by pyrophyllite. Kaolinite futher surrounds these and forms later small crosscutting veins (fig 3.15, 3.32).

Topaz and muscovite are less affected by the clay alteration and are commonly present as relatively unaltered relicts in highly altered Al_2SiO_5 rock, representing earlier veining of the same (fig 3.32). Muscovite may accompany some stages of clay alteration, but is not found in late stage kaolinite rutile rich veins (fig 3.30). It is often found in clay veins whose sequence is muscovite, pyrophyllite/kaolinite, rutile.

Extremely small (>5μm) crystals of Ca-La-Th-Ce aluminium phosphate mineral were detected by electron microporbe in some clay veins, the paragenesis of which is uncertain. Margins of these crystal appear indistinct under electron backscatter. Other crystals with a similar form were analysed as aluminium - phosphate - silicates, and do not correspond to any available analyses in the literature. They are most similar to viseite, a hydrated mineral of the zeolite group. This identification is supported by the presence of a broad illdefined peak on two clay XRF traces, which is typical of a zeolite (Cuff, Personal comm.) (appendix 2).

FIG. 3.28 - (A) Quartz - Al_2SiO_5 rock pervasively altered and veined by clays (DDH2, 206.5m).
(B) Al_2SiO_5 rock veined and pervasively replaced by clays and some fine grained diaspore and muscovite (field sample 22).

FIG. 3.29 - Outcrop of pervasively clay altered Al_2SiO_5 (- quartz) rock on the main ridge area 50m SWW of DDH4 . The rock is distinguished in the field by its softness.

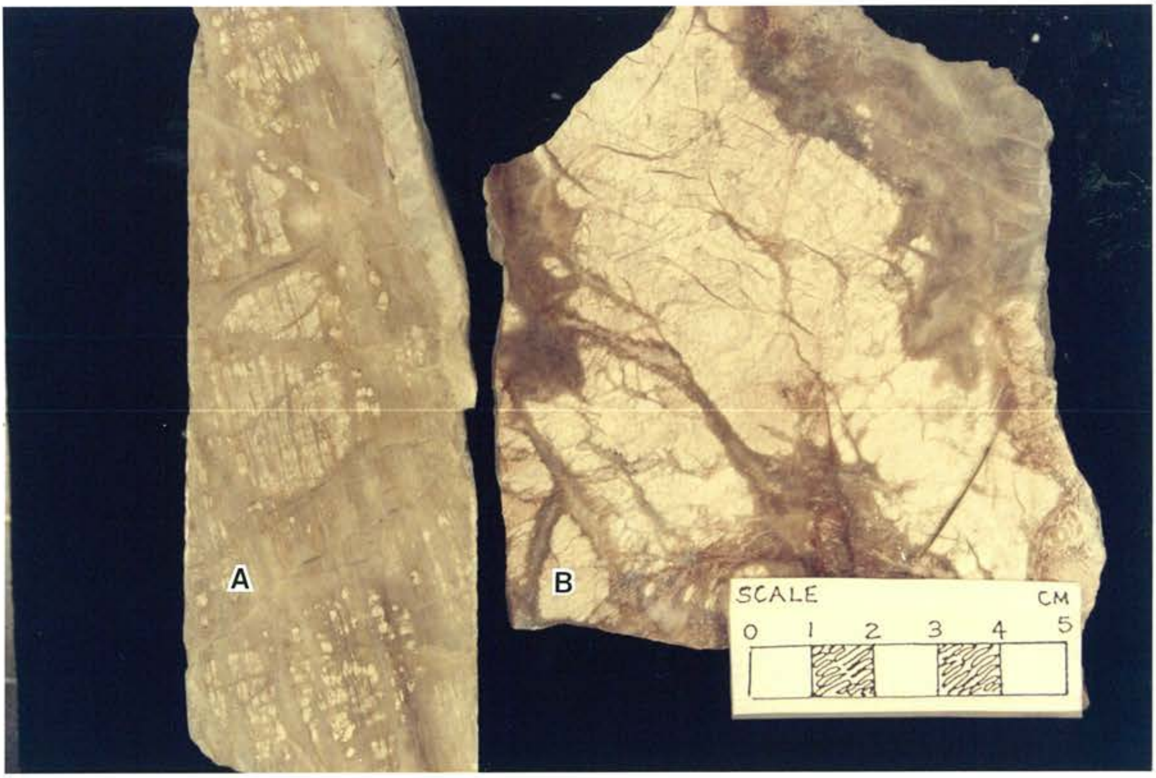

FIG. 3.28

FIG. 3.29

FIG. 3.30 - Highly clay altered quartz and kyanite veins. Kyanite has been veined by muscovite, and almost completely replaced by psuedomorphing clays, with some relict kyanite remaining. Quartz is veined by clays along crystal boundaries and fractures and is partly replaced. Field of view is 5.4mm (TS 134 from DDH4, 46.0m).

FIG. 3.31 - Clay psuedomorphs after andalusite. Andalusite cleavage traces are outlined by pyrophyllite. Veined and partly replaced quartz, irregular groups of rounded topaz grains and rare relict fragments of andalusite are identified in plane light by relief differences. Field of view is 5.4mm (field sample 28A, TS 116).

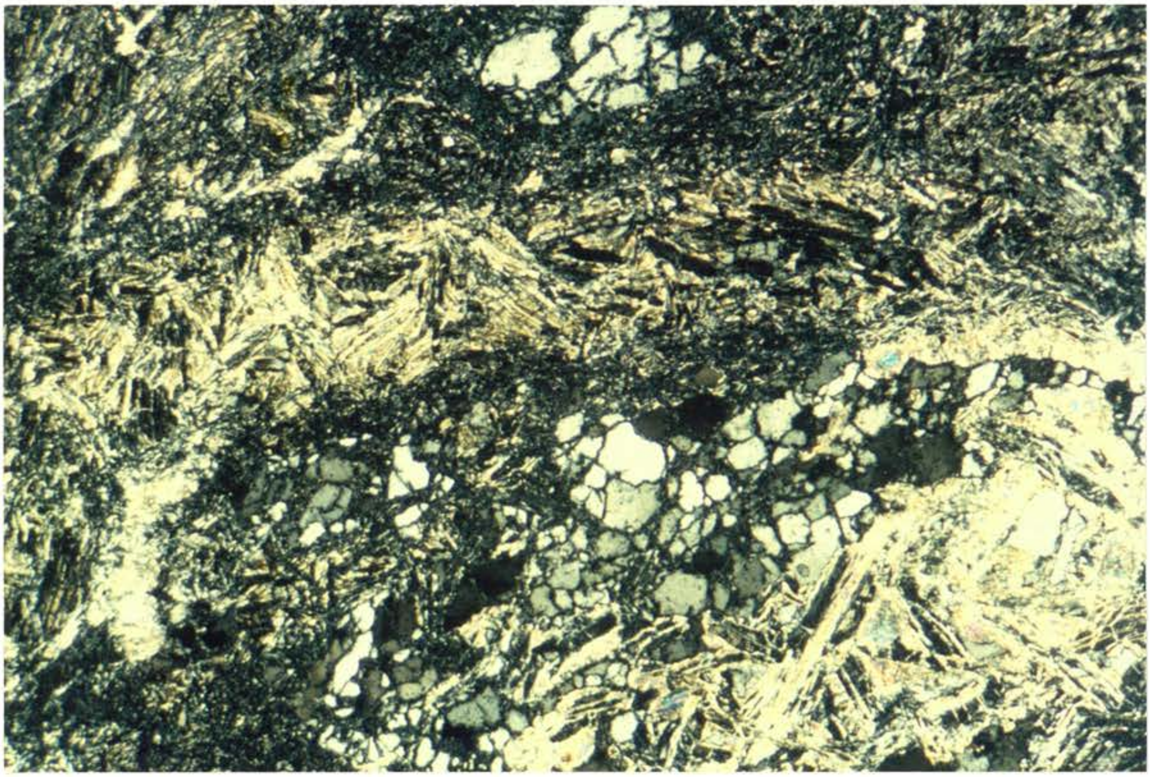

FIG. 3.30

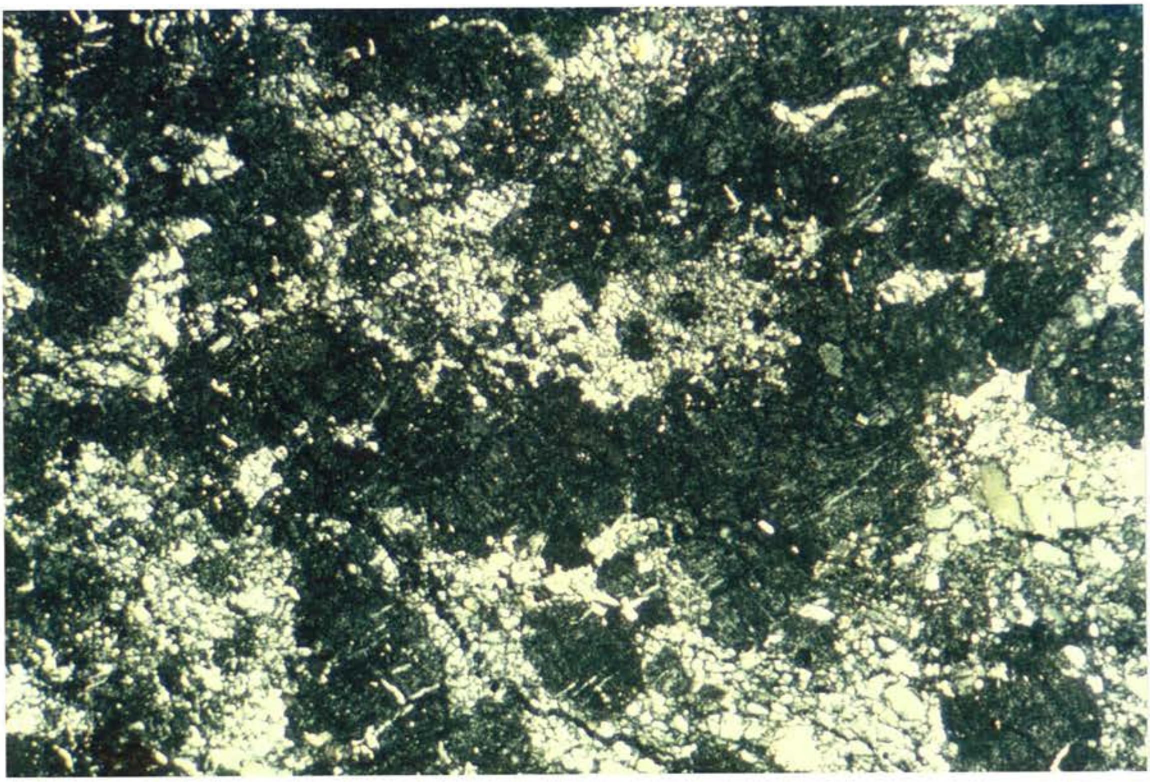

FIG. 3.31

FIG. 3.32 - Diaspore nodule within highly clay altered kyanite rock. Kyanite is partly to completely replaced by clays. Clay veins cut the through the diaspore nodule. Topaz (To) crystals at the bottom right of the frame are relatively unaltered in comparison to kyanite. Field of view is 5.4mm (field sample 21C, TS 162).

FIG. 3.33 - Late quartz veins with fluorite within quartz - topaz breccia rock, are veined and brecciated by multistage clay veins. In the left of the frame a pyrophyllite diaspore vein along a fracture contains angular quartz fragments, fine grained topaz (or topaz-quartz) fragments and muscovite flakes. This is cut by a dominantly pyrophyllite and kaolinite vein that extends across the top of the frame. It contains angular fragments of quartz, quartz - topaz rock and fluorite (± quartz inclusions). Atopaz vein in a quartz fragment is shown by To. Very fine grained rutile (R) is also in the vein. Field of veiw is 5.4mm (TS 142 from DDH3, 99.0m).

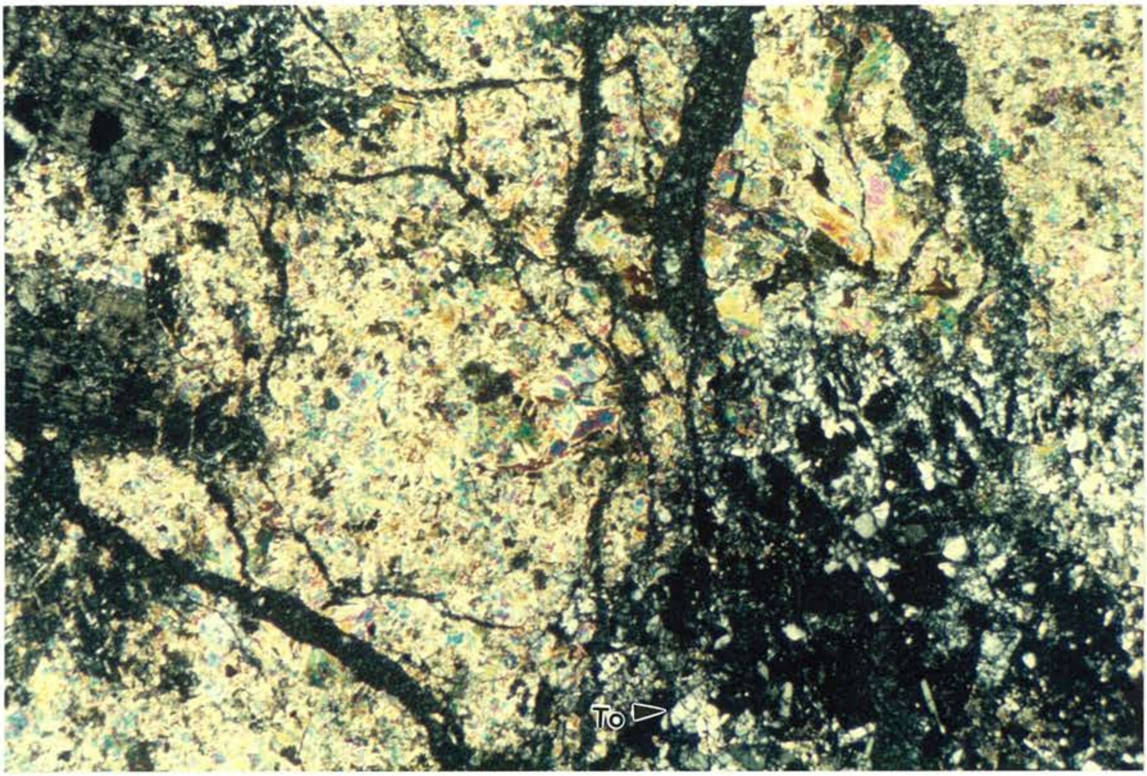

FIG. 3.32

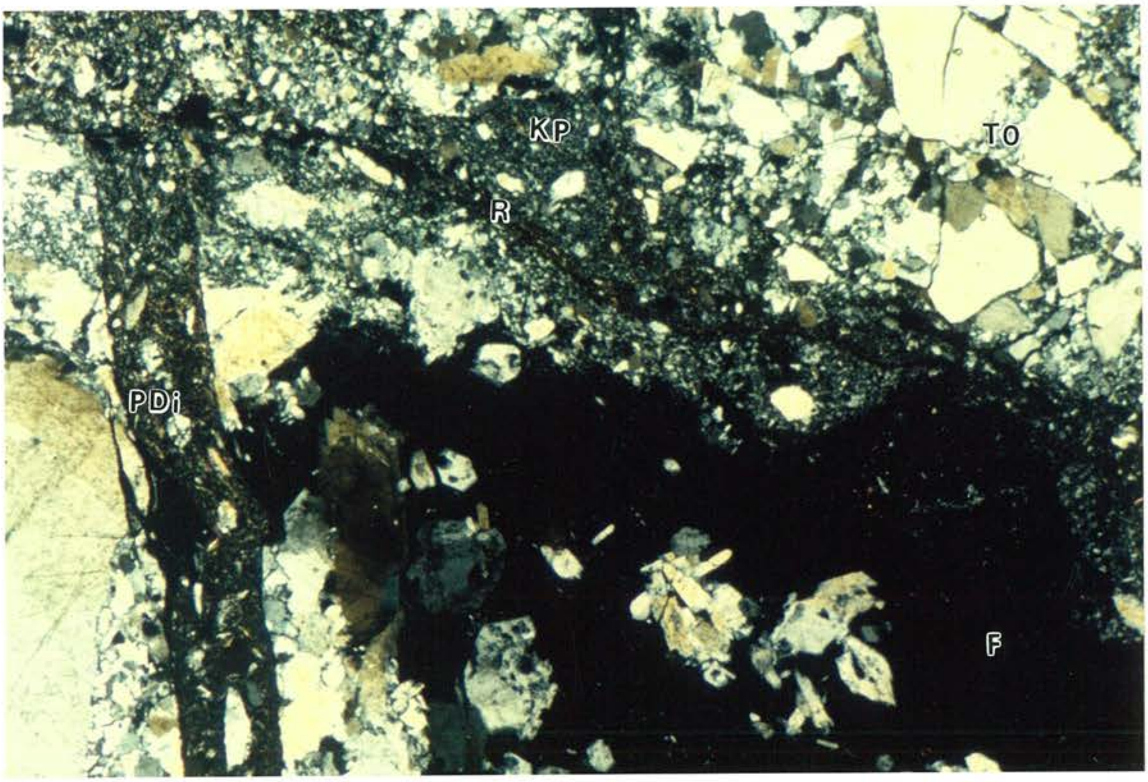

FIG 3.33

Clay alteration of siliceous topaz rocks

Clay alteration is fracture controlled and in places is associated with angular microscopic breccias of the topaz quartz rock and is multiphase (fig 3.33). Purple fluorite is frequently present particularly in the more brecciated quartz rich rocks (fig 3.24). Muscovite is not usually found with later clay veins in these rocks. Pyrophyllite/kaolinite also commonly veins earlier muscovite topaz (apatite, pyrite) veins, and topaz alteration pathways (fig 3.23, 3.25).

Shards of vein quartz and topaz altered quartz tectonite (1.5mm-50μm) are found within some fracture controlled clay veins and fluorite infillings (fig 3.33). Quartz is generally less replaced than in the aluminous rocks by the clay phases, as fragments and vein margins are 'sharper'.

Small amounts of extremely fine grained fibrous or nodular topaz possibly occur with pyrophyllite and fluorite in some early clay veins although identification is not certain. Very fine grained rutile is common as as a centerally placed string within prophyllite/kaolinite veins.

3.4 DISCUSSION OF ALTERATION PARAGENESIS

The overall paragenetic sequence of the alteration includes an early synmylonitic silicification that produced several lenslike bodies of fine grained quartz along the length of the ridge in addition to less intense silicification and quartz veining of the surrounding country rocks.

Aluminous alteration of these rocks resulted in pervasive developement of andalusite/kyanite along foliation planes and fine fractures; and the formation of larger Al_2SiO_5 veins associated with prexisting quartz veins. These veins have developed into elongate pods up to 15m long and 8m wide of medium to coarse grained Al_2SiO_5. These commonly contain diaspore and corundum alteration, and less commonly apatite and aluminium phosphates. Mineral textures indicate that both irregular brecciation with pervasive alteration of breccia fragments and probable subsequent replacement by crosscutting euhedral crystals (such as diaspore) were processes in an area of intense alteration and fluid flow.

The cause of the banded texture (fig 3.14) of the phosphatically altered andalusite rock is unclear. Possibly andalusite crystal growth was affected by residual rutile grains outlining an earlier foliation. The rocks outcrop as a group of large boulders (fig 3.8) about which the banding appears to be broadly concentric. This suggests that the banding is not related to an earlier foliation texture but may have been related to some chemical parameter.

Microtextural evidence indicates that topaz - muscovite alteration overprints aluminous alteration and is derived from futher evolution of a continuing alteration process. Some areas appear however to have only been affected by topaz - muscovite and clay alteration and not aluminous alteration i.e. andalusite and kyanite are not present in significant amounts (e.g. DDH3 - appendix 3). Narrow zones of intensley brecciated very fine grained siliceous topaz rock show a different style of fluid flow than indicated by textures in aluminus alteration, and rechanneling of main areas of fluid flow.

These topaz - quartz rocks are the only rock type to show any later quartz veining, and may represent remobilization within these more silicous rocks. The extent of topaz muscovite overprinting of aluminous rocks is not well known from field mapping as hand specimen identification is extremely difficult and large areas are obscured by later clay alteration.

Clay alteration is also seen as a continuation of the alteration process. Alteration of this sort involving microbrecciation is associated with brecciated siliceous topaz rock, and some clay veins even contain small amounts of very fine grained topaz. Larger scale breccias within aluminous alteration are the product of veining along tension fractures followed by intense pervasive alteration of aluminosilicates to clays.

3.5 RELATIONSHIP TO DEFORMATIONAL HISTORY

Orogenesis of the Balcooma Metavolcanics occured in the late Silurian to early Devonian during regional E-W compression (Van der Hor, 1989). Developement of ductile mylonites was associated with the later stages of this orogenesis during crustal thinning and heating. A mylonitic foliation was developed in the Balcooma Metavolcanics in this area, and the alteration zone parallels this foliation. The silicification and aluminous alteration appears to have taken place in the late and waning stages of the mylonitic deformation event. This is supported by the following observations:

(i) The silicified rock has a prototomylonitic foliation. In some areas tight folding and intensive subparallel crenulations of similar orientation were formed probably as part of the same event. Quartz veins in rocks affected by later alteration are commonly irregularly folded and enclose less deformed veins of Al_2SiO_5 minerals.

(ii) Al_2SiO_5 minerals within the quartz tectonite typically show slight undulose extinction, but are not highly deformed, and veins may crosscut the quartz foliation (fig 3.5). However the foliation can also be seen wrapping around Al_2SiO_5 minerals (fig 3.37). These minerals may also contain inclusions that display relict foliations, which have been destroyed in the matrix during the mylonitic event. Al_2SiO_5 veined quartz tectonites are often recrystalized to an equigranular texture (fig 3.5).

(iii) Al_2SiO_5 rock is typically undeformed and muscovite within this rock is not schistose (fig 3.14 A).

(iv) Muscovite within quartz tectonite rock is highly crenulated in places (fig 3.34). At the margins of the unaltered siliceous body muscovite - topaz veins are largely unfoliated (fig 3.35). Occasionally quartz - topaz - muscovite - apatite rocks are highly sheared (fig 3.36). Orientations of these deformations are unknown as samples are from drillcore.

(v) Clay alteration crosscuts all foliations and does not appear to have been affected by deformations.

In general the post silicification alteration has been deformed to varying degrees in localised areas, but is largely less deformed in comparison to the quartz tectonite. The mylonitic foliation probably developed late during the D5 stage of the orogeny, as defined by Van der Hor (1989). A later weak D6 was also noted by Van der Hor (1989), and muscovite crenulations may have developed during this stage. Late stage clay alteration may have been post tectonic.

Angular haematitic fault breccias occur where fault zones cut the quartz tectonite. There are two sets of brittle faults trending NE and E which displace the ridge. This faulting may have occured much later than the major orogenesis.

The alteration appears to have been late syn to post mylonitic in age, and has been affected by relatively minor later faulting.

FIG. 3.34 - Deformed quartz - muscovite - topaz rock. Several subparallel crenulation sets are well developed in the muscovite without topaz (To) in the bottom right area of the frame. Field of view is 5.4mm (TS 132 from DDH3, 103.6m).

FIG. 3.35 - Unfoliated muscovite - topaz vein in the quartz tectonite. The sample was taken approximately 30cm from the contact of the main quartz body with a highly altered area with all main phases of alteration overprinted. The vein also contains also contains clay psuedomorphs after Al_2SiO_5 minerals (K). Field of view is 5.4mm (field sample 27A, TS 167).

FIG. 3.34

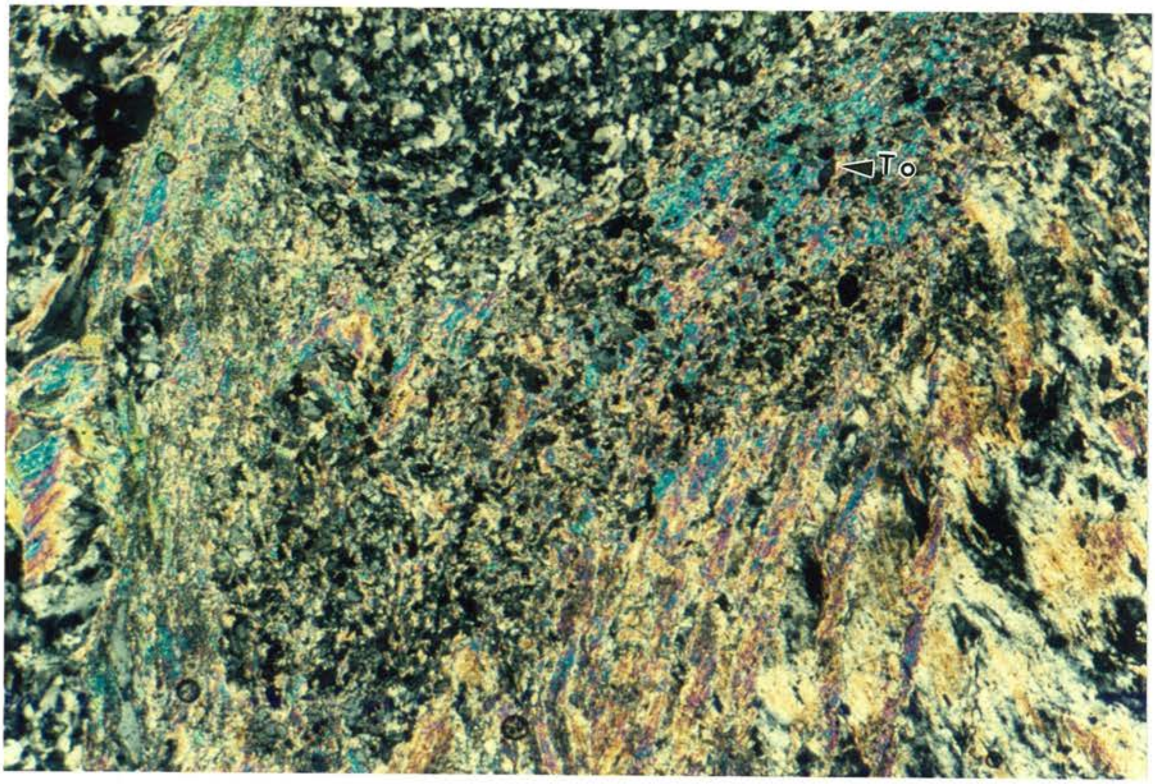

FIG. 3.35

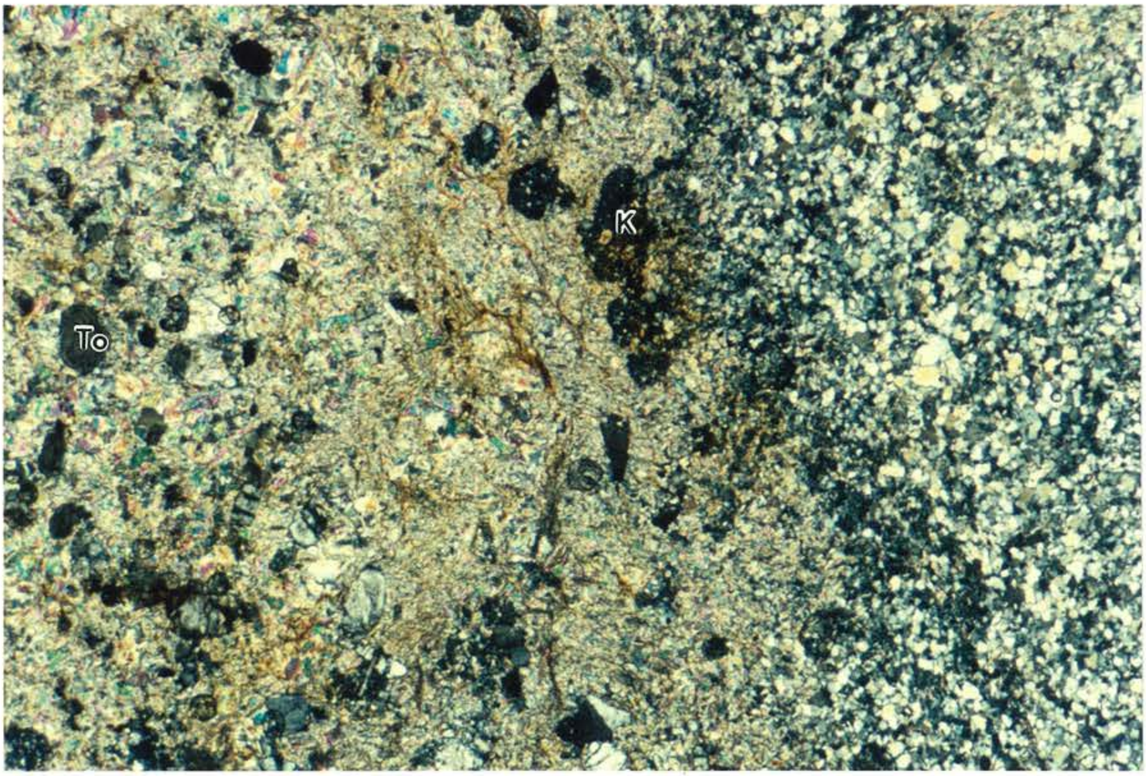

FIG. 3.36 - Highly sheared quartz - topaz rock. Deformation partitions around patches of fine grained topaz alteration (To) in a matrix of fine grained quartz and muscovite. A deformed muscovite-apatite (Ap) - topaz vein is in the bottom right of the frame. Field of view is 5.4mm (TS 127 from DDH3, 124.3m).

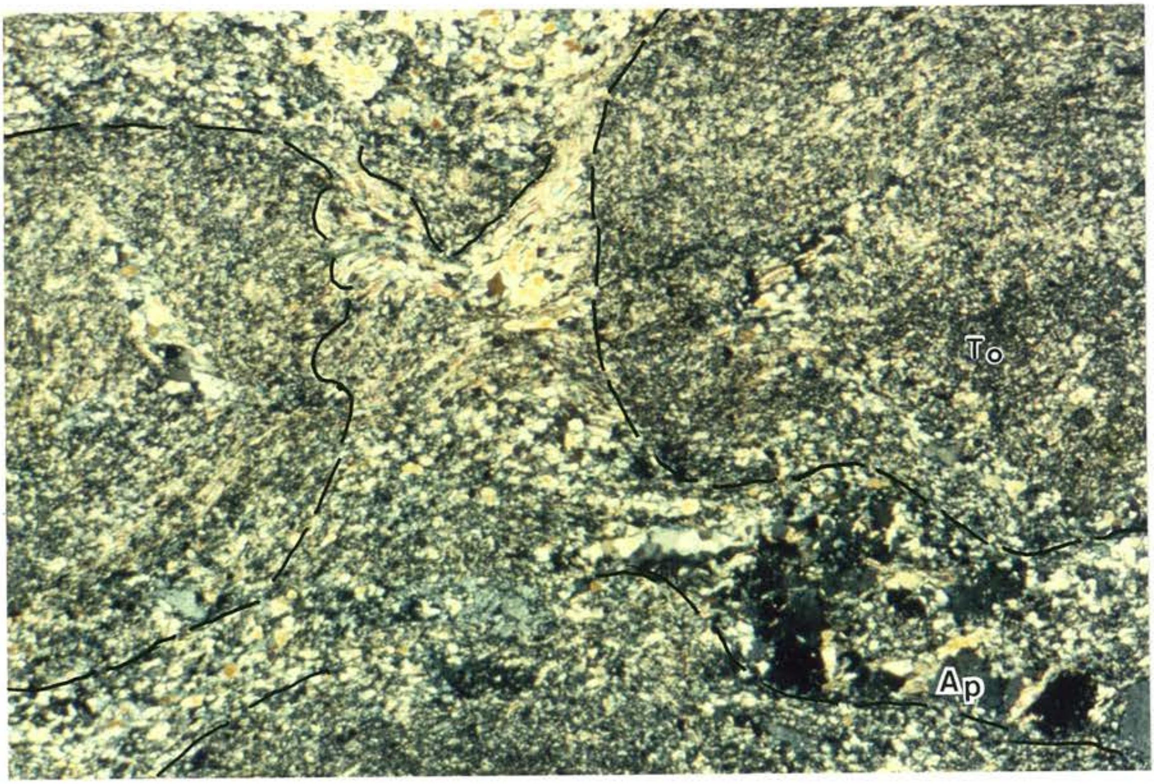

FIG. 3.36

FIG. 3.37 - Foliation wraps around a fractured andalusite (An) in the quartz tectonite. The andalusite is partly replaced by clay (PK), and muscovite (Mu) may have initially filled the fracture void. Field of view is 3mm (field sample 32, TS 161).

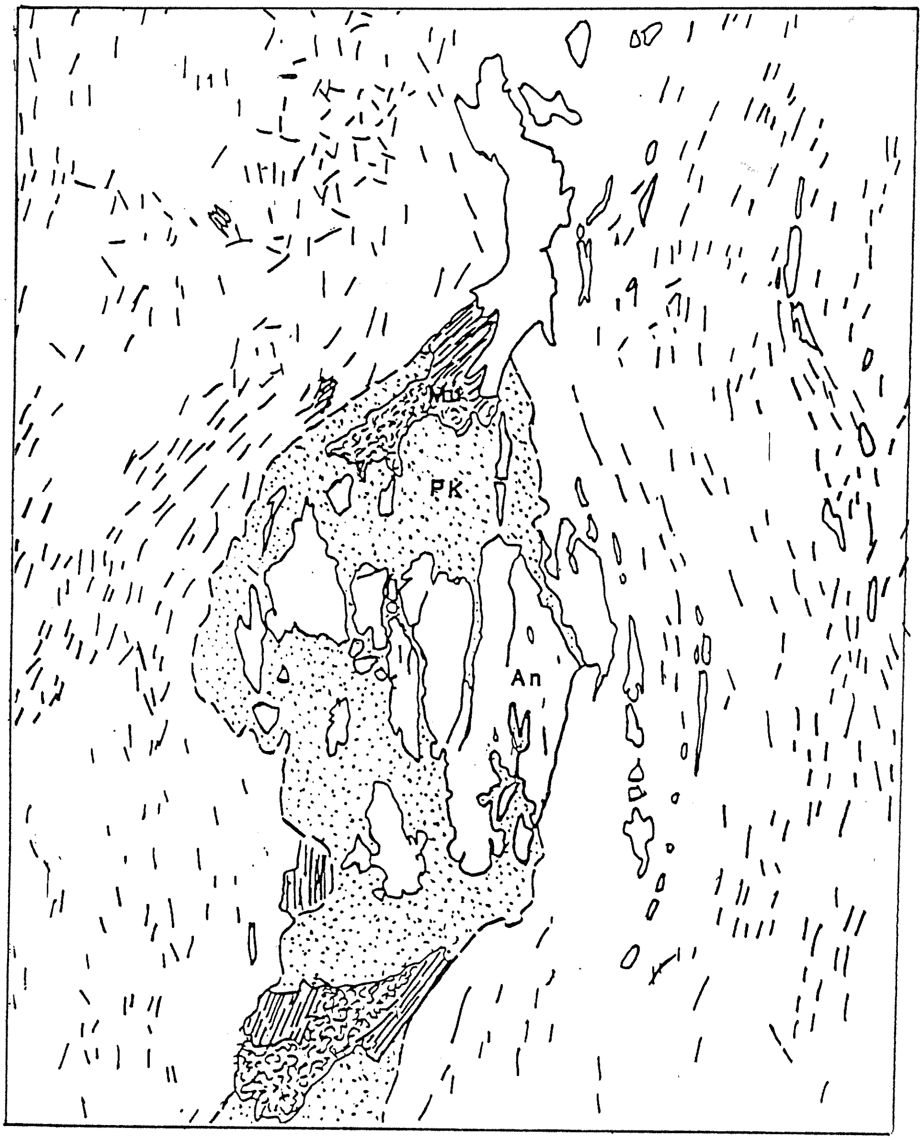

FIG. 3.37

CHAPTER 4 - GEOCHEMISTRY

4.1 INTRODUCTION

Geochemical analyses of the alteration zone show general trends in major element variations being extremely low cation values and a high percentage of Al_2O_3, and anomalous levels of some minor elements such as fluorine and strontium. This is consistant with observed mineralogy. In interpreting bulk analyses, values are normally considered as a ratio with an immobile standard, so that actual volume loss or gain during alteration does not cause an apparent depletion in a component due to dilution. No standard reference frame appears to be suitable as textures of titanium and other 'immobile' elements suggest they are mobile. Thus although anomalously low values of any component most probably indicates depletion, this is actually based on the assumption of constant volume which may or may not be the case.

Bulk XRF analyses of 12 samples of 20m intervals of split drill core selected by CEC were carried out by Australian Assay Laboratories in Perth. The samples were analysed for SiO2, Al2O3, K_2O, Na_2O, CaO, Fe_2O_3, MgO, P_2O_5, TiO_2, F, Sr, Ba and Cl. (Table 4- the results for Cl are not included as all were below the level of detection. Cl is not found as a constituent of significance in many rock forming minerals and is highly volatile, and thus would be unlikely to remain even if the rocks had been altered by chloride rich fluids. Apatite can be Cl bearing, but microprobe analyses did not indicate that it is in this case.) Variations in alteration lithology over the length of the samples and overprinting of alteration phases precludes a detailed interpretation of XRF results with individual mineral assemblages.

Results are grouped according to dominant alteration mineralogy and include a sample of dominantly country rock at the margin of the alteration envelope.

Systematic sampling of the drillcore by CEC consisted of assays for Au, Cu, Pb, Zn, Ag, As and Bi (by Australian Assay Laboratories in Townsville) over 2m intervals for the length of each hole (appendix 3).

4.2 MAJOR ELEMENT RESPONSES

Comparison of SiO_2, Al_2O_3, K_2O, CaO, Na_2O, Fe_2O_3, MgO, P_2O_5 and TiO_2 can be made with the country rock interval (75666) and whole rock analyses of other Balcooma Metavolcanics by Withnall (1988) (appendix 4). The country rock interval from the foot wall of DDH2is dominantly comprised of a meta andesite with altered phenocrysts of albite in a quartz - chlorite (biotite) schistose groundmass with sericite and epidote and acessory apatite, pyrite, ilmenite and sphene. A metasedimentary quartz - biotite schist is at the base of the interval.

The interval is veined by quartz and calcite associated with sericitic alteration, and appears depleted in Ca, Na, Mg and enriched in silica for an andesite (Cox et al., 1979). This is probably because of the presence of the quartz - biotite rock in the interval. The extent of bulk chemical changes related to the earlier sericitic alteration is unknown.

Cation depletion

The alteration zone has low levels in all major cations except aluminium, relative to the Balcooma Metavolcanics and would appear to have undergone substantial cation depletion. Areas with substantial muscovite alteration are less depleted in K_2O (as expected). Highly altered clay zones have extremely low levels with K_2O, Na_2O, CaO, Fe_2O_3 and MgO all <1%. Intervals containing massive Al_2O_3 corundum and diaspore bearing rock is slightly higher in all of these, and is likely associated with a mineralogically similar zone at the surface where scorzalite (Mg phosphate) is found.

Fe_2O_3 (total Fe is as Fe_2O_3) content is up to 4% in quartz rich topaz muscovite altered rocks. These often contain appreciable pyrite associted with topaz and muscovite and within late quartz veins.

Phospate

P_2O_5 has a fairly uniformly low value from around 0.3 to 0.1%, but is slightly higher in sample 75669, a highly aluminous zone extensively overprinted by topaz/muscovite and clay alteration, at 0.9%. Apatite is fairly common in some topaz - quartz - muscovite veins and breccias common in this interval (a higher CaO value for this interval is consistant with apatite as the main phosphate bearing phase). Aluminium phosphates were not observed in any of the thin section samples from the drill core and may or may not be present. P_2O_5 distribution is reasonably consistant with the low solubility of H_3PO_4.

Titanium

TiO_2 content is remarkably consistant throughout the alteration zone at about 0.5%. The country rock has a reasonably high TiO_2 content for a andesitic rock, with Ti bearing accessory minerals such as ilmenite and sphene, at 1.26%. The ubiqutous presence of small amounts of rutile throughout the alteration reflects the known insolubility of Ti^{++} and instability of other usual Ti bearing minerals within the alteration enviroment.

Aluminium

An Al_2O_3 content of about 30% is found in intervals with a large proportion of Al_2SiO_5 rock, reflecting a mineralogy composed almost entirely of aluminosilicates and quartz. Overall this would not represent a large substantial net increase if the original rock was a quartz mica schist. However overprinting of the margins of the alteration obscures the relationship of the earlier silicic and aluminous alteration to the host rocks. There is however no evidence to suggest that a quartz mica rock was a precursor. Metavolcanics of dacitic to andesitic composition are the dominant host and would be expected to have a maximum Al2O3 content of around 17% (Withnall, 1988; Cox et al., 1979).

Al_2SiO_5 veins up to 8m across would require significant concentration and mobility of aluminium even if the precursor was highly aluminous. Transport of aluminium is thought to occur even in chloride bearing fluids (aqueous Al decreases with increasing chloride contents (Anderson et al., 1988)) under metamorphic conditions as alkali silica complexes (Woodland and Walther, 1987). Aluminium is known to form readily soluble hydrated fluoro complexes in HF aqueous solutions (Cotton and Wilkinson, 1972).

4.3 MINOR ELEMENT VARIATIONS

Gold and base metals

Drillcore analyses show a general trend of for depletion of Cu, Pb and Zn in comparison to the host rocks. All three are consistently below 25ppm within the alteration zone, with the exception of slightly higher levels of Cu (and Zn) found in the peripheral muscovite alteration zones. Host rocks have consistently higher background levels for these elements.

Slightly anomalous gold levels (> 0.05ppm) are not uncommon in the host rocks and are associated with shear zones and quartz veins, and anomalous base metal values and rarely As. Soil anomalies of Au and As (fig 3.0) are probably derived from these host rock sources, and auriferous veins are known from the Balcooma Metavolcanics a few kilometres to the south. Muscovite alteration in the foot wall area of DDH2 is also associated with slightly anomalous Au and Cu.

Fluorine and strontium

Bulk XRF analyses show anomalous values of both F and Sr, particularly associated with topaz muscovite alteration. Sr is quite variable and is actually at notably low values in some zones. Al_2SiO_5 rocks with the Sr bearing aluminium phosphates goyazite and svanbergite would also be expected to be Sr anomalous. These minerals seem to have similar timing to the late phases of topaz muscovite alteration. Sr and REE bearing aluminium phosphate mineral (probably florencite) may be associated with clay veining.

Although quantitative analyses of fluorine bearing minerals was not available, the level of anomalous flourine over the 20m interval indicates that the F/OH ratio must be high. Ba content is quite low generally. The nature of sampling means real levels of enrichment on a smaller lithologically based scale are not discernable.

TABLE 4.1 – BULK XRF ANALYSES

Sample no. and location	Rock	SiO_2%	Al_2O_3%	K_2O%	Na_2O (ppm)	CaO%	Fe_2O_3%	MgO%	P_2O_5%	TiO_2%	Sr (ppm)	F (ppm)	Ba (ppm)
75666 (DDH2 280-300m)	Propyllitic albite - quartz - chlorite schist, and quartz - biotite schist.	73.0	15.7	2.35	2062	0.34	3.22	0.48	0.284	1.26	410	560	97
75662 (DDH2 168-188.3m)	Muscovite - kaolinite - quartz rock, and 30% quartz - Al_2SiO_5 rock.	74.0	13.9	1.89	2656	0.07	3.02	0.09	0.078	0.47	147	370	183
75663 (DDH2 188.3- 208m)	Quartz - Al_2SiO_5 rock (variably clay altered).	76.3	18.3	0.35	930	0.02	0.84	<0.01	0.071	0.47	170	320	37
75670 (DDH4 44-66m)	Quartz - Al_2SiO_5 rock (variably clay altered).	75.1	17.0	0.92	1308	0.12	1.61	0.01	0.100	0.46	110	480	66
75671 (DDH4 66-86m)	Quartz - Al_2SiO_5 rock (plus kyanite veins 3-4cm) variably pyritic and altered to clays.	76.4	17.0	0.64	1000	0.05	1.36	<0.01	0.108	0.48	89	640	63
75664 (DDH2 208-228m)	Quartz - Al_2SiO_5 rock (variably clay altered) with numerous Al_2SiO_5 veins up to 10cm.	68.9	22.0	0.99	1469	0.02	0.49	0.04	0.096	0.46	304	560	59
75673 (DDH4 106-126m)	Massive Al_2SiO_5 rock with diaspore and corundum veined by clays.	55.8	28.5	2.05	2550	0.85	2.00	0.75	0.181	0.58	344	600	337
75667 (DDH3 42-62m)	Quartz - muscovite - topaz - Al_2SiO_5 rock (variably clay altered).	73.9	17.1	1.02	1432	0.04	4.03	0.01	0.112	0.49	168	320	93
75668 (DDH3 62-82m)	Quartz - muscovite - topaz rock (with quartz - topaz - (fluorite - pyrite) veins and breccia) (variably clay altered).	71.4	17.8	1.44	1698	0.03	4.23	0.20	0.094	0.51	310	400	120
75669 (DDH3 106-126m)	Massive Al_SiO_5 rock and quartz - muscovite - topaz - $Al_{2S}iO_5$ rock and quartz - topaz - fluorapatite - (fluorite - pyrite) breccias (with variable clay alteration).	65.4	23.4	2.27	1901	0.67	1.97	0.10	0.911	0.53	2812	2200	564
75672 (DDH4 86-106m)	Al_2SiO_5 - (quartz) - topaz - muscovite rock, extensively altered to clays.	55.9	32.4	0.29	1267	0.06	0.90	0.04	0.137	0.47	386	950	35
76665 (DDH2 228-248m)	Al_2SiO_5 - quartz - topaz - muscovite rock, extensively altered to clays.	70.3	26.8	0.67	1321	0.10	0.71	0.18	0.098	0.61	159	1300	47

CHAPTER 5 - MINERAL REACTIONS AND STABILITY FIELDS

5.1 INTRODUCTION

Stabilities of minerals, defined in terms of the variables temperature, pressure, bulk chemical composition of solid phases and solution composition, provide a framework which can be used to interpret alteration enviroments. The different alteration assemblages at Quartzite Ridge are compositionally restricted, comprising dominantly quartz, aluminosilicates, hydrated aluminosilicates and muscovite. Most reactions within the alteration assemblage can be described within (or part thereof) the system (HK_{-1})-Al_2O_3-SiO_2-H_2O-(F_2O_{-1}). Major reaction processes that can be postulated to have taken place are :

(1) Hydrolysis reactions are decomposition reactions in which either H^+ or OH- ion is selectively consumed thereby changing the ratio of these ions in the solution. These will generally be base leaching reactions with silicate minerals in which the reacting phases are depleted in cations (such as K^+, Ca^{++}, Mg^{++}, Na^+) by exchange with H^+ from acidic fluids.

(2) Hydration reactions are a chemical combination of H_2O with another substance without selective consumption of H^+ or OH-, and without the release of another ion to solution.

(3) Silicification /desilicification reactions in which aqueous silica H_4SiO_4 is added to, or depleted from the reactant phase (aluminium oxide, hydroxide or silicate) and is thus conversely effected in the fluid.

(4) Hydrofluorination reactions are those of HF from acidic solutions with silicate minerals involving the exchange of one or two HF per H_2O, for O or OH.

The physio-chemical conditions during the developement of the alteration assemblage, can be determined from the experimental data for reactions interpreted to have occurred in the course of its formation. This is most easily done by the application of mineral stability diagrams from the literature.

5.2 HYDROLYTIC ALTERATION

Direct evidence for extensive hydrolytic alteration has been obliterated by the overprinting halo topaz/muscovite and clay alterations. However for such a large scale change in bulk chemistry to have occurred, in which virtually all cations excepting aluminium have been massively depleted, hydrolytic processes must have been operating. The F bearing nature of the fluids (indicated by the occurance of topaz and fluorite) means that they were of an acidic nature with a tendency towards producing peraluminous alteration and alkali or base leaching (fig 5.1) (Burt, 1981).

The peripheral muscovite alteration of the country rocks, is overprinted by kaolinite and is probably representitive of this alteration process. Quartz - albite - chlorite - epidote schist shows a fairly sudden transition to a quartz - muscovite - (pyrite) schist.

Stability fields of minerals as a function of temperature and cation ratio with H^+ in a coexisting aqueous phase at 500 bars (fig 5.2), show in principle how all systems conserve Al_2O_3 among solids, and contain excess SiO_2 and H_2O (Beane, 1982). Although during the development of the main aluminous alteration zone, fluids are presumed to be locally quartz undersaturated, initial alteration

FIG. 5.1 - Vector diagram showing showing chemical potentials and alteration types related to increasing μHF (acidity) andd μKF (salinity) in the presence of quartz and an aqueous phase in the system K_2O-Al_2O_3-SiO_2-H_2O-F_2O_{-1} (μH_2O is externally controlled) (Burt, 1981).

FIG. 5.2 - Calculated stability relations among minerals as a function of temperature and cation activity ratios in a co-existing aqueous phase at 500bars. All systems conserve Al_2O_3 among solids and and contain excess SiO_2 and H_2O (Beane, 1982).

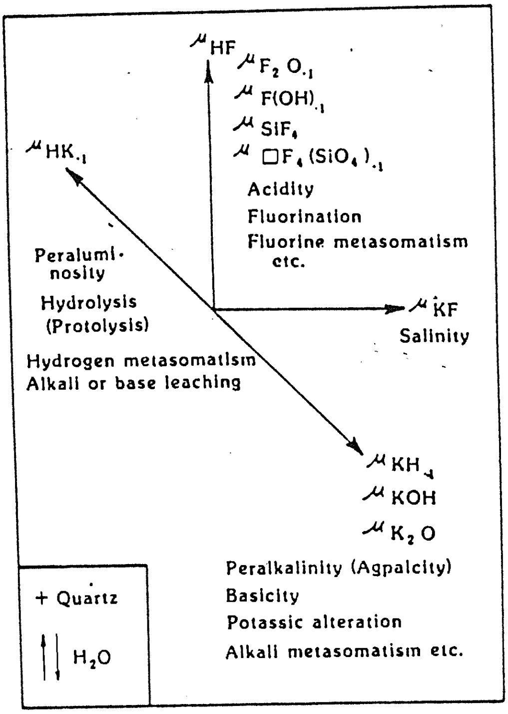
μHF
μF₂ O₋₁
μ F(OH)₋₁
μ SiF₄
μ □F₄ (SiO₄)₋₁
Acidity
Fluorination
Fluorine metasomatism etc.
μHK₋₁
Peraluminosity
Hydrolysis
(Protolysis)
Hydrogen metasomatism
Alkali or base leaching
μKF
Salinity
μKH₋₁
μKOH
μK₂O
Peralkalinity (Agpaicity)
Basicity
Potassic alteration
Alkali metasomatism etc.
+ Quartz
H₂O

FIG. 5:1

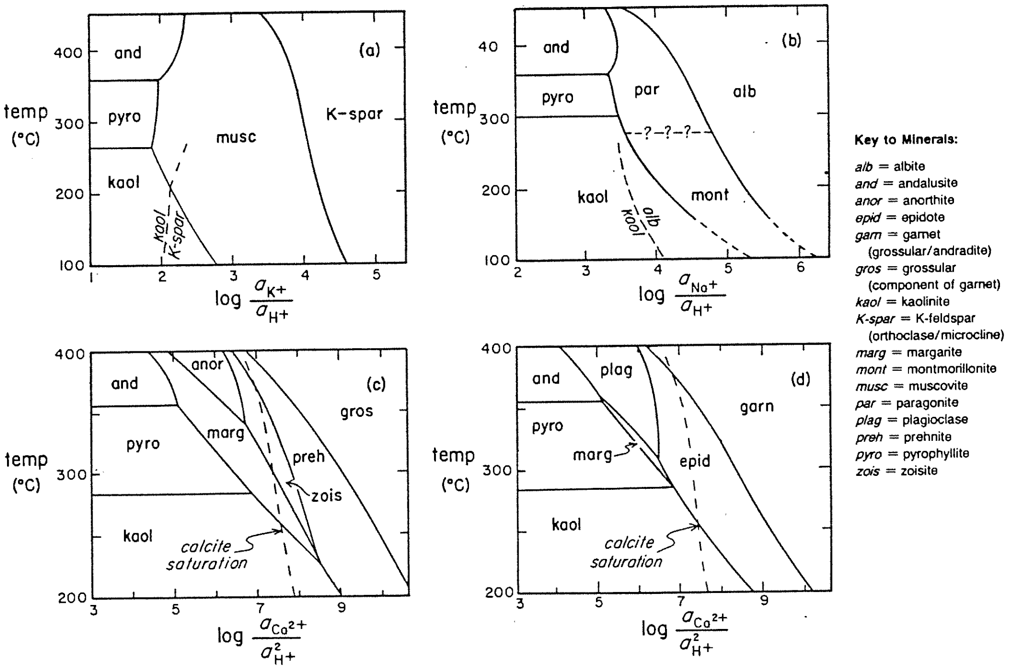
(a)
temp (°C)
400
300
200
100
and
pyro
kaol
musc
K-spar
kaol
K-spar
1
2
3
4
5
log a_K+ / a_H+
(b)
temp (°C)
40
300
200
100
and
pyro
par
alb
?-?-?
kaol
mont
alb
kaol
2
3
4
5
6
log a_Na+ / a_H+
(c)
temp (°C)
400
300
200
and
anor
gros
pyro
marg
preh
zois
kaol
calcite saturation
3
5
7
9
log a_Ca2+ / a²_H+
(d)
temp (°C)
400
300
200
and
plag
garn
pyro
marg
epid
kaol
calcite saturation
3
5
7
9
log a_Ca2+ / a²_H+
Key to Minerals:
alb = albite
and = andalusite
anor = anorthite
epid = epidote
garn = garnet (grossular/andradite)
gros = grossular (component of garnet)
kaol = kaolinite
K-spar = K-feldspar (orthoclase/microcline)
marg = margarite
mont = montmorillonite
musc = muscovite
par = paragonite
plag = plagioclase
preh = prehnite
pyro = pyrophyllite
zois = zoisite

FIG. 5.2

involving intense silicification is most likely to be coeval with muscovite alteration involving cation base leaching reactions.

Some rutile may have formed at this stage by the hydrolysis of ilmenite, which is known to occur in the host rocks. The reaction is:

$$\underset{\text{Ilmenite}}{FeTiO_3} + H^+ = FeOH^+ + \underset{\text{rutile}}{TiO_2} \qquad (15)$$

5.3 REACTIONS WITHIN ALUMINOUS ALTERATION : THE SYSTEM Al_2O_3-SiO_2-H_2O

Pressure and temperature

The presence of both andalusite and kyanite means that physical conditions are close to the polymorph boundary. This is shown (fig 5.4) on the PH_2O - T diagram, also showing dehydration reaction curves for the Al_2O_3 - SiO_2 - H_2O system. The presence of corundum in both andalusite and kyanite, then suggests a maximum pressure of 2.7Kb during the formation of corundum, and a temperature of 450° (at PH_2O=Ptotal). This means that the assemblage has formed at depth (approximately 10km) during orogenesis. A P of 2Kb is therefore used for the $aSiO_2$ / T diagram (fig 5.5).

Kyanite is in equlibrium with, or in places appears to have formed slightly later than andalusite, which is consistant with isobaric conditions and falling temperature. If andalusite and kyanite had formed by prograde regional metamorphism then kyanite would have to have been formed first.

FIG. 5.3 - Schematic stability of minerals in the system K_2O-Al_2O_3-SiO_2-H_2O as a function of μH_2O and μHK_{-1}. This assumes low to moderate pressure and temperature, and isothermal, isobaric conditions. Heavy lines indicate quartz bearing systems (Rose and Burt, 1979).

FIG. 5.4 - Calculated pressure temperature curves in the system Al_2O_3-SiO_2-H_2O based on 1Kb stability relationships and derived from thermodynamic data. (K = kaolinite, P = pyrophyllite, D = diaspore, C = corundum,

Q = quartz, K = kyanite, A = andalusite, Si = sillimanite,

W = water) (Hemley et al., 1980).

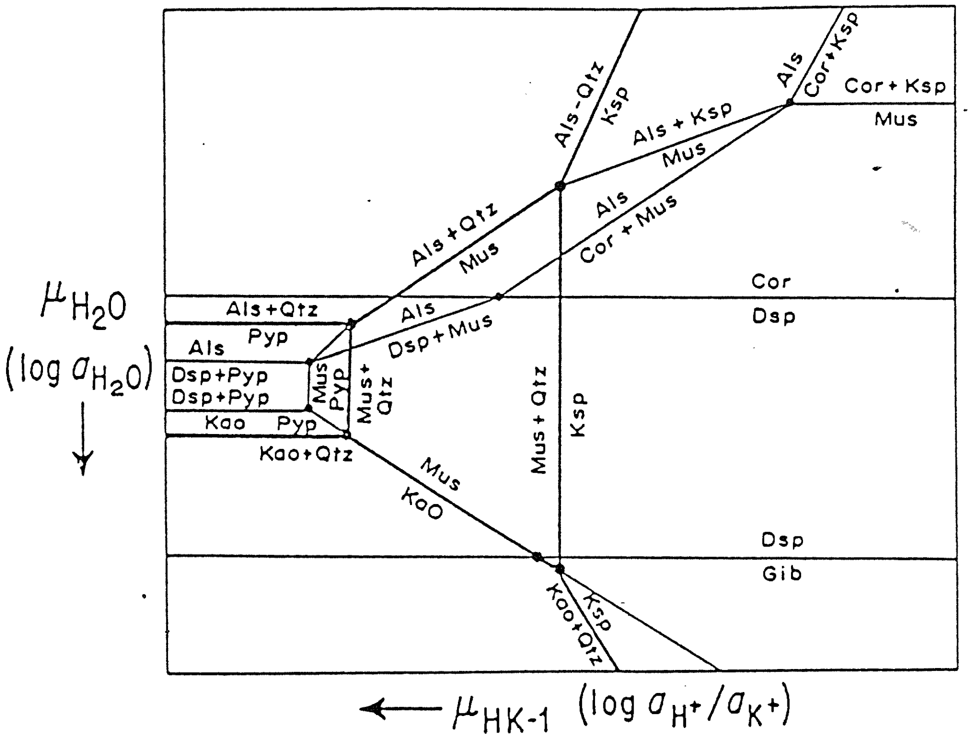
Als-Qtz
Ksp
Als
Cor+Ksp
Cor + Ksp
Mus
Als + Ksp
Mus
Als
Cor + Mus
Als + Qtz
Mus
Cor
Dsp
μ_{H_2O}
$(\log a_{H_2O})$
Als+Qtz
Als
Pyp
Dsp+Mus
Als
Dsp+Pyp
Dsp+Pyp
Mus
Pyp
Mus+Qtz
Mus + Qtz
Ksp
Kao
Pyp
Kao+Qtz
Mus
KaO
Dsp
Gib
Kao+Qtz
Ksp
μ_{HK-1} $(\log a_{H^+}/a_{K^+})$

FIG. 5.3 -

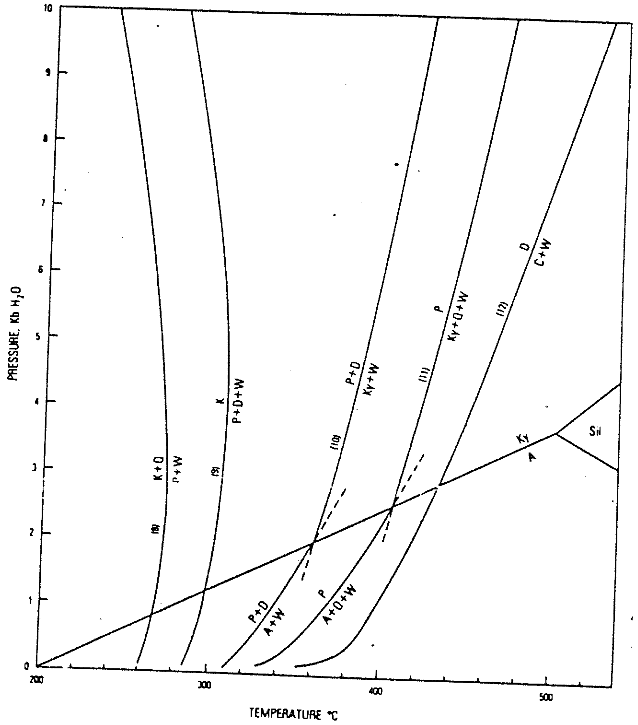
10
9
8
7
6
5
4
3
2
1
0
PRESSURE, Kb H_2O
200
300
400
500
TEMPERATURE °C
K+D
P+W
(8)
K
P+D+W
(9)
P+D
Ky+W
(10)
P
Ky+D+W
(11)
D
C+W
(12)
P+D
A+W
P
A+D+W
Ky
A
Sil

FIG. 5.4

Silica activity and temperature

Prograde and retrograde reactions occuring in aluminous alteration can be described within the system Al_2O_3-SiO_2-H_2O, the dominant controls being $aSiO_2$ and temperature. A mineral stability field diagram for this system as a function of these variables, at 2Kb, (experimentally derived) is shown in fig 5.5 (Hemley et al 1980). Reactions that textural evidence suggests occur are :

prograde:

Al_2SiO_5 + $2H_2O$ = corundum + H_4SiO_4 (aq) (1)

retrograde:

Al_2SiO_5 + $3H_2O$ = diaspore + H_4SiO_4 (aq) (2)

Al_2SiO_5 + $3H_4SiO_4$ (aq) = pyrophyllite + $5H_2O$ (3)

2 Al_2SiO_5 + $4H_4SiO_4$ (aq) = pyrophyllite + kaolinite + $5H_2O$ (4)

corundum + H_2O = 2 diaspore (5)

2 diaspore + $4H_4SiO_4$ (aq) = pyrophyllite + $8H_2O$ (6)

pyrophyllite + H_2O = kaolinite + 2HSiO4 (aq) (7)

Highly aluminous rocks, such as Al_2SiO_5 rock, contain no quartz, but are hosted by quartz rich rocks. Quartz at the margins of Al_2SiO_5 veins shows dissolution and replacement (fig 3.4) and fluids that formed Al_2SiO_5 rock, must have been locally undersaturated with respect to quartz. Futher, corundum and diaspore, common alteration products of this rock can only form from quartz undersaturated fluids. Compositional restrictions of Al silicates are displayed on fig 5.6.

FIG. 5.5 - Stability relationships in the system Al_2O_3-SiO_2-H_2O at 2Kb H_2O, derived experimentally (Hemley et al., 1980).

FIG. 5.6 - Composition diagram and compatability triangles in the system Al_2O_3-SiO_2-H_2O (Hemley et al., 1980).

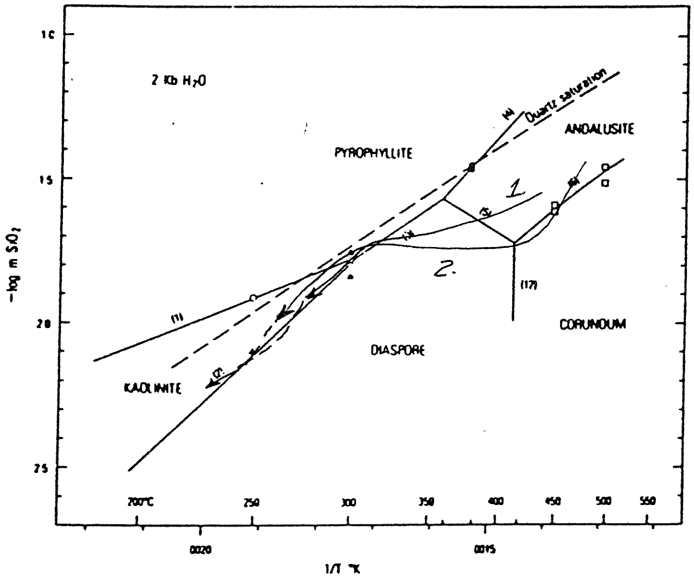
2 Kb H_2O
PYROPHYLLITE
Quartz saturation
ANDALUSITE
(4)
1.
2.
(17)
CORUNDUM
DIASPORE
KAOLINITE
(1)
-log m SiO_2
10
15
20
25
200°C
250
300
350
400
450
500
550
0020
0015
1/T °K

FIG. 5.5

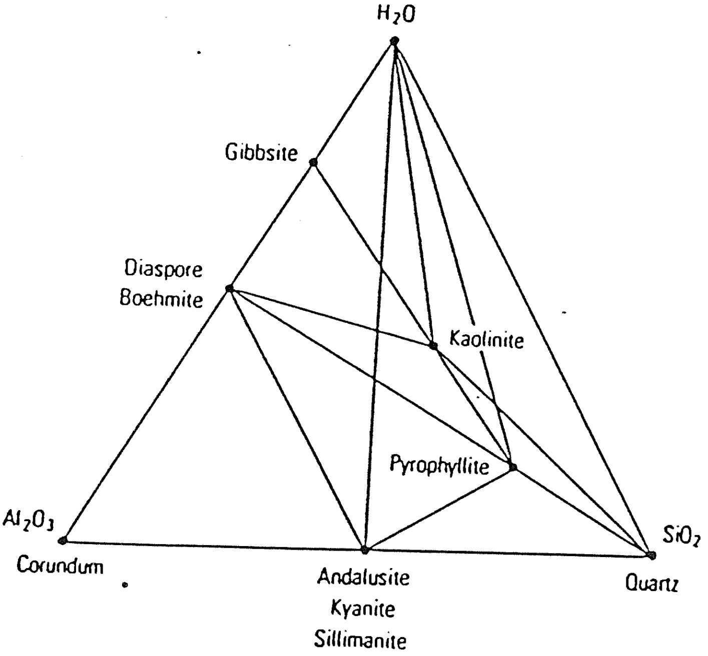
H_2O
Gibbsite
Diaspore
Boehmite
Kaolinite
Pyrophyllite
Al_2O_3
Corundum
Andalusite
Kyanite
Sillimanite
SiO_2
Quartz

FIG. 5.6

A possible path for fluid evolution in $aSiO_2$ vs 1/T space then will be below the quartz saturation curve, and is shown as line 1 (fig 5.5). This cannot be representitive for all aluminous alteration however, since the silica activity of the fluid appears to have had a considerable spatial variation.

Bulk composition would initially be that of Al_2SiO_5, and local increases in temperature would have caused the growth of corundum, since generally increasing temperature favours nonstochiometric dissolution of silica over aluminium. Alternatively a local decrease in $aSiO_2$ would also promote the formation of corundum, and futher decreases in temperature result in diaspore and kaolinite as low $aSiO_2$ alteration products (fig 5.5, line 2).

Diaspore has commonly replaced andalusite and kyanite with decreasing temperature. Small amounts of interstitial pyrophyllite in some diaspore nodules, and pyrophyllite alteration rims to diaspore prisms may indicate a slight rise in $aSiO_2$, and a position close to the pyrophyllite - diaspore reaction curve. Otherwise pyrophyllite represents a later change in $aSiO_2$ and overprints a stable diaspore occurrence.

Andalusite and kyanite more usually show pyrophyllite alteration rims sometimes accompanied by small amounts of fine grained diaspore followed by almost complete replacement by kaolinite. Corundum bearing Al_2SiO_5 minerals are shifted to a higher Al bulk composition and were replaced dominantly by diaspore, with minor kaolinite, and in places veined by later pyrophyllite. The reaction path then varies somewhat in silica activity throughout time and space as to its position relative to the pyrophyllite - diaspore boundary, but with futher decreasing temperature and silica activity would enter the kaolinite stability field.

Quartz fragments and relicts within highly altered rocks show pyrophyllite alteration rims representing active removal and replacement of quartz by pyrophyllite and finally kaolinite, reflecting the silica undersaturated nature of the fluids.

5.4 TOPAZ - MUSCOVITE ALTERATION AND THE SYSTEM K_2O-Al_2O_3-SiO_2-F_2O_{-1}

Muscovite and topaz, both of which formed during later evolution of the alteration fluid, represent a change from a completely Al dominated fluid to gradually increasing K^+ and F-. Topaz became the dominant aluminium silicate, replacing, and forming instead of andalusite or kyanite., while muscovite forms as an additional phase in response to increasing K^+, and slightly decreasing T, from existing aluminium silicates. Compositional variations based on the addition of HF to aluminosilicates are shown on fig 5.7.

Mineral stability fields within the system K_2O-Al_2O_3-SiO_2-F_2O_{-1} are shown on fig 5.8 (Burt, 1981) in an isobaric, isothermal diagram whose axes are μHF (acidity, where $\mu HF = \mu HCl + \mu FCl_{-1}$) and μKF (salinity, where $\mu KF = \mu NaCl + \mu KNa_{-1} + \mu FCl_{-1}$). The diagram assumes conditions of quartz and fluid saturation and is purely qualitative.

Muscovite stability field

Variation in K^+/H^+ controls the boundary of the muscovite stability field over that of the aluminium silicates and is shown on fig 5.2A as a function of temperature (as discussed in section 5.1). This serves only to demonstrate that muscovite becomes stable over a wide range of temperatures with increasing K^+/H^+, and slight T decrease from the andalusite stability field will promote muscovite formation. The muscovite stability field is also controlled by μH_2O, (fig 5.3) (Rose and Burt, 1979) and at high μH_2O values (which correspond closely to decreases in temperature) and reasonably high H^+ it is replaced by kaolinite. The hydrolysis reactions that bound the muscovite stability field with the aluminium silicate field are:

$$\text{andalusite} + 2KF + 3H_4SiO_4 = 2\ \text{muscovite} + 2HF + 3H_2O \qquad (8)$$

$$2\ \text{muscovite} + 2HF + 6H_4SiO_4 = 3\ \text{pyrophyllite} + 2KF + 12H_2O \qquad (10)$$

FIG. 5.7 - Composition diagram showing the limiting buffering assemblage for topaz solid solutions on the join Al_2SiO_4-H_2O-F_2O_{-1} in the system Al_2O_3-SiO_2-H_2O-F_2O. HF represents the limit of topaz buffering as compositions above this are unobtainable. Tie lines are schematic. (v=vapour, tpz=topaz, and=andalusite) (Barton, 1982).

FIG. 5.8 - Schematic diagram of the system Al_2O_3-SiO_2-H_2O-F_2O, as a function of μHF and μKF at fixed pressure, temperature and μH_2O (Burt, 1981).

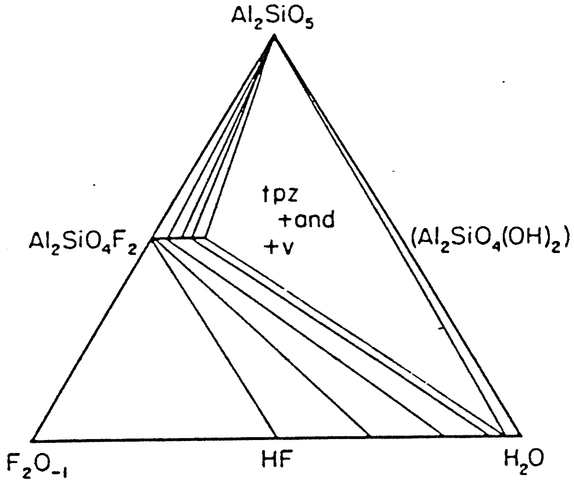
Al_2SiO_5
tpz
+and
+v
$Al_2SiO_4F_2$
$(Al_2SiO_4(OH)_2)$
F_2O_{-1}
HF
H_2O

FIG. 5.7

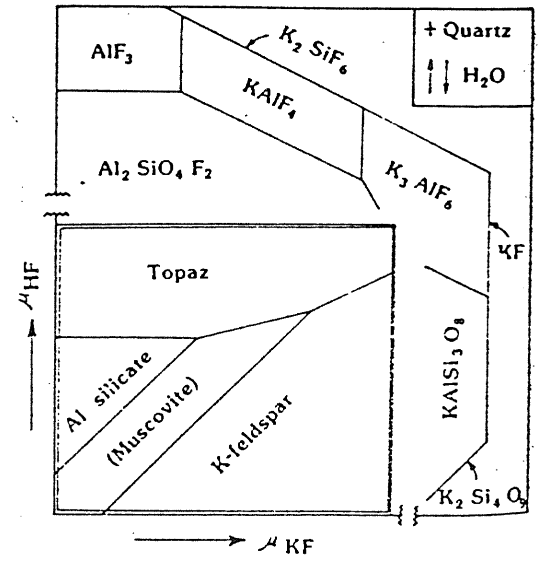
AlF_3
K_2SiF_6
$KAlF_4$
+ Quartz
H_2O
$Al_2SiO_4F_2$
K_3AlF_6
KF
Topaz
μ_{HF}
Al silicate
(Muscovite)
K-feldspar
$KAlSi_3O_8$
$K_2Si_4O_9$
μ_{KF}

FIG. 5.8

muscovite + HF + $2H_2O$ = 3 kaolinite + KF (9)

These reactions can also be written using HCl in the place of HF, however in this instance the fluids are known to be F bearing and the use of HF is appropriate (a small amount of Cl was detected as a minor constituent in some qualitative micropropbe analyses, so fluids are likely to have had a chloride component).

Muscovite is found veining and replacing andalusite and kyanite, and is also replaced by later clay alteration according to the above reactions. However these reactions occur also in the Al_2SiO_5 rock which are thought to be silica -undersaturated. Reactions (8) and (10) are silica dependant, however silica undersaturation is variable and may have been higher during topaz/muscovite alteration.

Hydroxymuscovite undergoes significant substitution by one HF for each H_2O, and thus acts as a buffer for aqueous HF (Burt, 1981) according to the reaction :

$KAl_2(AlSi_3O_{10})(OH)_2$ + 2HF = $KAl_2Si3O_{10}F_2$ + $2H_2O$ (11)
hydroxymuscovite fluormuscovite

The extent of this substitution in muscovites at Quartzite Ridge is unfortunately unknown as a fluorine standard was unavailable for the electron microprobe.

Topaz stability field

Under increasingly fluorine rich conditions topaz usurpes the role of aluminium silicates (Barton,1982) and replaces andalusite or kyanite and buffers HF according to the reaction:

Al_2SiO_5 + 2HF = $Al_2SiO_4F_2$ + H_2O (12)
andalusite topaz

Topaz commonly exists with muscovite. The reaction boundary between the stability fields for the two minerals is given by:

$$\underset{\text{muscovite}}{2KAl_2(AlSi_3O_{10})(OH)_2} + 8HF = \underset{\text{topaz}}{3Al_2SiO_4F_2} + 2KF + 3SiO_2 + 6H_2O$$

Thus topaz more effectively buffers HF than muscovite and is stable at higher μHF values (fig 5.8). Topaz and muscovite coexist and appear to be in equilibrium, although topaz is commonly present without muscovite indicating that the K^+/H^+ has fluctuated in time and space to intersect the muscovite stability field during the later stages of aluminous alteration (i.e. fluid was on the and-musc boundary), as K^+ increased (fig 5.2A). The topaz field is then intersected as HF increased, and topaz and muscovite were stable together until HF increases out of the muscovite stability field (fig 5.8). The less common association of pyrophyllite-muscovite-topaz shows that K^+/H^+ was periodically in the vicinity of the triple point,and the amount of K^+ available for the formation of muscovite varies periodically. In later stages futher increasing HF is shown by the formation of late stage fluorite.

HF variations and buffering

Physical processes such as boiling or cooling will affect the acidity and salinity of the fluid. These processes and their effects are summarised in fig 5.9.

Given the inferred depth of 10km for the alteration system, it is considered unlikely that boiling caused the the initial increase in acicidity and decrease in salinity of the fluid. Alternative explanations are:

(1) decreases in temperature causing oxidation and ionization of acid and neutral complexes

(2) sudden pressure and density changes caused by fluid throttling in constricted openings

(3) dilution of magmatic fluids with meteoric waters
(Burt, 1981)

FIG. 5.9 - Vector diagram showing the hypothetical effects of various processes on μHF (acidity), and μKF (salinity) in porphyry type systems (Burt, 1981).

FIG. 5.10 - Schemmatic diagram showing the possible intersection of $F(OH)_{-1}$ substitution or exchange reactions with F_2O_{-1} substitutions as a function of log ^{f}HF and temperature (Burt, 1981).

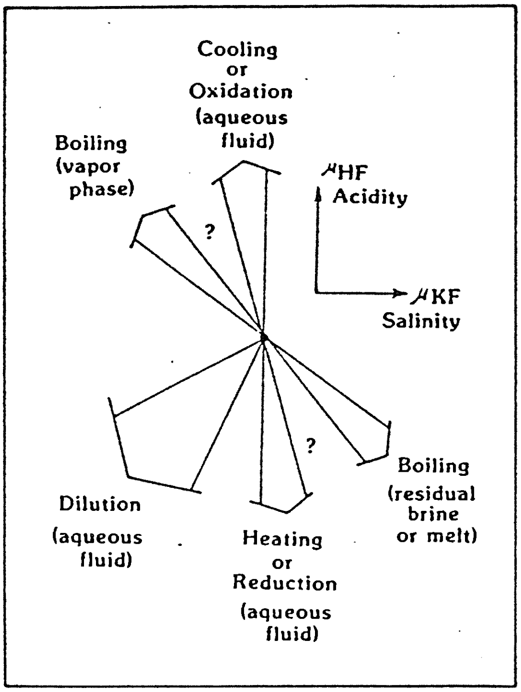

FIG. 5.9

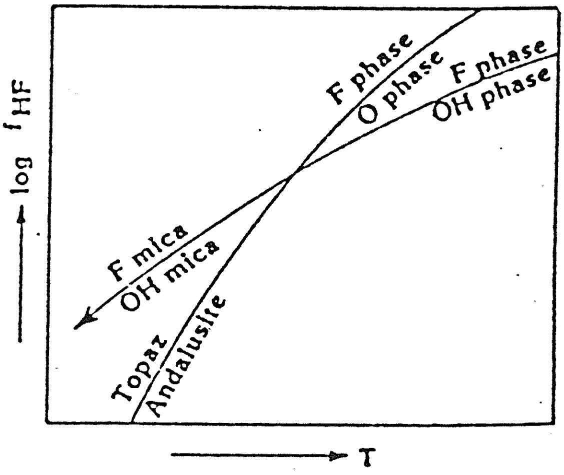

FIG. 5.10

A temperature decrease alone can lead to apparent or relative increases in μHF. Fluorination reactions are of two types: F exchange for O or OH. An example of the first type then involves the exchange of 2HF's for each H_2O in the conversion of andalusite to topaz - reaction (12). Hydroxal substitution exchanges one HF for one H_2O as in the formation of fluormuscovite - reaction (11) (Burt, 1981).

If hydroxyl exchange is the dominant control on HF/H_2O ratio of the fluid, then a temperature decrease with a corresponding increase in μH_2O can cause the oxygen exchange reaction to go the right (Burt, 1976b) (reaction 12) thus resulting in the late formation of topaz followed by fluorite as seen at Quartzite Ridge. The difference in HF coefficents cause the reactions to have different T dependence. The process is schematically displayed on fig 5.10.

The effect of Fluorine complexing

At high temperatures and pressures fluorine is significantly complexed by silica, and HF and KF concentrations are relatively low. However below about 500°C, fluoride concentrations that are constrained by assemblages involving fluorite and topaz are too low to contribute significantly to the transport of silicon (Haselton et al, 1988).

Aluminium has been observed experimentally to be increasingly soluble in fluoride solutions that are alkali free, with increasing temperature.A likely explanation is the formation of fluoro-aluminium complexes (Haselton et al 1988). Hydrated fluoride complexes of aluminium such as $AlF_3.nH_2O$ (n=3or9) are easily formed in HF aqueous solutions and are very soluble in water (Cotton and Wilkinson, 1972). Within silicate melts Al is beleived to be progressively removed from the tetrahedral network by complexing with F (Manning et al, 1980).

In geologic transport processes, the concentrations of fluoride complexes are probably extremely low for most elements at temperatures less than 500°C because the topaz and flourite bearing assemblages buffer HF to low values. At higher temperatures fluoride complexing may be significant with regard to silicon and aluminium transport (Hasselton et al, 1988).

5.5 THE FORMATION OF ALUMINIUM PHOSPHATES

Aluminium phosphates are comparatively rare minerals and their occurrance and origin within hydrothermal alteration systems has received little attention in the literature. Al phosphates found at Quartzite Ridge are of two types whose origin and timing are slightly different, but both reflect the high activity of H_3PO_4 in the fluid. The solid solution series for the relevant phoshate minerals are given in table 5.

Table 5 - Aluminium phoshate minerals

Mineral	Chemical Formula		Occurs at QR
Lazulite	$FeAl_2(PO_4)_2(OH)_2$		
Scorzalite	$MgAl_2(PO_4)_2(OH)_2$		*
APS minerals:	general formula - $RAl_3(PO_4)_{1+x}(SO_4)_{1-x}(OH)_{6-x}.H_2O$		
Svanbergite	$SrAl_3\ (PO_4)(SO_4)\ (OH)_6$	x=0	*
Woodhouseite	$CaAl_3\ (PO_4)(SO_4)\ (OH)_6$	"	
Goyazite	$SrAl_3\ (PO_4)_2\ (OH)_5.H_2O$	x=1	*
Crandallite	$CaAl_3\ (PO_4)_2\ (OH)_5.H_2O$	"	
Florencite	$(CeLaThSr)Al_3\ (PO_4)_2\ (OH)_6$	x=1	*

(after Stoffregen and Alpers,1987)

The lazulite - scorzalite series are Fe - Mg bearing Al phoshates and are found commonly in phoshate bearing pegmatites, and high alumina alteration zones in volcanic rocks, (Nriagu amd Moore, 1984) similar to that at Quartzite Ridge. The mineral was recently noted occuring with sericite in an advanced argillic alteration assemblage associated with a trachyandesite intrusive at Camp Oven Mountain, North Queensland (Morrison, Personal Comm.).

Aluminium phosphate-sulfate minerals (APS) have the generalized formula given in table 5 and belong to an isostructural group of minerals that includes alunite $KAl_3(SO_4)^2(OH)_6$ (Stoffregen and Alpers, 1987). APS minerals have been documented at some 30 locations in the world. These occur mostly in high alumina alteration zones such as Quartzite Ridge, but have been noted more recently with advanced argillic alteration in epithermal gold-copper and porphyry copper deposits (Stoffregen and Alpers, 1987).

Scorzalite

Scorzalite occurs earlier than the APS minerals at Quartzite Ridge and appears to replace andalusite. The proposed reaction is:

$$\underset{\text{andalusite}}{Al_2SiO_5} + H_3PO_4 + Mg^{++} = \underset{\text{scorzalite}}{MgAl2(PO_4)_2(OH)2} + SiO_2$$

Investigations into the system Al_2O_3-$AlPO_4$-H_2O by Wise (1976)(establishing stability fields for berlinite $AlPO_4$; augelite $Al_4(PO_4)_3(OH)_3$; and trolleite $Al_4(PO_4)_3(OH)_3$), suggests that Al phosphates in the presence of phosphoric acid are far more stable than any silicate. The equilibrium constant for the conversion of andalusite to augellite is equal to $1/aH_3PO_4$ so that the extent of the conversion is only dependant on the amount of H_3PO_4 present.

The origin and controls on the magnesium bearing member scorzalite are not clear. However obvious scorzalite replacement of andalusite is veined by later andalusite with apatite, and apatite, unaccompanied by any other phosphate phases, also veins and replaces kyanite. Thus the presumed inevitability of the above reaction in the presence of H_3PO_4 is not always the case. The reason for an extremely localized conversion of andalusite to a magnesium bearing Al phosphate in an otherwise extremely cation depleted enviroment is not known.Insufficent information is available on stabilities of phosphates to identify the factor controlling the phosphate phase present in this case. (possibly temperature, or cation availability).

APS minerals

APS phases (goyazite and svanbergite) are intimately associated with, and appear to replace apatite. They also replace scorzalite, andalusite/kyanite and diaspore. Florencite occurs as fine grained indistinct crystals within later clay veins.

Stoffregen and Alpers (1987) suggest that APS minerals form by the replacement of apatite or in response to apatite dissolution in the low pH enviroments such as in advanced argillic alteration, where they occur as inclusions in alunite at lower temperatures and in increasing solid solution with alunite at higher temperatures.

Considerable substitution of $(PO_4)^{3-}$ for $(SO_4)^{2-}$ can occur in alunite (Wise 1975), and monovalent cations are replaced by the divalent cations Ca^{2+} and Sr^{2+} with little effect on crystal structure. Deviations in the 1:1 ratio between phosphate and sulfate occur and result in the addition of trivalent ions such as Ce to compensate the charge imbalance (e.g Florencite) (Stroffregen and Alpers, 1987).

A stability field diagram (fig 5.11) for the APS mineral woodhouseite with apatite, alunite, muscovite and kaolinite (as a function of aH_3PO_4 and pH at 250° C) shows that apatite can not coexist with alunite or kaolinite at these conditions. APS minerals form in response to apatite dissolution, the composition of which is dependant on the SO_4 content of the fluid. In higher temperature aluminous alteration systems (as opposed to advanced argillic assemblages), apatite is more stable and pH is usually more a function of HF than H_2SO_4, so APS minerals with variable SO_4 substitution are commonly present while alunite is rare (alunite requires a high H_2SO_4 concentration to form in equilibrium with kaolinite (Hemley et al., 1969)).

At Quartzite Ridge the exact degree of sulfate substitution is not known, as a S standard was not available for quantitative microprobe analysis, however qualitative analyses of APS minerals demonstrated that $SO4^=$ is present (see appendix 1). Varying degrees of substitution probably explains the variation in aluminium to phosphate ratios. This is also the case for Sr, which qualitiative analyses showed is present as a substantial component. In the absence of other cations, the low to extremely low Ca content of the qauntitative analyses suggests that the minerals are closest to the Sr end members.

Source of phosphate

Phosphate may be relatively concentrated within the alteration zone by residual enrichment as H_3PO_4 is extremely insoluble. Apatite was observed as an accessory mineral in andesitic host rocks. Alternatively phosphate may have been introduced in the fluid, but there is no reason why this would be the case. Aluminuim phosphates are known from pegmatites however suggesting phosphate is concentrated in fractionated phases.

5.6 PHYSICAL AND CHEMICAL CONDITIONS OF FORMATION IMPLIED BY PARAGENESIS

Overall mineral assemblages show that the host rocks have undergone substantial bulk compositional change to consist dominantly of SiO_2 and Al_2O_3. Evidence for timing and reactions involved in this process has been obliterated by later alteration. Replacement of albite, chlorite and biotite by muscovite has occured at the margins of the alteration zone but the presence of rare topaz suggests that this is related to later overprinting. However a similar process of cation leaching can be postulated to have occured initially, possibly concurrent with early silicification. Futher increases in acidity would promote the removal of K^+ and even SiO_2, causing a relative enrichment in Al_2O_3.

The early formation of rutile by hydrolysis of ilmenite from host rocks may have occured in this manner, TiO_2 being resistant to leaching. A residual enrichment of P_2O_5 could occur in the same way, the solubility of H_3PO_4 being extemely low.

The scale of the formation of large masses of nearly pure Al_2SiO_5 minerals in veins suggests that Al has been introduced to some extent by fluids rather rather than being solely the product of residual enrichment processes. Al could conceivably be transported by F ligands (although at the relative time of formation of these large Al_2SiO_5 veins there is no evidence that F was present in appreciable amounts) or alkali silica complexes (this would be unlikely since the system is known to be depleted in cations).

A study of the $aSiO_2$ vs T diagram for the system Al_2O_3 - SiO_2 - H_2O, shows that Al_2SiO_5 can readily be altered to corundum with decreasing $aSiO_2$ or increasing temperature. Diaspore, pyrophyllite and kaolinite are retrograde alteration products of Al_2SiO_5 minerals formed sequentially with decreasing temperature under conditions of undersaturation in SiO_2 shown on fig 5.3 by path 1. The higher Al_2O_3 assemblage of corundum bearing Al_2SiO_5 is altered to diaspore and kaolinite via path 2.

Local conversion of andalusite to scorzalite/lazulite during aluminous alteration was probably a function of H_3PO_4 abundance (apatite is common within late aluminous and topaz/muscovite alteration) and cation availability (apatite requires Ca and scorzalite/lazulite requires Mg/Fe). Later apatite became the dominant phosphate bearing mineral to form but was locally replaced by APS minerals in response to decreasing pH or increasing $aH_2SO_4=$

FIG. 5.11 - Calculated stability relations among selected minerals in the system $CaO-K_2O-Al_2O_3-SO_3-P_2O_5-H_2O$ as a function of pH and dissolved phosphate at 250°C and 40bars (vapour saturation) (Stoffregen and Alpers, 1981).

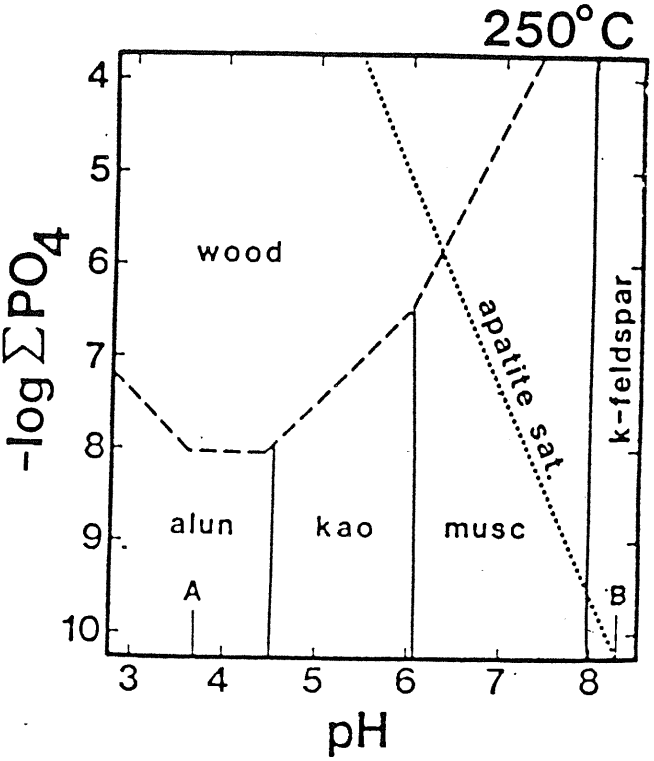
250°C
-log ΣPO4
4
5
6
7
8
9
10
3
4
5
6
7
8
pH
wood
alun
kao
musc
apatite sat.
k-feldspar
A
B

FIG. 5.11

and anomalous Sr levels.

Muscovite alteration of Al_2SiO_5 rocks would have occured as H^+/K^+ increased slightly, as would be expected during hydrolytic exchanges in conjunction with decreasing temperature would intersect the muscovite stability field (figs 5.2A & 5.3).

Decreasing temperature promotes an increase in μHF thus promoting the alteration of both andalusite and muscovite to topaz and eventually the formation of fluorite in late quartz and clay veins. The association of very fine grained topaz and quartz in narrow brecciated veins indicates a change to a higher $aSiO_2$, at least locally.

Dominant overprinting by clay alteration (pyrophyllite/kaolinite) occurred with futher decreasing temperature (and possible increasing μH_2O), and a probable futher increase in μHF shown by the presence of fluorite. Veining and replacement of quartz by kaolinite and pyrophyllite shows that at this stage the fluid must be undersaturated with respect to quartz, and probably aluminous. If Al is transported in connection with F this would be appropriate.

The occurrance of corundum in both kyanite and andalusite pinpoints this stage on the P/T diagram. This shows that the assemblage formed at appreciable depths and pressures (2-3 Kb) if PH_2O = Ptotal. In a system with such extensive metasomatic replacement this would be expected to be the case. A maximum T of approximately 435° is indicated.

CHAPTER 6 - DISCUSSION AND CONCLUSIONS

6.1 PARAGENESIS

An extensive elongate high alumina siliceous zone within the dominantly intermeadiate metavolcanics of the Cambrian - Ordivician Balcooma Metavolcanics crosscuts the stratigraphy at a low angle, but is parallell and with the dominant mylonitic foliation. The siliceous body is mylonitically foliated while the large Al_2SiO_5 veins were observed to be largely undeformed. Less competant muscovite-quartz-topaz rocks are commonly foliated and occaisionally topaz - quartz rocks show high strain deformation.

Both the siliceous and aluminous rocks are thought to be the product of a hydrothermal alteration event that can be divided into 4 stages:

(1) Silicification
(2) Aluminous alteration
(3) Topaz / Muscovite alteration
(4) Clay alteration

Mineralogy associated with these stages is summarised in table 3. A largely schematic representation of the above sequence of events (fig 6) shows their gross spatial relationships and most important textural features. Aluminous alteration is characterised by incipient veining and replacement of silicified rock, and possibly some brecciation of quartz and vein material particularly in the more aluminous larger veins i.e. with corundum alteration. Replacement of Al_2SiO_5 minerals by unorientated euhedral crystals of

FIG. 6.1 - Diagramatic three dimensional representation of alteration at Quartzite Ridge, showing gross spatial relationships and some of the most important textural features. Clay alteration is not represented for simplicity. The alteration zone has been exagerated in width by a factor of 2, and represents the area shown on the map between the two road crossings of the ridge.

A Corundum alteration of andalusite, overprinted by muscovite

B Unaltered quartz tectonite

C Fine and coarse veins of andalusite or kyanite in quartz tectonite with deformed quartz veins

D Muscovite - topaz alteration of andalusite/kyanite rock

E Fine grained topaz veining and multiphase brecciation of quartz tectonite

F Muscovite - topaz alteration of quartz tectonite

G The margin of the unaltered siliceous lens is irregularly veined along the preferential foliation by muscovite and topaz

H Pervasive developement of andalusite/kyanite along foliation planes in the quartz tectonite/associated with crosscutting veins

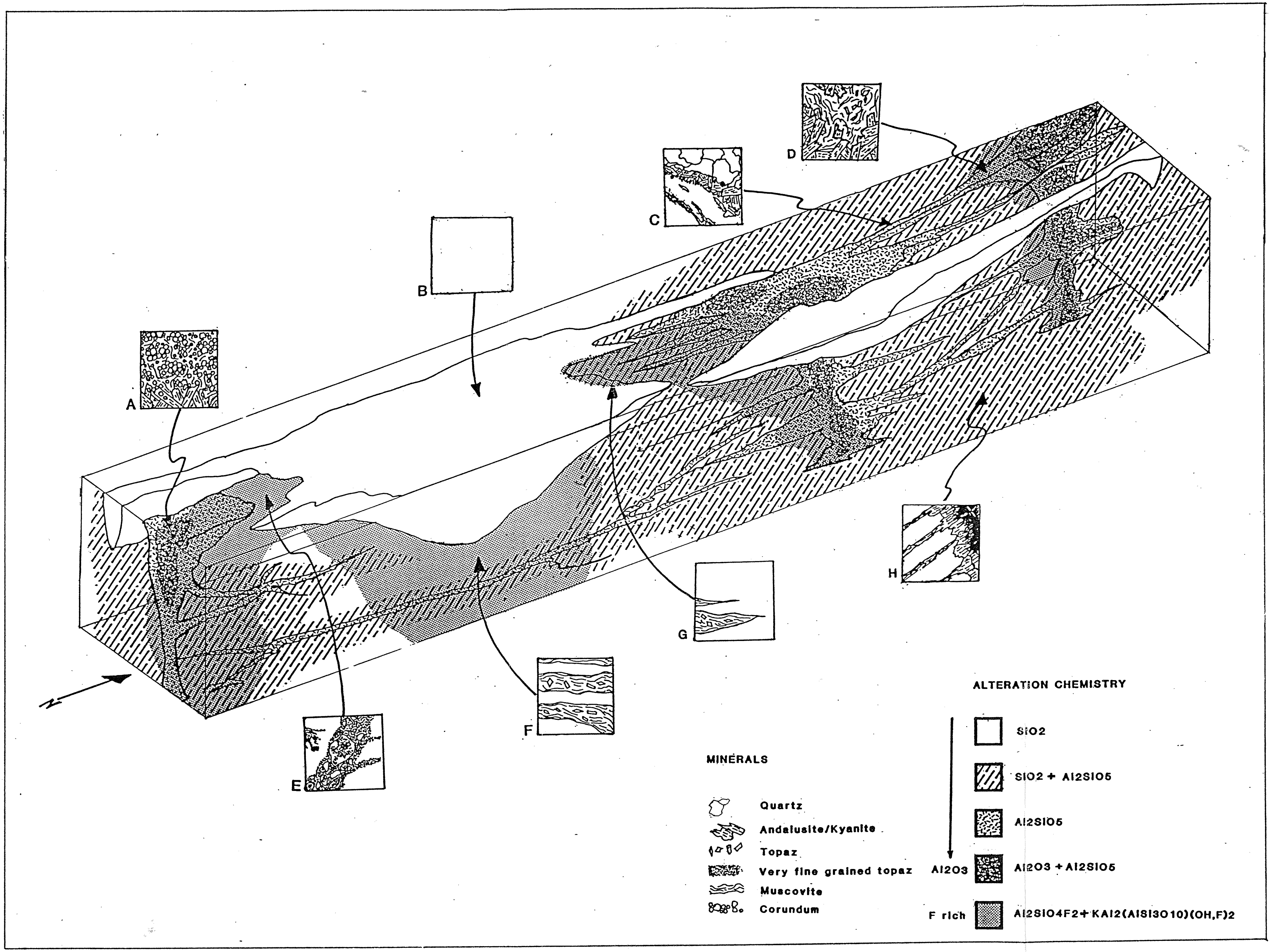
D
C
B
A
H
G
F
E
ALTERATION CHEMISTRY
SiO2
SiO2 + Al2SiO5
Al2SiO5
Al2O3
Al2O3 + Al2SiO5
F rich
Al2SiO4F2+KAl2(AlSi3O10)(OH,F)2
MINERALS
Quartz
Andalusite/Kyanite
Topaz
Very fine grained topaz
Muscovite
Corundum

FIG. 6

diaspore, apatite and phosphate minerals is probably facilitated by moderate lithostatic pressure. Topaz - muscovite alteration is characterised by a fine grained texture (of topaz) and frequent microbrecciation, which is possibly related to a change in hydrostatic to lithostatic pressure ratio. However topaz is known to occur in a similar fine grained form associated with aluminous alteration at other localities (see section 6.3) and may be related to the nature of topaz crystalization under certain conditions. Alteration to clays is extensive at 210m depth and veining and microbrecciation textures confirm that was not a supergene process.

Silicification

Silicification occurred during the late stages of the ductile mylonitic event within, and probably facilitated by, a local high strain zone. It is possible that silicification was accompanied by quartz - mica alteration associated with hydrolytic leaching that formed the protolith for the aluminous alteration. However no evidence exists that this was the case, or it has been completely obliterated by later overprinting alteration.

Silicification through leaching would produce a volume loss that would facilitate veining by aluminosilicates rather than blocking the channelway by the introduction and precipitation of silica from the fluid. Massive replacement by silica though can occur without volume change. The intensely siliceous largely unaltered quartz massif (map - appendix 4) however is more probably a lens of replacement silica introduced through veins.

Aluminous alteration

Aluminous alteration was determined by textural relationships to have formed by veining and replacement of the siliceous body by Al rich fluids, or possibly synchronous with at least part of the silicification. Residual enrichment of Al by hydrolytic leaching of the host rocks almost certainly occurred, but the formation of massive pods and veins of structureless Al_2SiO_5 rock must have occured by Al mobilisation in fluids. Al_2SiO_5 minerals occurring along foliation planes within the quartz tectonite are introduced from larger crosscutting Al_2SiO_5 veins.

Corundum alteration areas of Al_2SiO_5 rock, of which there are several of limited extent, are probably indicative of high temperature fluid flow, since increasing temperature and low $aSiO_2$ (by removal through high fluid flow rate) promote nonstochiometric disolution of silica over aluminium. Diaspore is also indicative of a quartz undersaturated enviroment but forms at a lower temperature as a retrograde alteration product of aluminous minerals.

Thus to this stage the alteration is seen as the product of a progressively more acidic fluid. Initial leaching removed most cations from the host rock, residually concentrating silica and aluminium, and other relatively insoluble minerals such as TiO_2 and P_2O_5. Increasing acidity and probably temperature, then began to favour even the dissolution of silica over aluminium, producing highly aluminous assemblages within regions of high fluid flow i.e. along Al_2SiO_5 veins intensifying in corundum bearing areas.

Residual concentrations of rutile along previously existing foliation planes within the original rock may have been a controlling factor in the formation of the banded nature of some rutile bearing andalusites.

In addition to textural evidence for the primary formation of Al_2SiO_5 veins from hydrothermal fluids, P/T considerations of Al_2SiO_5 polymorphs precludes their formation from prograde regional metamorphism of aluminous clays. Kyanite has replaced andalusite in one sample. This is consistant with decreasing temperature under isobaric conditions (see fig 5.2). If the Al_2SiO_5 were the product of prograde regional metamorphism, kyanite would always occur first.

Muscovite - topaz alteration

A gradual decrease in temperature and slight rise in K^+/H^+ is postulated as having promoted muscovite alteration of the aluminous assemblage and produced an overprinting alteration halo of the surrounding rocks. A narrow peripheral muscovite zone was formed that replaced the meta-andesite minerals. Decreasing temperature also increased HF content, as muscovite, with increasing μH_2O ceases to be an effective buffer of HF (see reaction 12). Apatite probably also acts as an OH exchange buffer as fluorapatite is found in veins with topaz.

Topaz becomes the stable aluminosilicate as temperature futher decreased and μHF increased. Very fine grained topaz - quartz rock multiphase milled and subangular breccias may indicate that these were now high fluid flow areas. $aSiO_2$ is locally increased as these are the only rocks to contain late silicification. This is accompanied by fluorapatite or fluorite and pyrite.

Clay alteration

In the waning stages of the alteration pervasive alteration of aluminosilicates to pyrophyllite and kaolinite occurs over large areas. The change in fluid pathways is again demonstrated where microscopic angular multiphase brecciation of topaz - quartz rocks occurs by clay veins. Clay alteration of Al_2SiO_5 veins and rocks is largely along passive tension cracks and by incipient replacement, and is quartz undersaturated.

Phosphate alteration

A variety of rare aluminium phosphates occurs at Quartzite Ridge, some of which correspond to no available analysis, however these occur only in trace amounts. Two main types have been observed in any abundance, and these only within a restricted location within andalusite rock. Apatite however is widespread but not of volumetric significance except within the aluminium phosphate bearing rocks.

Scorzalite/lazulite occurs as an alteration product of andalusite during aluminous alteration, probably forming as a function of high H_3PO_4 instead of apatite, controlled by Mg:Ca cation availability. APS minerals svanbergite and goyazite probably form in response to the presence of H4SO4 and Sr, from apatite dissolution prior to clay alteration. They also directly replaced andalusite and diaspore.

Phosphate is either residually enriched in a similar manner to titanium, due to its resistance to hydrolytic leaching or alternatively may be introduced by the fluid. Neither process offers an explanation for the localised abundant occurance of these minerals. If H_3PO_4 is highly insoluble then large concentration of the species by fluids would seem unlikely. In addition, apatite is unstable at low pH's unless the aqueous PO_4 concentration is high (fig 5.9).

6.2 CONDITIONS OF FORMATION

Pressure

A pressure of 2.5 - 3.0Kb is indicated for the formation of the aluminous alteration from the association andalusite - kyanite-corundum provided PH_2O = Ptotal (hydrobrecciation of topaz - quartz rocks indicates that either this is the case, or that there has been a lithostatic pressure decrease between aluminous alteration and topaz - muscovite alteration). This suggests that the depth of formation was in the order of 10Km. Such a substantial P and depth for the formation probably explains the difficulties encountered in interpretation of replacement and infill textures.

Temperature

Temperature at the same reaction triple point (andalusite-kyanite-corundum, fig 5.4) is approximately 435°C. Using Hemley et al.s (1980) diagram for $aSiO_2$ vs T, based on the mineral assemblage at 2Kb, a range of 435-220°C is shown for the alteration assemblage.

Age

The Early Devonian Conjuboy Formation is a shallowly dipping unit unconformably overlying the Balcooma Metavolcanics to the north. A proposed depth of formation of around 10Km means that the alteration must have occured a geologically reasonable time before the Early Devonian to allow for erosion close to the modern surface before then.

The alteration is considered to have occurred concurrently with the late stages and cessation of the mylonitic deformation event. Van der Hor (1989) dates the mylonitic event as Silurian. The alteration is therefore of probable Silurian age.

Fluid

The fluid responsible for the alteration was highly acidic and fluorine rich, and possibly strontium rich. The scale of metasomatism proposed would have to involve very large volumes of fluid the origin of which is uncertain. Two general possibilities can be proposed. The extreme depth of formation in conjunction with a deep crustal disturbance and proposed crustal thinning in the late stages of the orogeny (Van der Hor, 1989), suggest fluids derived from anatectic or other deep seated metamorphic dewatering processes could be channeled in the mylonite zone during the orogeny. Alternatively magmatically derived fluids, probably from an intrusive emplaced during orogeneis are a possible source.

The extreme disequilibrium of the fluid with respect to the host rocks, suggests the fluid was not metamorphically derived. The fluorine rich, acidic nature of the fluids suggests a granitic source.

The Dido Tonalite is a highly differentiated composite batholith of a fairly mafic nature overall and isotope dating indicates an Early Silurian or older age, and does not seem a likely source. The Ringwood Park Microgranite is considered by Withnall (1989) to be coeval with the Balcooma Metavolcanics, and by Vander Hor (1989) to be syntectonically emplaced. This could conceivably be a possible fluid source and outcrops 2Km east of Quartzite Ridge. Two bulk chemical analyses of the Ringwood Park Microgranite are presented by Withnall (1989), but both are of low K_2O granodiorites.

6.3 FUTHER WORK

Futher investigations, particulary more detailed and prepared microprobe analyses, would assist interpretation of this alteration style at Quartzite Ridge. Quantitative analyses of APS minerals for S and Sr would be desirable as the substitution properties of these minerals are not well known. Additional rare phosphate minerals are probably also present, and warrant investigation. Quantitative fluorine analyses of topaz and muscovite would elucidate μHF buffering processes. An isotope study of the alteration zone and granites from the surrounding area would assist in determining the actual origin of the fluid.

6.4 MODELS FOR THE FORMATION OF HIGH ALUMINA ALTERATION ZONES

Fluorine and phosphate bearing high alumina alteration zones

High alumina alteration zones with remarkably analogous mineral assemblages to that at Quartzite Ridge are known from Precambrian and Palaeozoic felsic to intermeadiate metavolcanics from several localities in the world (table 6.1). These characteristically occur associated with and hosted by siliceous bodies that are usually roughly strataform, or, less commonly, pipelike and crosscutting the stratigraphy. Stratigraphy is usually steeply dipping and within slate belt deformational regimes. The distinctive mineral association is defined by the association:

quartz
kyanite or andalusite
muscovite (sericite)
pyrophyllite
diaspore
topaz
rutile
Al phosphates

TABLE 6.1 – HIGH ALUMINA ASSEMBLAGES IN ADVANCED ARGILLIC ALTERATION ENVIRONMENTS

LOCATION	QTY HIGH ALUMINA MINERALS	PHOSPHATE MINERALS	ALTERATION CHEMISTRY	MINERALIZATIO	REFERENCE
Equity (British Columbia)	A sillimanite, A andalusite, corundum, A pyrophyllite A (tourmaline, dummortierite)	A scorzalite c apatite c svanbergite	acid-sulphate, V. high Al	Ag-Cu-Au (Sb-As)	Cyr et al., (1984) Wodjak and Sinclair, (1984)
Summitville (Colarado)	A alunite/kaolinite A sericite	r woodhouseite r svanbergite r hindsdalite	V. high S	Au-Cu-Ag	Stoffregen and Alpers, (1987)
El Salvador (Chile)	A pyrophyllite A diaspore c corundum c tourmaline c alunite		high k-high Al high S porphyry	Cu	Gustafson and Hunt, (1975)
Butte (Montana)	A andalusite A corundum c pyrophyllite ? topaz ? zunyite ? sericite		high S and Al porphyry	Cu	Brimhall, (1977)
La Granja (Peru)	A pyrophyllite A andalusite c diaspore	r woodhouseite r apatite	high Al epithermal	Cu-Mo	Stoffregen and Alpers, (1987)
Kounrad (USSR)	A andalusite c corundum c topaz r diaspore r dummortierite c alunite		high S and Al porphyry	Cu-Mo	Schmidt, (1985)
Tapaada and Tombuililato (North Sulawesi),	c andalusite c pyrophyllite c diaspore c corundum		high Al porphyry	Cu-Au	Schmidt, (1985)
Peak Hill (Australia)	A pyrophyllite r diaspore r topaz r/c alunite	r apatite r goyazite r wavellite	high K epithermal	Au	Open file report, anon. (1986?)
Elkhorn (Montana)	r andalusite r corundum		high K porphyry	Cu-Mo	Steefil and Atkinson, (1984)
Vunda (Fijii)	c sericite c/r diaspore	r gorceixite	K-Al? porphyry	Au	Schmidt, (1985)
Roseki (Japan)	A andalusite A corundum A pyrophyllite A kaolinite c diaspore c alunite c sericite r topaz r zunyite r dummortierite	r augelite r apatite r wilkeite	V. high Al acid-sulphate		Kamitani, (1985)

In several localities they are accompanied by gold, chalcopyrite and subeconomic amounts of Mo and Sn (Schmidt, 1985). All these occurrences have in common that they appear to have formed by hydrolytic processes from strongly acidic fluorine bearing fluids. Direct association with acid intrusives has been noted at Brewer Mine (US) (Schmidt, 1985) and Chizeuil (France) (Stoffregen and Alpers, 1987). They vary however considerably in depth of formation, the more strataform zones being shallower and crosscutting ones deeper (Schmidt, 1985).

Within belts of Paeleozoic acid to intermeadiate metavolcanics such as the Carolina slate belt (USA), and the Kazakhstan region (USSR), high alumina alteration zones of varying intensity are common and economic porphry Cu - Mo and porphry Au deposits that include high alumina alteration zones within their alteration assemblages also occur (Schmidt, 1985).

Thus some of these fluorine rich and Al phosphate bearing aluminous alteration zones are observed to be directly the result of alteration by magmatically derived fluids. Tourmaline, dummortierite, barite, zunyite or alunite may also be present and represent the introduction of boron, barium, chlorine or sulphate respectively in the fluid (Hemely et al. 1980, Wise, 1975).

High alumina mineral suites within advanced argillic alteration

High alumina assemblages are commonly present within advanced argillic alteration zones within acid to intermediate volcanics formed by contact metamorphism with acid intrusives, solfarctic systems and porphyry and acid sulphate systems. Hydrothermally produced andalusite, pyrophyllite diaspore and corrundum have all been observed within alteration in porphyry systems (table 6.2).

Andalusite, corundum, diaspore, pyrophyllite and kaolinite and quartz occur in the Roseki Ores (Japan) as alteration products within a lacustrine sediment by meteoric circulating waters during the intrusion of a quartz monzonite stock. A central ' griesen zone'

TABLE 6.2 - ANALAGOUS HIGH ALUMINA ALTERATION SYSTEMS

LOCALITY	Sillimanite	Andalusite	Kyanite	Topaz	Muscovite	Diaspore	Corundum	Pyrophyllite	Kaolinite	Rutile	Pyrite	PHOSPHATE MINERALS	OTHER MINERALS	ORE MINERALS	HOST ROCKS	AGE	ORIGIN PROPOSED	REFERENCE
Chizeuil (France)		X				X	X	X	X	X	O	Sv	Ba	Au, Ch,	quartzite? in granite	C	associated with muscovite granite dykes	Stoffregen and Alpers (1987)
Pazmand (Hungary)				X		O		X	O	O	X	APS unident.	Alu, Zu,		quartzite?	?	2 phase hydrothermal alteration, granite then andesite fluid sources, F to SO_4 rich	Nemecz, (1984)
Boliden (Sweden)		X	O		X	X	X		X	X	X	(F)Ap, Sv,		Au, Ch, As, BiT,	quart/sericite altered metavolcanics	PC	multiple phase hydrothermal alteration from granitic fluid source	Geijer, (1963)
Halljoberget (Sweden)		O	X		X			O		X	O	Lz, Sc, Ap, Aug, Wg, Sv,	Pa, Ba, To, Ha, Il, Mg,		sedimentary quartzite in granitic gneisses	PC	hydrothermal alteration by 'post magmatic processes'	Geijer, (1963)
Dicksberget (Sweden)			X		X						X	(Mn)Ap, Lz,	Ha, Il,		as above	PC	as above	Geijer, (1963)
Vastana (Sweden)		O	X		X			X		O		(F)Ap, Lz, Sv, Aug, Br, Tr,	Ct		sedimentary quartzite in metasedimentary and metavolcanic rocks	Pz	as above	
Semis Bugu (Kazakhstan - USSR)		X			O		X			O	O		Alu, Ba, Zi,		silicified volcanic flows and pyroclastics	?	magmatic fluids with declining temperature and changing composition	Geijer, (1963)
Zhanet (Kazakhstan - USSR)		X		X		O	X					Ap,	Alu, Du, To, Ha, Di,		as above	D-C	fumarolic hydrothermal alteration, adjacent to a volcanic vent	Schmidt, (1985)
Zhorg Massiff (Kazakhastan - USSR)				X	X			X	X			Sv,	Ba,		as above	?	as above	Stoffregan and Alpers (1987)
Poffadder (South Africa)	X			X	X	X	O	X	X	O	O	Ho,	Il, Za, Na,	Ch, Co,	quartzite in quartz feldspar gneiss	PC	hydrothermal alteration of metamorphic sillimanite	Schoch et al., (1985)
Mt. Perry (Australia)		X			X			O		X		Aug, Lz,	Ha	rutile	quartzite in altered volcanics	Tr	pneumatolytic replacement and brecciation by F rich vapour phase from granitic intrusion	Denaro, (1963)
Kiowa Mtn. (Mexico)		X	X		X					O		Ap,	Ha, Il, Zi,		altered acid metavolcanics	PC	hydrolysis of feldspars to muscovite and Al silicate by fluid of unknown source	Gresens, (1971)

TABLE 6.2 - CONT'D

LOCALITY	Sillimanite	Andalusite	Kyanite	Topaz	Muscovite	Diaspore	Corundum	Pyrophyllite	Kaolinite	Rutile	Pyrite	PHOSPHATE MINERALS	OTHER MINERALS	ORE MINERALS	HOST ROCKS	AGE	ORIGIN PROPOSED	REFERENCE
USA																		
Farmville (Virginia)		O	X		X	O		X	O	O	X	Go, Va, Lz, Cr, Ap,	To, Ba, Zu,		sedimentary quartzites in intermediate metavolcanics and pyroclastics	PC-early Pz	Metamorphic kyanite is remobilized by later pegmatite veins	Espanshade and Potter (1960)
Graves Mtn. (Georgia)		O	X					X		X	O	Lz	Ba, Pa,	Au	silicified intermediate metavolcanics and pyroclastics	" "	metamorphism of an earlier shallow hydrothermal alteration	Schmidt, (1985) Sykes and Moody, (1978)
Hillsborough (North Carolina)		X	O	X	X	O		X		O		Lz	Cl		as above	" "	as above	
Brewer Mine (South Carolina)		X		X	X			X			O			Co, Ch, En, Au,	as above	" "	as above	Schmidt, (1985)
Pilot Mtn (North Carolina)		X		X	X			X		O			Cl,	rare Cu, Mo sulphates	as above	" "	hydrothermal alteration by subvolcanic intrusives	Schmidt, (1985)
White Mtn (California)		X		O	X					X	O	Lz, Wdh, Aug, Tr,	Ba, Alu, To, (Sr,Na)Alu,		silicified rhyolitic - rhyodacitic meta volcanics.	Mz	hydrothermal alteration by an adjacent granite	Wise, (1975)
Dover Mine (Nevada)		X			O	X		X			O	Sv	(Sr)Ba, To, Ca		altered rhyolitic - dacitic	Mz	hydrothermal replacement by a fluid of unknown source	Switzer, (1949)
Vitrefax (California)			X					X			O	Sv			unspecified metavolcanics	Mz	hydrolytic leaching of muscovite quartz metavolcanics and introduction of PO_4, F etc.from a magmatic source	Wise, (1975)
Oreana (Nevada)	X				X					O			Du, Zi, To, Sp		as above	Tr	as above,but source of fluid is identified as associated granite porphyry and quartz monzonite	Wise, (1975)

MINERAL ABBREVIATIONS:

PHOSPHATES

Ap	apatite	Ca5(PO4)3OH
(F)Ap	fluorapatite	$Ca_5(PO4)_3F$
(Mn)Ap	manganiferous apatite	$(Ca,Mn)_6Ca(PO_4)_6F$
Aug	augelite	$Al_2PO_4(OH)_3$
Br	berlinite	$AlPO_4$
Cr	crandallite	$CaAl_3(PO_4)_2(OH)_5.H_2O$
Go	goyazite	$SrAl_3(PO_4)_2(OH)_5.H_2O$
Cr	crandallite	$CaAl_3(PO_4)_2(OH)_5.H_2O$
Go	goyazite	$SrAl_3(PO_4)_2(OH)_5.H_2O$
Ho	hotsonite	$11Al_2O_3.2P_2O_5.6SO_3.53H_2O$
Lz	lazulite	$(Mg,Fe^{2+})Al_2(PO_4)_2(OH)_2$
Sv	svanbergite	$SrAl_3(PO_4)(SO_4)(OH)_6$
Tr	trolleite	$Al_5(PO_4)_3(OH)_4$
Va	varsicite	$AlPO_4.2H_2O$
Wg	wagnerite	$(Mg,Fe,Mn,Ca,)_2PO_4F$
Wdh	woodhouseite	$CaAl_3PO_4SO_4(OH)_6$

OTHER MINERALS

Alu	alunite
(Na)Alu	natroalunite
(Sr,Na)Alu	strontium, natro alunite
Ba	barite
Ca	carnotite
Di	dickite
Du	dummortierite
Ha	haematite
Ho	hotsonite
Il	illmenite
Mg	magnetite
Pa	pargonite
Sp	spinel
To	tourmaline
Za	zaherite
Zi	zircon

ORE MINERALS

Au	gold
As	arsenopyrite
BiT	bismuth tellurides
Ch	chalcopyrite
Co	covellite
En	enargite

within the andalusite zone (intensely altered) consists of topaz, dummortierite, augelite (Al phosphate),wilkeite (apatite group),pyrite and muscovite. These were considered to have formed from high temperature fluid seperated directly from the magma (Kamitani, 1977).

Aluminium phosphates are known from the Equity Silver Mine (British Columbia), a Ag-Cu-Au acid sulphate deposit, in association with andalusite, corundum and tourmaline as part of an aluminous alteration suite (Cyr et al., 1984). APS minerals in association with alunite have been recognized recently in several porphyry Cu deposits by Stoffregen and Alpers (1987). They are considered to form from the alteration of pre-existing apatite from the host rocks. Goyazite and apatite are noted as rare acessory alteration minerals at the acid sulphate deposit of Peak Hill (Australia) (Cordery, 198?).

APS minerals may form by the alteration of apatite, however apatite is more likely an alteration mineral itself. Small amounts of APS mineral encounted in advanced argillic alteration in association with alunite are a function of the sulfate rich nature of the fluids.

Quartzite Ridge and analogical high alumina zones

Quartzite Ridge is strikingly similar to those less strataform high alumnina zones described by Espanshade and Potter (1962), and Schmidt (1985) of the Carolina Slate Belt. Espanshade and Potter state - "Silicification was the first stage of mineralization; the aluminous minerals vein and replace quartz. Kyanite occurs in irregular bodies and crosscutting veins in kyanite quartz rock. Topaz forms irregular masses and networks of veins...". Mineralogy and configurations of the Pilot Mountain and Brewer deposits suggest that they formed at relatively low pressures - less than 2Kb (andalusite is widespread, but kyanite has been observed in small local concentrations) - and temperatures ranging from 300 to 400°C (Schmidt, 1985).

Information on the high alumina alteration zones of the Kazakstan (USSR) in english was unobtainable, but Espanshade and Potter (1962), after Ozerov (1933), describe lenticular bodies of high alumina rock occuring in fracture zones in silicified volcanic flows and tuffs that are intruded by granite and granodiorite. The lenses are principally andalusite with corrundum predominating in the centre. The volcanic rocks were silicified at an early stage; decomposition of feldspar provided Al2O3 and SiO_2 for the formation of andalusite, which was later replaced by corrundum. Magmatic (or meteoric fluids with a magmatic component) fluids of declining temperature and changing composition were responsible.

Both the above systems (and others in table 6.1) have similar settings to Quartzite Ridge within Palaeozoic metavolcanics, and are of comparable size and form. Quartzite Ridge is highly elongate due to the local structural controls. In all systems an early silicification is later veined by aluminous alteration. The consistancy of this relationship indicates both were formed by a single continously evolving hydrothermal event. The same is true for the regular occurance of topaz, which many authors (Sykes and Moody, 1978; Nemecz, 1984) interpreting a system in isolation have ascribed to a seperate hydrothermal event rather than a change in fluid μHF.

Quartzite Ridge seems to have formed at a higher pressure than Schmidt interprets for Brewer and other systems. Andalusite and corundum are commonly reported but significant amounts of kyanite with corundum are not. Quartzite Ridge seems to have formed at greater depth than most other systems.

Associated features of slate belt high alumina zones

Highly strataform occurances of Al_2SiO_5 quartz schists within the Carolina Slate Belt, without large veins of Al_2SiO_5 rock, and having a generally more restricted mineral assemblage, are interpreted to have formed from regional metamorphism (and or associated with heating by intrusives), of a high alumina precurssor (Schmidt, 1985;

Allard and Carpenter, 1980; Espanshade and Potter, 1962). The high alumina precurssor is suggested to have formed by fumarolic action during the evolution of a submarine felsic volcanic pile, altering dacite tuffs to an advanced argillic assemblage, the protoliths of the Al_2SiO_5 quartzites (Allard and Carpenter, 1980). Adjacent exhalitive assemblages hosting massive and disseminated Zn - Cu - Pb - Au - Ag mineralization are assumed to be associated (Allard and Carpenter, 1980).

The strataform kyanite quartzite at Galah Dam described by Withnall (1989) (see chapter 2.4) seems similar to this type, but no firsthand observations were made. It is of interest that base metal mineralization of presumed volcanogenic origin is found close to Quartzite Ridge. In the Seventy Mile Range Group (a slate belt of Cambrian - Ordivician felsic metavolcanics similar lithology and age to the Balcooma Metavolcanics), a pyrophyllite -sericite - quartz ± topaz alteration zone occurs a few kilometers along strike from the volcanogenic Reward massive sulphide deposit (Cu - Pb - Zn - Au) (Beams et al., 1989). These correlations may merely reflect the overall tectonic enviroment of lower Palaeozoic felsic volcanic regimes developed on continental margins.

6.5 CONCLUSION

The high alumina alteration at Quartzite Ridge was formed by hydrolytic alteration of intermediate volcanics and interbedded sediments by an acidic F rich fluid along a high strain zone. Leaching of the host rocks produced an initial silicification. Aluminium has been concentrated and mobilized (possibly due to the F rich nature of the fluids) to form substantial veins of Al_2SiO_5 and other aluminous minerals. At high temperatures SiO_2 has been removed by quartz undersaturated fluids increasing the Al concentration within the veins.

Decreasing temperature facilitated an increase in HF and the formation of F bearing minerals, and finally clays. P_2O_5 may have been introduced by the F rich fluid. A possible fluid source is the Ringwood microgranite.

The alteration formed in the Silurian at depth (approximately 10Km) with a temperature range of about 435 - 220°C, during the late stages of the mylonitic event.

High alumina alteration zones such as the one at Quartzite Ridge represent a distinctive alteration style that has been noted elsewhere. They are characterised by the veining of siliceous bodies within acidic to intermeadiate metavolcanics, by aluminosilicates from F rich fluids and the assemblage :

quartz
andalusite, kyanite
muscovite
pyrophyllite
topaz
diaspore
rutile
Al phosphates

They are distinct from aluminous advanced argillic assemblages by their low H_2SO_4, high F and overall higher temperature assemblage, and the presence of P_2O_5 and TiO_2. APS minerals are characteristically present instead of alunite. These high alumina alteration zones have genetic affinities with both porphyry Cu-Mo systems and greisens.

REFERENCES

Anon, 1984; Report on the portions of Authority to Prospect No. 2036M - "Balcooma" relinquished 27 October 1984. Open file report, Qld.Dept.Mines.

BARTON, M. D., 1982; The thrmodynamics of topaz solid solutions and some petrologic applications. Am. Mineralogist, **67**, 956-974.

BEAMS, S. D., LAING, P. W., O'NEILL, D. M., 1989; The exploration history and geology of the polymetallic Reward Deposit, Mt Windsor Volcanic Belt, North Queensland. NQ Gold '89 Conference, Pub. AUSIMM, 95-103.

BEANE, R. E., 1982; Hydrothermal alteration in silicate rocks : southwestern north america., in TITLEY, S. R. (Ed), Advances in the geology of porphyry copper deposits., The University of Arizona Press.

BRIMHALL, G. H., 1977; Early fracture controlled mineralisation at Butte, Montana. Econ. Geol., **72**, 37-59.

BURT, D. M., 1981; Acidity-salinity diagrams - Application to greisen and porphyry deposits. Econ. Geol., **76**, 832-843.

BURT, D. M., 1976b; Generation of high HF fugacities in miarolitic granites and pegmatites: the possible role of topaz [abs]. Geol. Soc. Am., Programs with Abstracts, **8**, 798.

CARPENTER, R. H., ALLARD, G. O., 1980; Mineralization, alteration and volcanism in the Lincoln-McCormick district, Georgia and South Carolina. Geol.Soc.Am., Abstracts with programs, v12-**7**, 398-399.

CLARKE D. E. 1971; Geology of the Ravenswood, 1 mile sheet area. Geol. Soc. Qld., report 53.

CORDERY, G., 198?; Epithermal alteration zonation at Peak Hill, N.S.W. Report on E.L. 1464, Peak Hill, NSW. Dept. Min. Resources, unpub.

COTTON, J. M., WILKONSON, P. W., 1972; Advanced inorganic chemistry - a comprehensive text. Interscience Publishers-John Wiley and Sons, New york, Sydney, Toronto.

COX, K. G., BELL, T. D., PANKHURST, R. G., 1978; The interpretation of igneous rocks.. London, George Allen & Unwin , Boston.

CYR, J. B., SCHROETER, T. G., 1984; Geology and mineralization at the Equity Silver Mine. Econ. Geol. 79, 947-968.

DENARO, T. J., 1986; The geology of the Mt Perry Rutile deposit. Geol.Soc.Aust.,Qld. Div. 1986 Field Handbook for the Burnett District.

ESPANSHADE, G. H., POTTER, D. B., 1960; Kyanite, sillimanite and andalusite deposits of thr southeastern states.

GEIJER, P., 1963; Genetic relationships of the paragenesis Al_2OSiO_5-lazulite-rutile. Ark. Min. Geol. 3, 423-464.

GRESENS, R. L., 1971; Application of hydrolysis equilibria to the genesis of pegmatite and kyanite deposits in Northern New Mexico. Mtn. Geolt. 8, 3-17.

GUSTAFSON, L. B., HUNT, J. P., 1975; The porphyry copper deposit at El Salvador, Chile. Econ. Geol., 70, 857-912.

HARVEY, K. J., 1980, The geooogy of the Balcooma Massive Sulphide Deposit, northeast Queensland. M.Sc. Thesis, J.C.U.N.Q., unpub.

HASELTON, H. T., CYGAN, C. L., D'ANGELO, W. M., 1988; Chemistry of aqueous solutions coexisting with fluoride buffers in the system K_2O-Al_2O_3-SiO_2-F_2O_{-1} (1Kb, 400-700ºC). Econ. Geol., **83**, 163-173.

HEMLEY, J.J., MONTOYA, J. W., MARIENKO, J. W., LUCE, R. W., 1980; Equilibria in the system Al_2O_3-SiO_2-H_2O and some general implications for alteration mineralization processes. Econ. Geol., **75**, 210-228.

HEMLEY, J. J., HOSTETLER, P. B., GUDE, A. J., MOUNTJOY, W. T., 1969; Some stability relationships of alunite. Econ. Geol. **64**, 599-612.

HENDERSON, R. A., 1987; An oblique subduction and transform faulting model for the evolution of the Broken River Province, Northern Tasman Orogenic Zone. Aust. J. Earth Sci. **34**, 237-249.

HENDERSON, R. A., 1986; Geology of the Mt. Windsor Subporvince - a Lower Palaeozoic volcano-sedimentary terrane in the northern Tasman Orogenic Zone. Aust. J. Earth Sci., **33**, 343-364.

KAMITANI, M., 1977; Genesis of the andalusite bearing Roseki Ore Deposits in the Abu District, Yamaguchi Prefecture,Japan. Japan Geol.Surv. Bull. **28**, 201-263.

KERRICK, D. M., 1988; Al_2SiO_5 - bearing segregations in the Lepontine Alps, Switzerland: Aluminium mobility in metapelites. Geology, **16**, 636-640.

MANNING, D. A., HAMILTON, D. L., HENDERSON, C. M. B., DEMPSEY M. J., 1980; The probable occurance of interstitial Al in hydrous F-bearing and F - free aluminosilicate melts. Contribs. Mineral. Petrol., **75**, 257-262.

McLENNAN, T.P.T., 1986; The geology of the Criagie outstation area, Broken river province, North Queenland. BSc Hons thesis, UQ, unpublished.

NEMECZ, E., 1984; Pyrophyllite 1TC occurrence at Pamand (Hungary) in Flourine-activized enviroment. Acta Geologica Hungarica. **27** (1-2), 191-202.

NRIAGU, J. O., MOORE, P. B.,(Eds) 1984; Phosphate Minerals. Springer - Verlag, Hîedelberg.

OVERSBY, B. S., WITHNALL, I. W., WARNICK, J. V., McLEOD, R. L., 1983; Einasliegh, Lyndhurst, Conjuboy, and Burges 1:100 000 sheet areas - catalogue of field geological compilation sheets. B. Min. Res.,Aust., Record 1983/17 (unpublished).

RICHARDS, J. R., WHITE, D. A.,WEBB, A. W., BRANCH, C.D., 1966; Isotopic ages of acid igneous rocks in the Cairns hinterland, North Queensland. B. M. R. Bull. **88**.

ROSE, A. W., BURT, D. M., 1979; Hydrothermal Alteration, in BARNES, H. L., (Ed); Geochemistry of hydrothermal ore deposits, 2nd ed. , Wilet Interscience, New York/Chichester/Toronto/Brisbane.

SCHMIDT, R. G., 1985; High-Alumina Hydrothermal systems in volcanic rocks and their significance to mineral prospecting in the Carolina Slate Belt. U.S. Geol.Surv. Bull. 1562.

SCHOCH, A. E., BEUKES, G. J., PRAEKELT, H. E., 1985; A natroalunite - zahaerite - hotsonite paragenesis from Poffader, Bushmanland, South Africa. Canada. Miner. **23**, 29-34.

STEEFEL, C. I., ATKINSON, W. W., 1984; Hydrothermal andalusite and corundum in the Elkhorn district, Montana. Econ. Geol. **79**, 573-579.

STOFFREGEN, R. E., ALPERS, C. C., 1987; Woodhouseite and svanbergite in hydrothermal ore deposits: products of apatite destruction during advanced argillic alteration. Canada. Miner. **25**, 201-211.

SYKES, M. L., MOODY, J. B., 1978; Pyrophyllite and metamorphism in the Carolina Slate Belt. Am. Mineralogist, 63, 96-108.

SWITZER, G., 1949; Svanbergite from Nevada. Am. Mineralog. **34**, 104-108.

VAN DER HOR, F., 1989; The geology of the Balcooma-Dry River region, with emphasis on deformational and metamorphic history. Ph. D. Thesis, J.C.U.N.Q., unpub.

WHITE, D. A., 1962 a; Clarke River - 1:250 000 Geological Series. B. M. R., Aust., Explanatory Notes (E/55-13).

WHITE, D. A., 1962 b; Einasleigh - 1:250 000 Geological Series. B. M. R., Aust., Explanatory Notes (E/55-9).

WHITE, D. A., 1965; The geology of the Georgetown/Clarke River area, Queensland. B. M. R., Aust., Bull. 71.

WITHNALL, I. W., 1989; The Precambrian and Palaeozoic geology of the Southeastern Georgetown Inlier, North Queensland. GSQ Report 2, pub. Qld. Dpt. Mines, Brisbane.

WITHNALL, I. W., 1982; The geology of the Greenvale-Balcooma area., in Withnnall I. W., (Ed); 1982 Field Conference, Charters Towers-Greenvale area., Geol. Soc. Aust., Qld. Div., 31-46.

WITHNALL D. A., MACKENZIE, D. E., 1980; New and revised stratigraphic units in the Proterozoic Georgetown Inlier, North Queensland. Q. G. M. J., **81**, 28-43.

WISE, W. S., 1975; The origin of the assemblage quartz + Al silicate + rutile + Al-phosphate. Fortschr. Miner. **52**, Spec. Issue; IMA papers, 151-159.

WISE, W. S., 1975; Solid solution betwwwen the alunite, woodhouseite and crandellite mineral series. N. Jb. Miner. Mh., **12**, 540-545.

WISE, S.W., LOH, E. S., 1976; Equilibria and the origin of minerals in the system Al_2O_3-$AlPO_4$-H_2O. Am. Mineral. **61**, 409-413.

WOJDAK, P. J., SINCLAIR, A. J., 1984; Equity Silver Silver-Copper-Gold deposit: Alteration and fluid inclusion studies. Econ. Geol. **79**, 969-990.

WYATT, D. H., PAINE, A. G. L., CLARKE, D. E., GREGORY, C. M., HARDING R.R., 1971; Geology of the Charters Towers 1:250 000 sheet area, Queensland. B. M. R., Aust., Report 137.

APPENDIX 1 - MICROPROBE ANALYSES

Qualitative Analyses

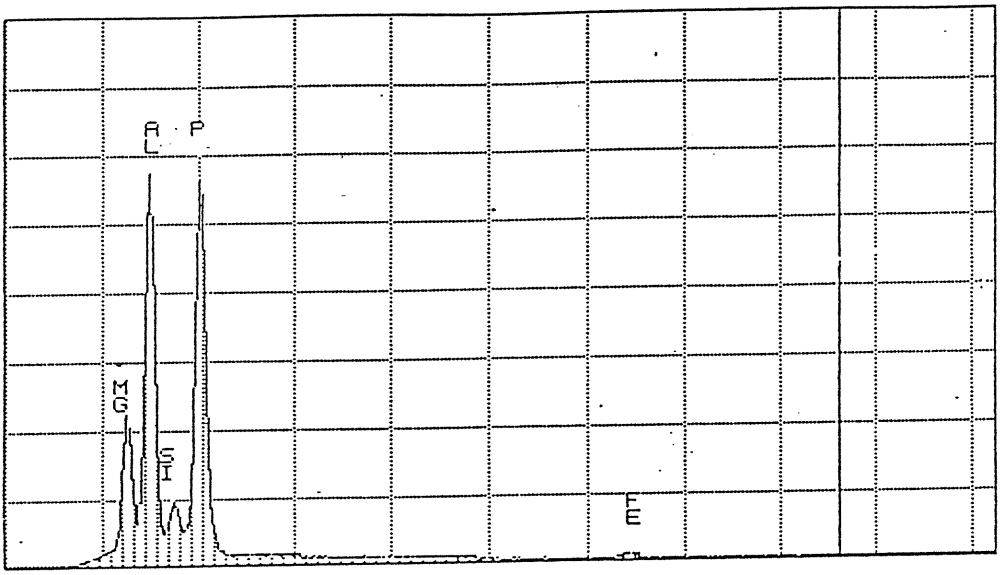

TS 158: Scorzalite

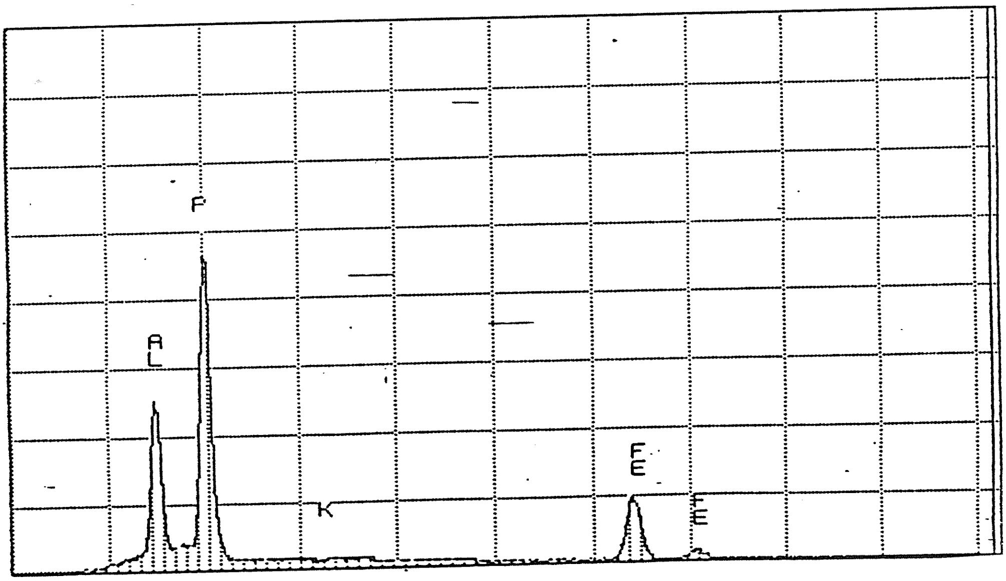

TS 154: Souzalite, a dark green hexagonal mineral occuring as an alteration product of scorzalite and associated with pyrite

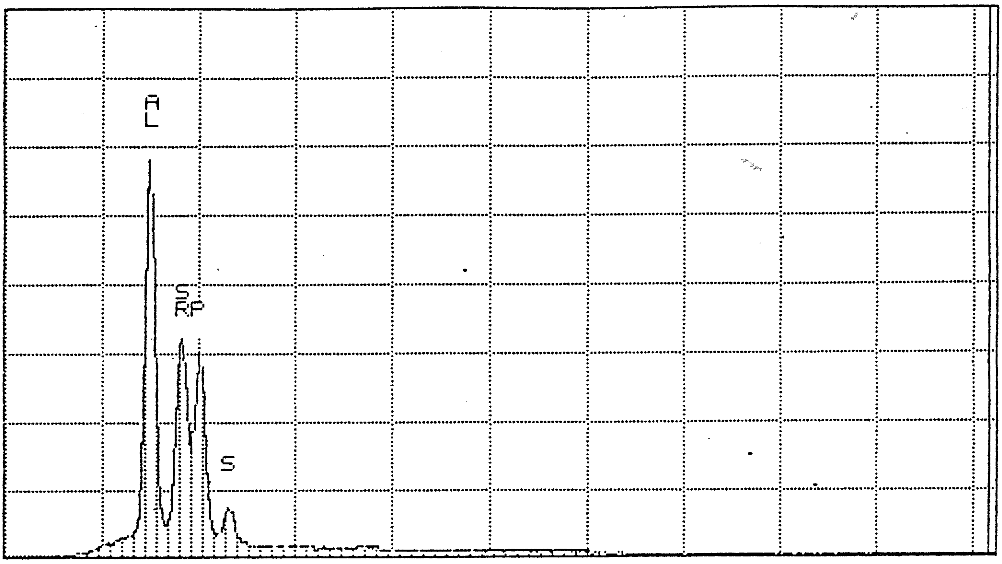

TS 148: Svanbergite

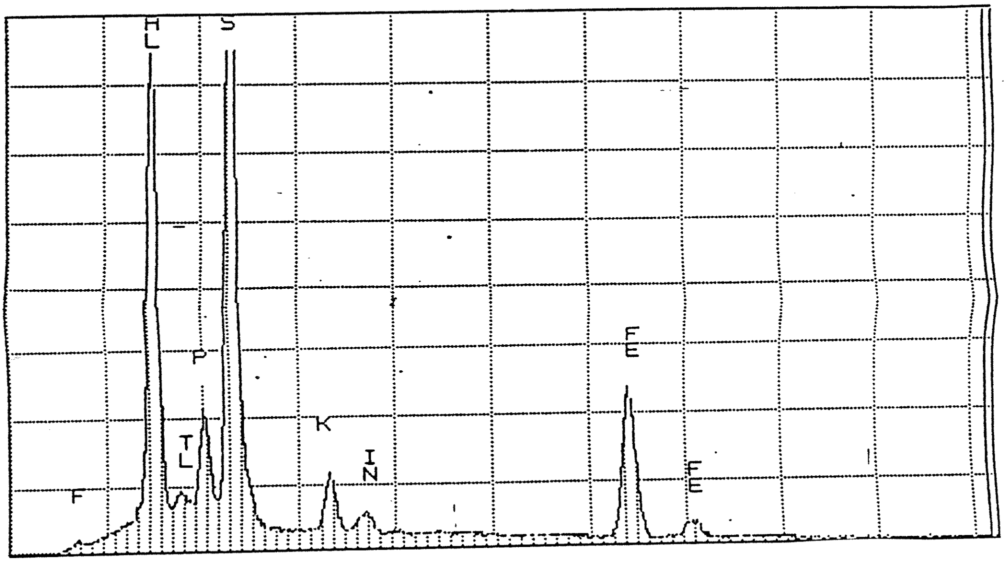

TS 154: Hallotrichite, the Fe rich member of the alunite group, occuring as a alteration product of pyrite.

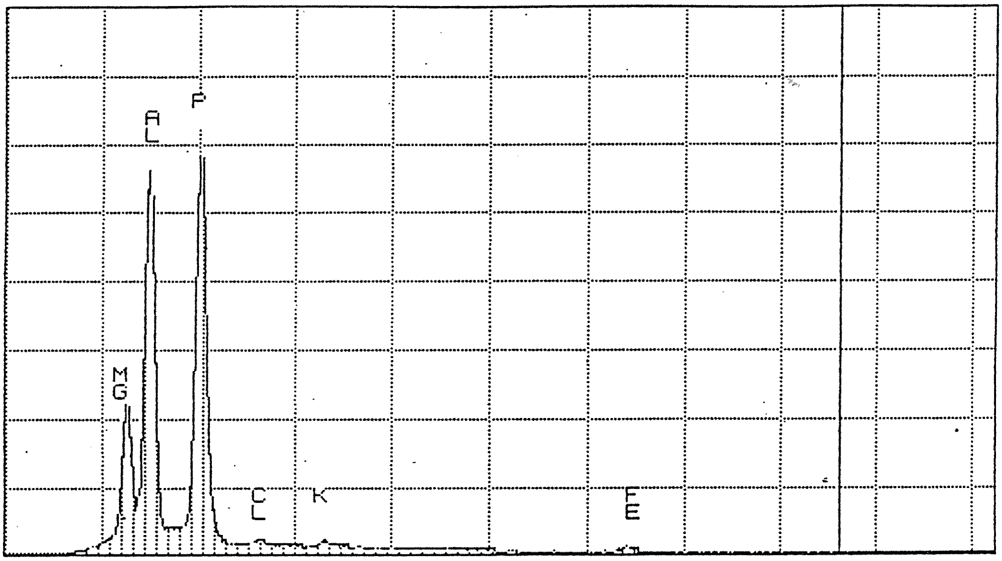

TS 158: Scorzalite

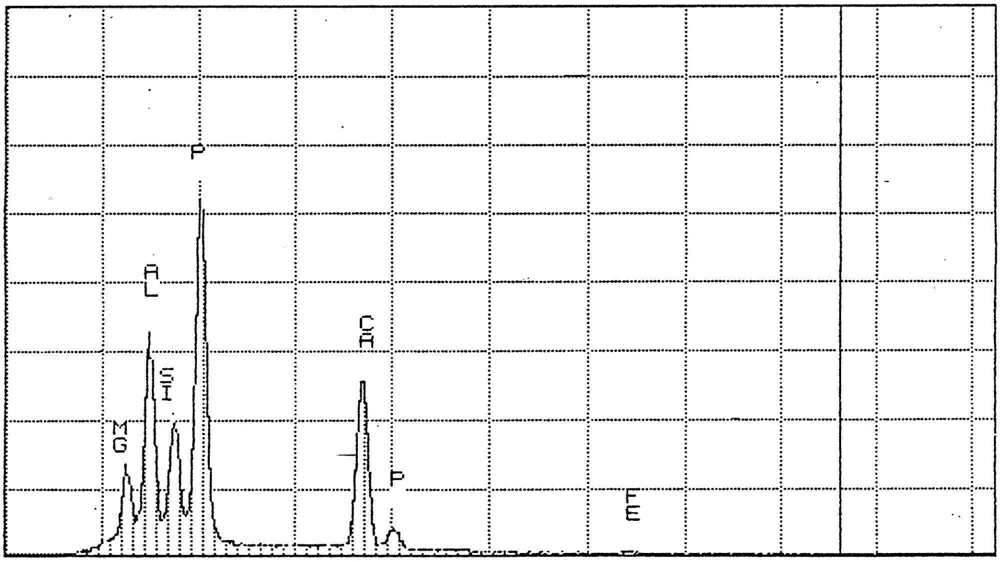

TS 158: Unidentified, possibly a zeolite, in a clay vein

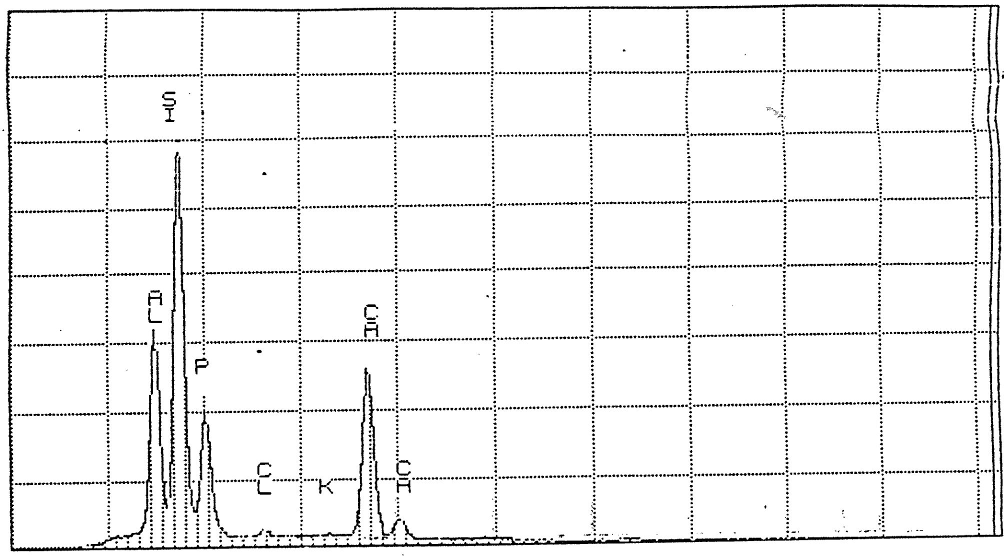

TS 158: Possibly a zeolite, e.g. viseite ($5CaO.6Al_2O_3.3SiO_2.3\ 1/2P_2O_5.\ 1\ 1/2F.36H_2O$), in a clay vein

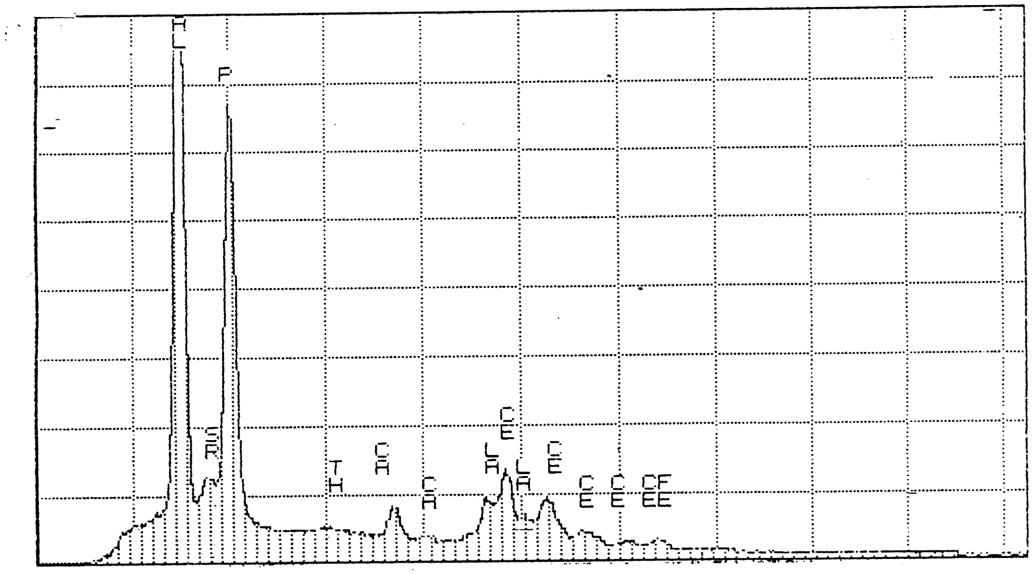

TS 162: Florencite, in a clay vein

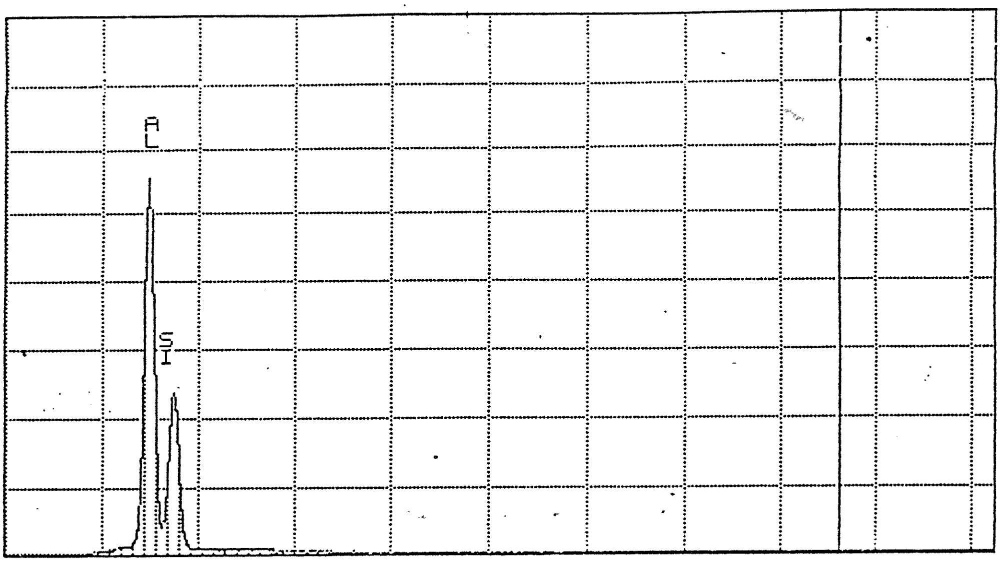

TS 158: Kaolinite in a vein

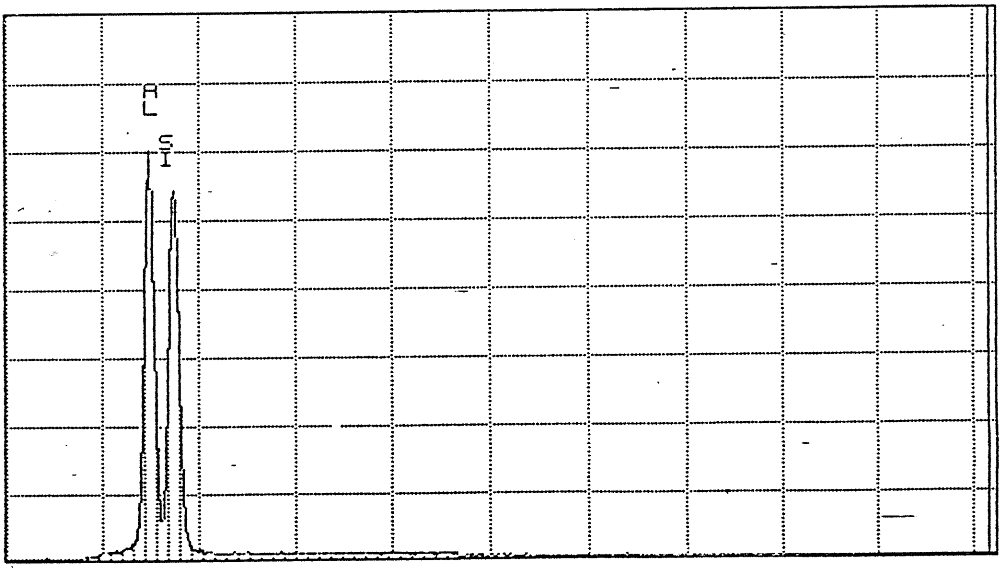

TS 158: pyrophyllite in a vein

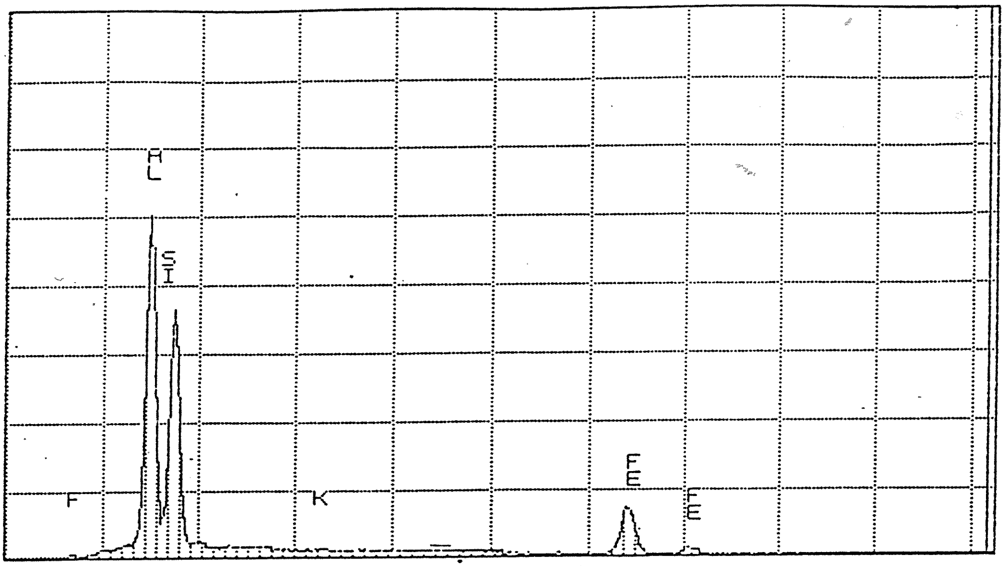

TS 154: Tiny crystal in andalusite

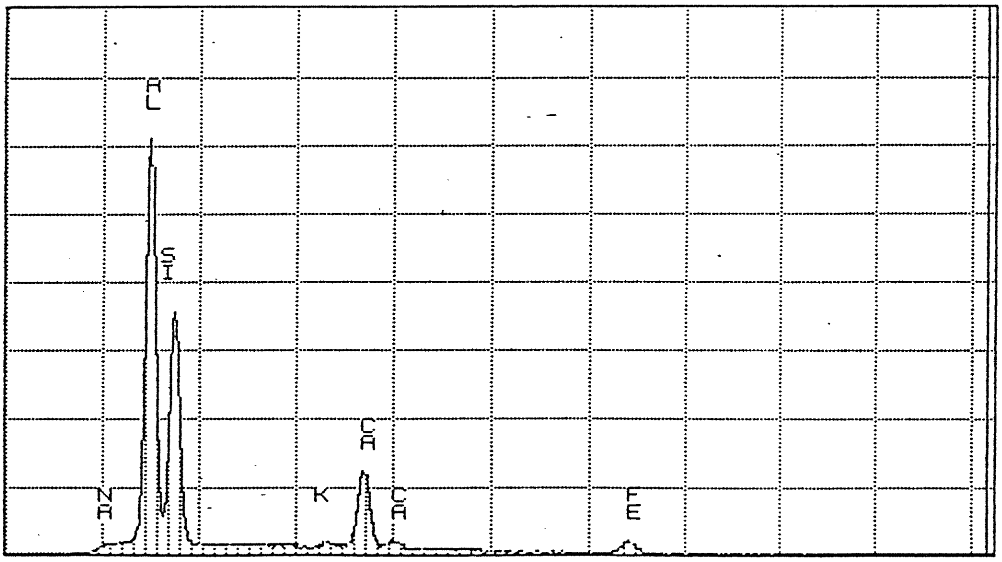

TS 154: Tiny euhedral crystal in andalusite

Quantitative analyses

ALUMINIUM SILICATES

Al2SiO5 (Andalusite/ kyanite)

TS:	158	159	159	130
SiO_2	36.52	38.55	36.74	36.46
Al_2O_3	64.64	64.57	65.23	61.37
MgO	0.16	0.00	0.11	0.00
K_2O	0.04	0.00	0.00	0.00
TiO_2	0.00	0.12	0.00	0.00
CaO	0.00	0.12	0.05	0.00
MnO	0.00	0.00	0.10	0.38
TOTAL:	101.37	103.30	102.56	98.22

DIASPORE

				CORUND.
TS:	163	163	159	159
SiO_2	2.899	0.3965	0.6012	0.1805
Al_2O_3	86.60	90.64	87.66	102.69
TiO_2	0.059	0.00	0.00	0.00
FeO	0.00	0.1617	0.00	0.00
TOTAL:	89.55	91.20	88.52	103.00

MUSCOVITE

TS:	130	130	159	161	162
SiO_2	45.95	46.73	49.88	47.79	50.26
Al_2O_3	36.63	38.25	38.32	38.72	40.15
FeO	0.25	0.25	0.017	0.265	0.148
MgO	0.19	0.14	0.212	0.181	0.00
CaO	0.00	0.10	0.00	0.00	0.00
Na_2O	0.32	0.08	0.702	0.309	0.271
K_2O	6.72	3.58	7.93	6.22	8.58
TiO_2	0.00	0.00	0.194	0.00	0.00
TOTAL:	90.05	89.14	96.84	93.63	99.77

KAOLINITE			PYROPHYLLITE		
TS:	130	159	130	130	159
SiO_2	47.65	41.21	67.79	64.89	51.45
Al_2O_3	38.32	49.00	28.42	28.10	39.86
FeO	0.08	0.095	0.00	0.00	0.00
MgO	0.00	0.114	0.00	0.00	0.00
CaO	0.10	0.00	0.00	0.00	0.00
Na_2O	0.00	0.18	0.00	0.00	0.00
K_2O	0.06	1.75	0.00	0.00	0.00
P_2O_5	0.00	0.1240	0.00	0.12	0.00
TiO_2	0.00	0.118	0.00	0.00	0.00
TOTAL:	86.21	92.50	96.33	93.12	91.31

TOPAZ

TS:	148	120	120
SiO_2	34.16	32.12	32.79
Al_2O_3	53.58	56.59	56.61
FeO	0.20	0.00	0.11
MgO	0.00	0.098	0.00
CaO	0.00	0.00	0.10
Na_2O	0.15	0.00	0.00
Rb_2O	1.1408	0.00	0.00
TOTAL:	88.38	88.71	90.75

(F peak observed in qualitative analyses)

PHOSPHATES

APATITE

TS:	148	120	120
P_2O_5	42.44	40.42	40.76
CaO	56.2	53.95	55.38
TiO_2	0.09	0.00	0.00
Cl	0.07	0.00	0.00
SiO_2	0.00	0.87	0.81
Al_2O_3	0.00	0.15	0.13
TOTAL:	98.6	95.49	98.18

SVANBERGITE/GOYAZITE

TS:	148	148	148	148	158	158	148	159
P_2O_5	18.38	1.47	1.13	18.31	5.18	18.56	13.51	40.30
Al_2O_3	36.41	40.51	37.96	36.56	43.68	36.62	39.75	38.19
SiO_2	1.49	21.23	22.19	0.78	24.60	1.20	1.04	12.20
CaO	0.25	0.05	0.00	0.19	2.65	0.25	0.354	0.197
MgO	0.13	0.06	0.12	0.15	0.27	0.24	0.26	0.180
Na_2O	0.16	0.14	0.17	0.11	0.22	0.14	0. 00	0.00
TiO_2	0.00	0.90	0.81	0.18	0.44	0.00	0.00	0.34
TOTAL:	57.16	64.36	62.38	56.11	77.10	57.35	54.92	91.49

(These are observed to contain appreciable S and Sr in qualitative analyses)

Also unusual phosphate minerals not closely corresponding to available analyses were observed in small amounts. 'Phosphate Minerals' (Nriagu and Moore,1984) contains a comprehensive listing of common and rare phosphate minerals with analyses, if available.

TS:	159	159
P_2O_5	53.47	18.31
Al_2O_3	37.09	73.12
SiO_2	0.768	0.98
CaO	0.081	0.00
MgO	0.00	0.212
Na_2O	0.09	0.195
TOTAL:	92.04	93.13

APPENDIX 2 - XRF DATA

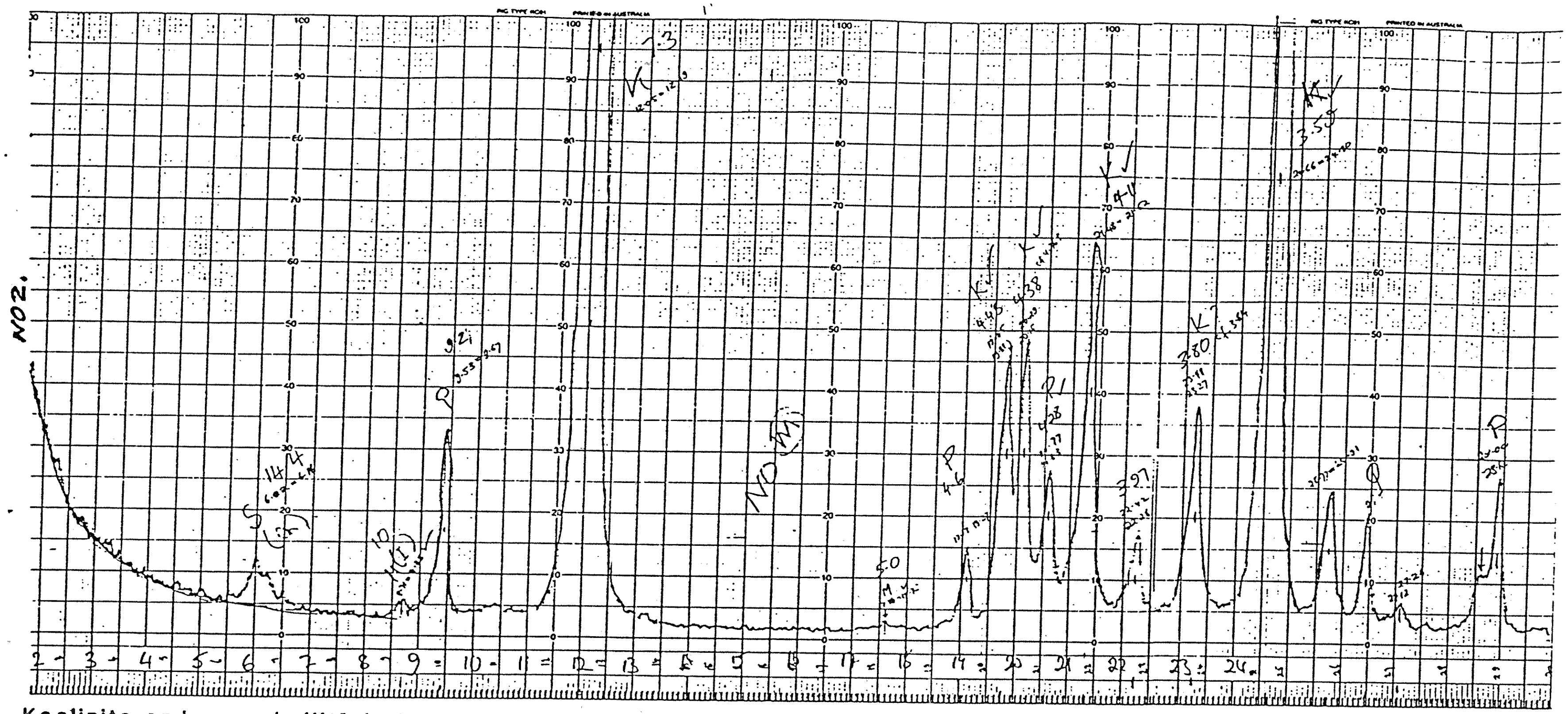

DDH2 234.2m

Kaolinite and pyrophyllite in translucent vein (possibly smectite)

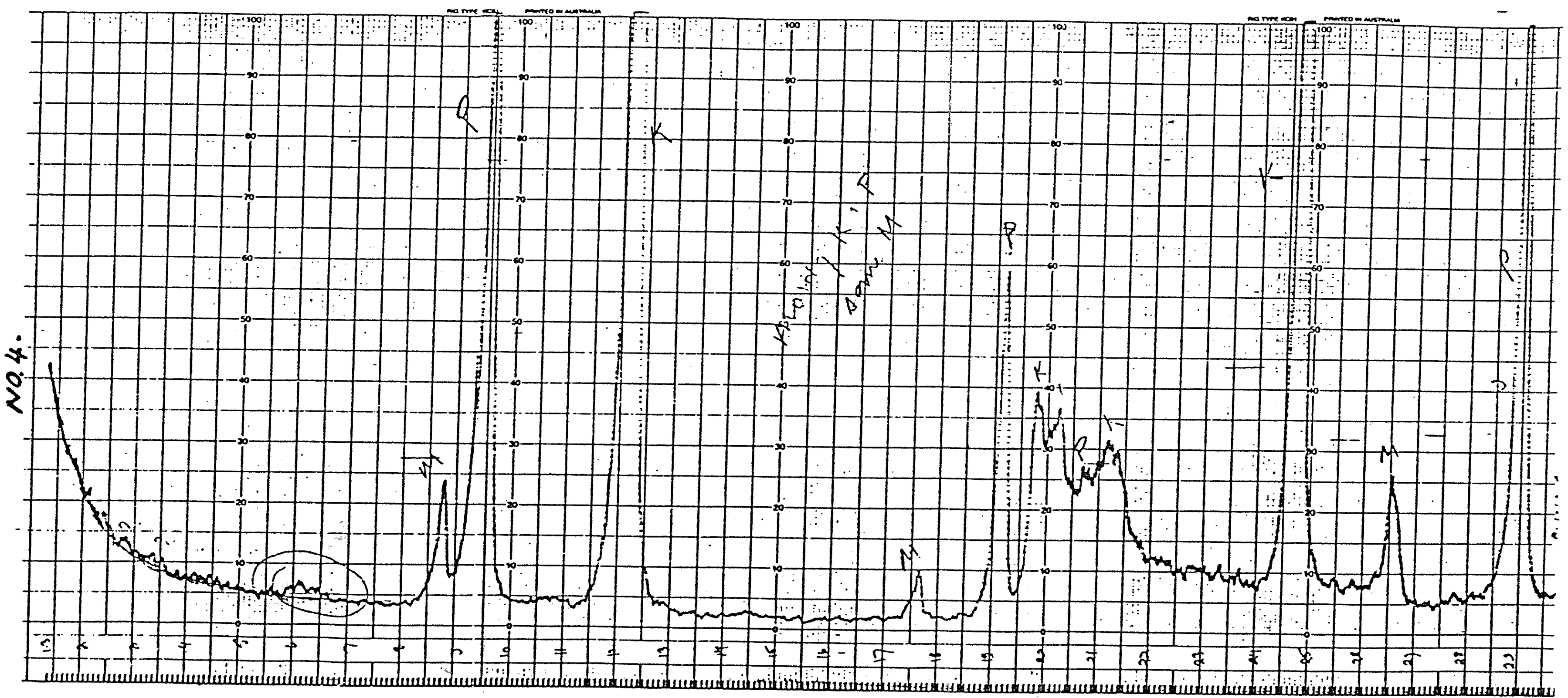

DDH2 231.9m

Kaolinite and pyrophyllite in white vein (lesser muscovite, low T)

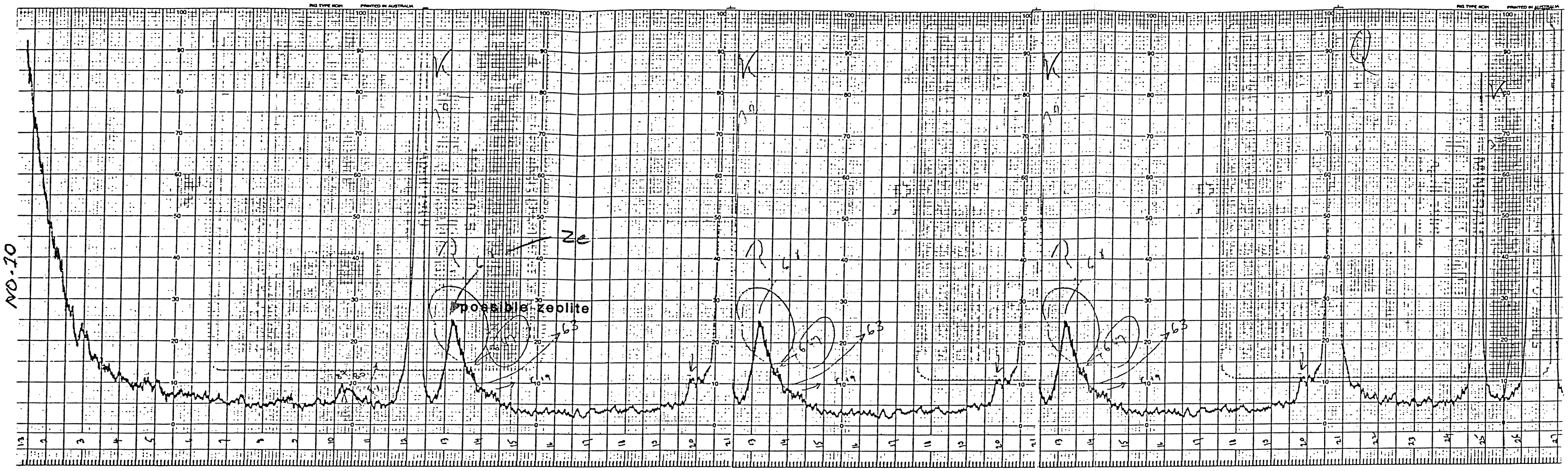

FIELD SAMPLE 28F Quartz vein, in intensley clay altered area

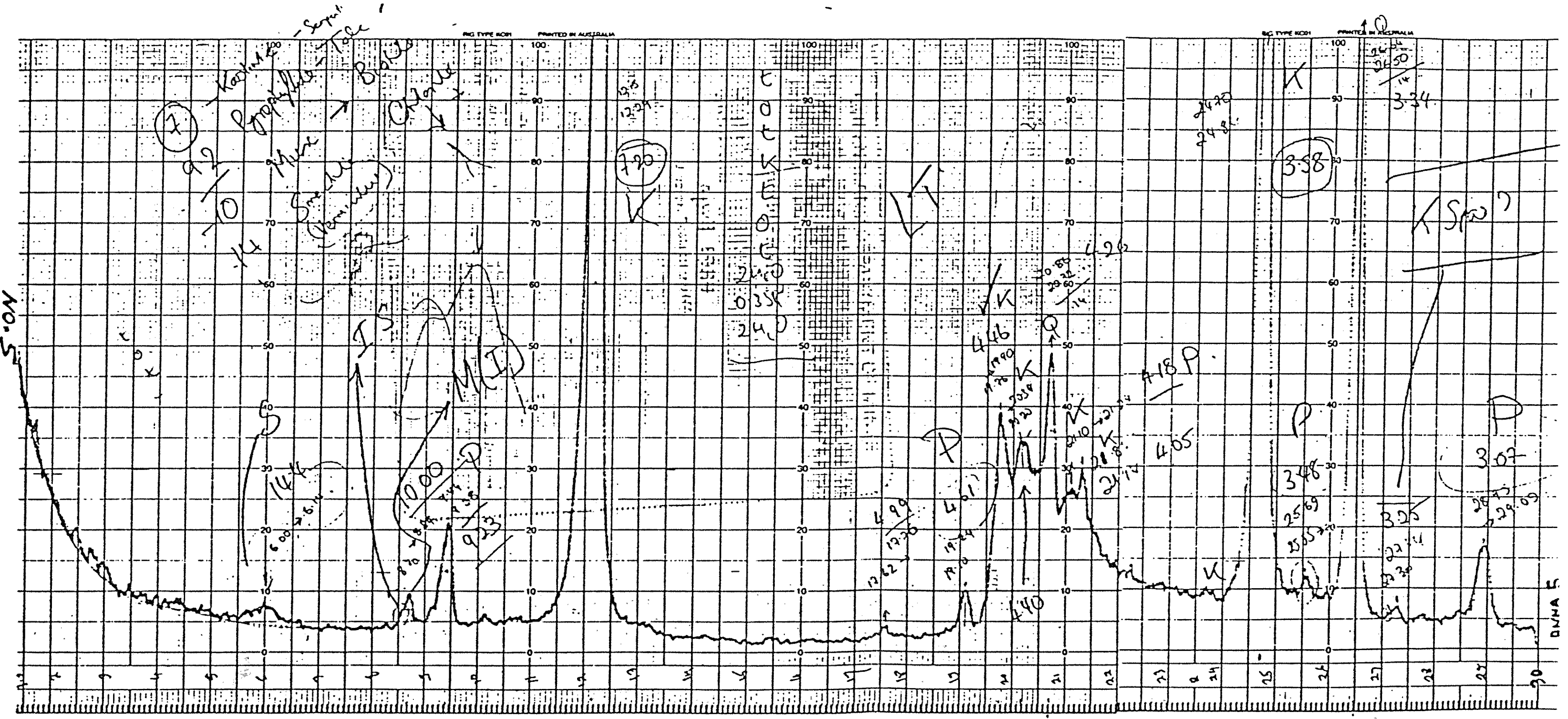

DDH4 119.4m

Dark translucent matrix to clay alterated rock: mostly kaolinite, also pyrophyllite and quartz, lesser muscovite/illite and smectite

NO.7

DDH4 44.3m

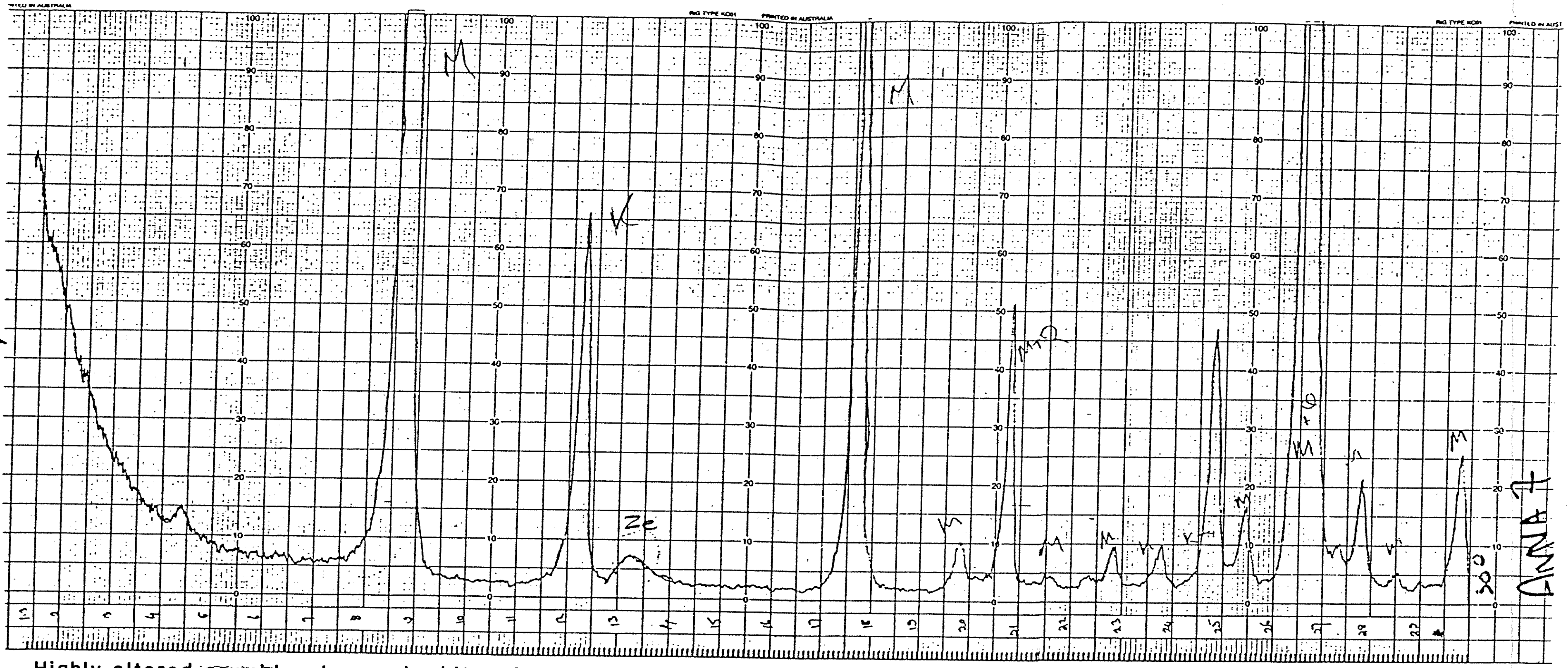

Highly altered crumbly clay and white mica zone: dominantly muscovite, lesser kaolinite and alittle quartz.

NO.8

DDH4 81.5m

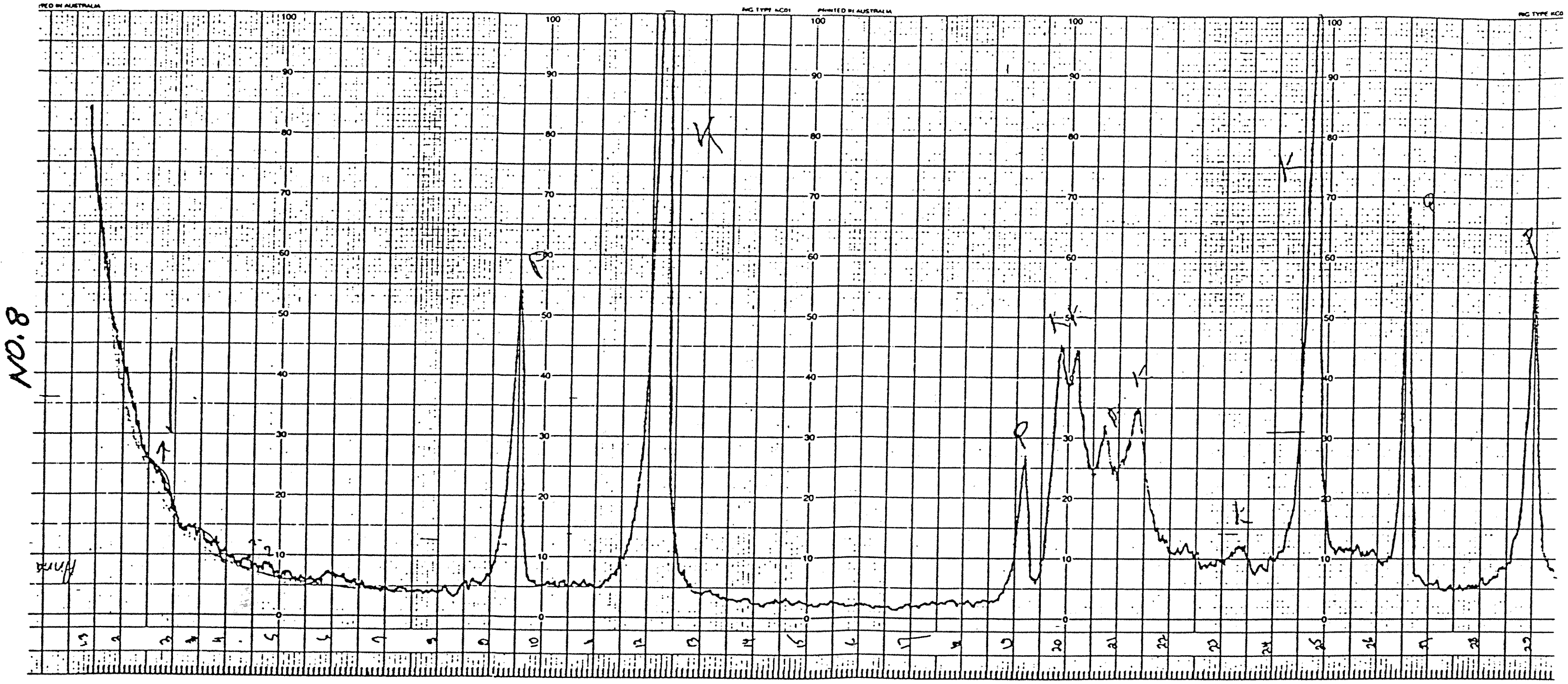

Pyrophyllite kaolinite vein

DDH4 64.0m

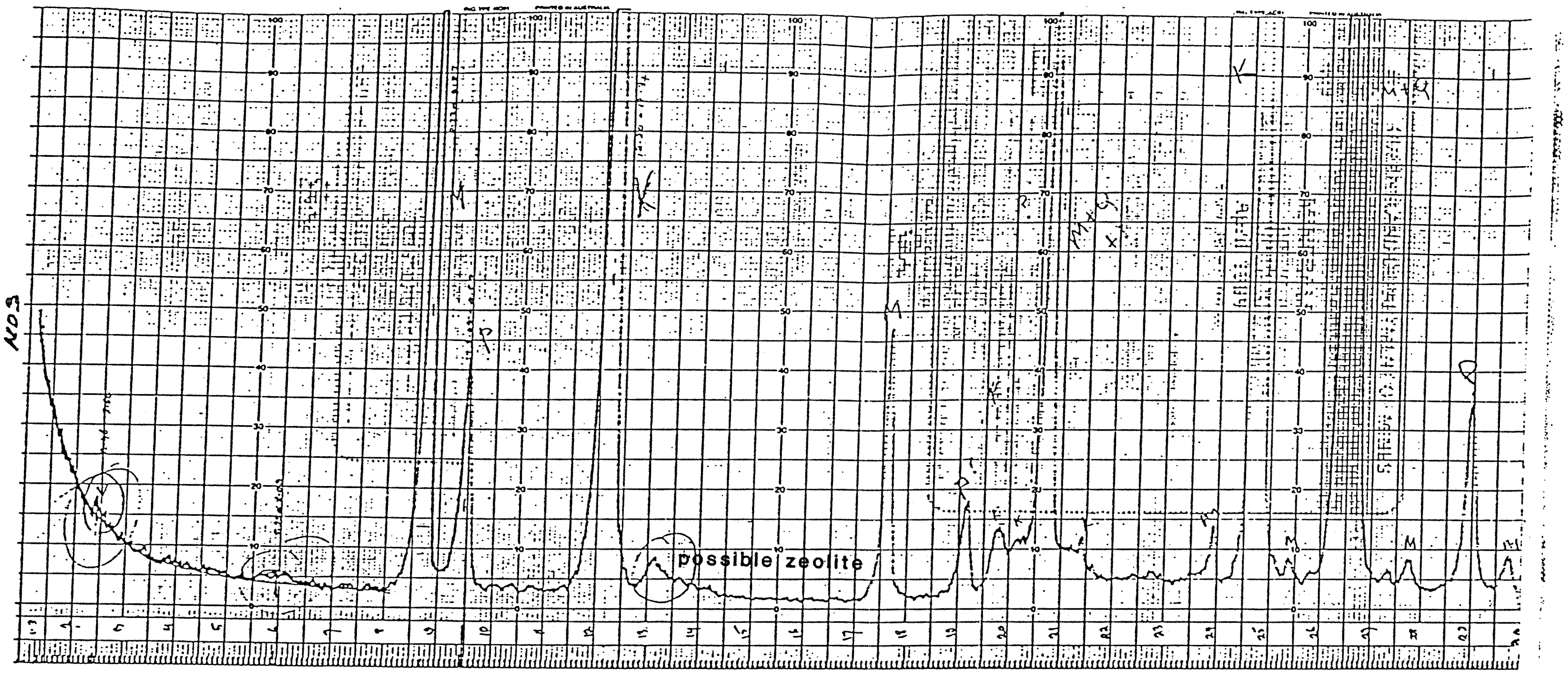

Translucent matrix to clay altered rock: pyrophyllite and kaolinite, lesser muscovite.

DDH4 57m

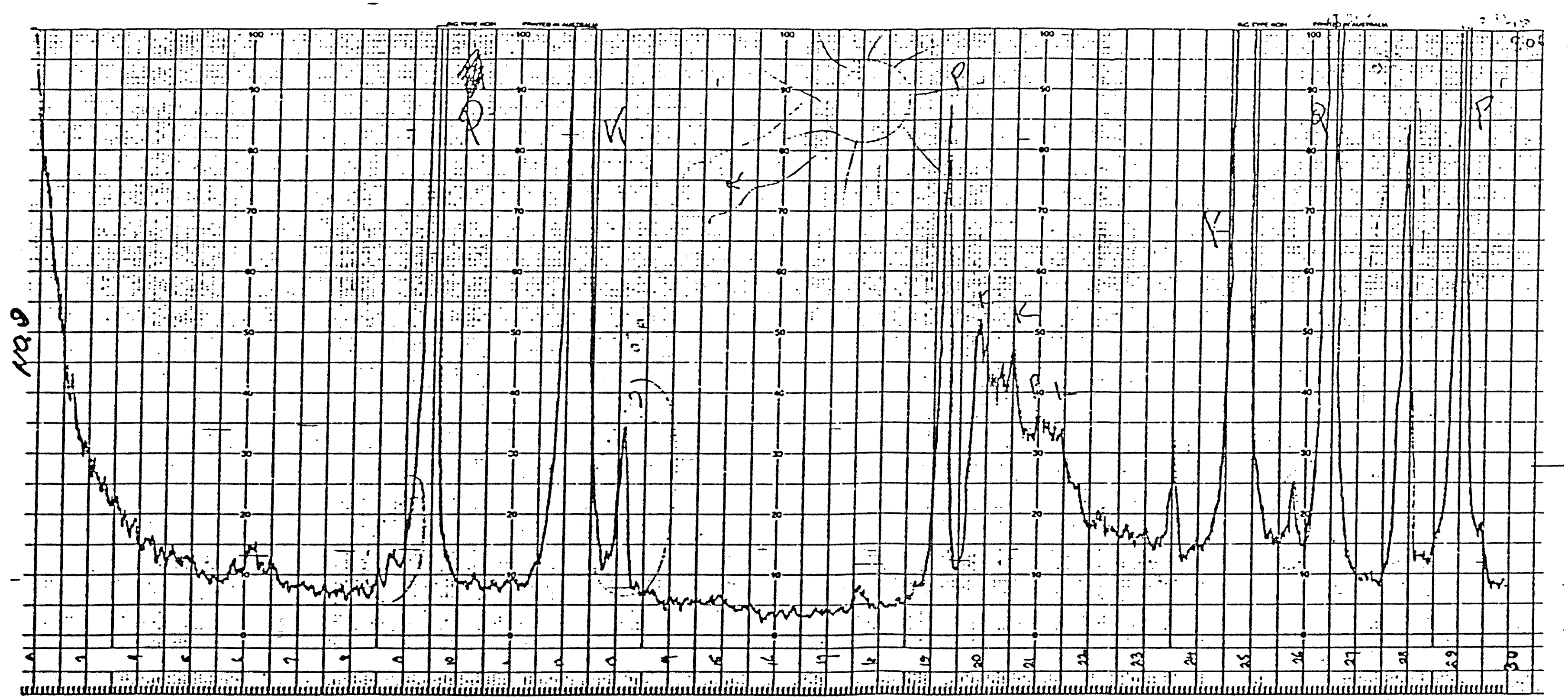

Highly altered kyanite vein: pyrophyllite and kaolinite,quartz, kyanite.

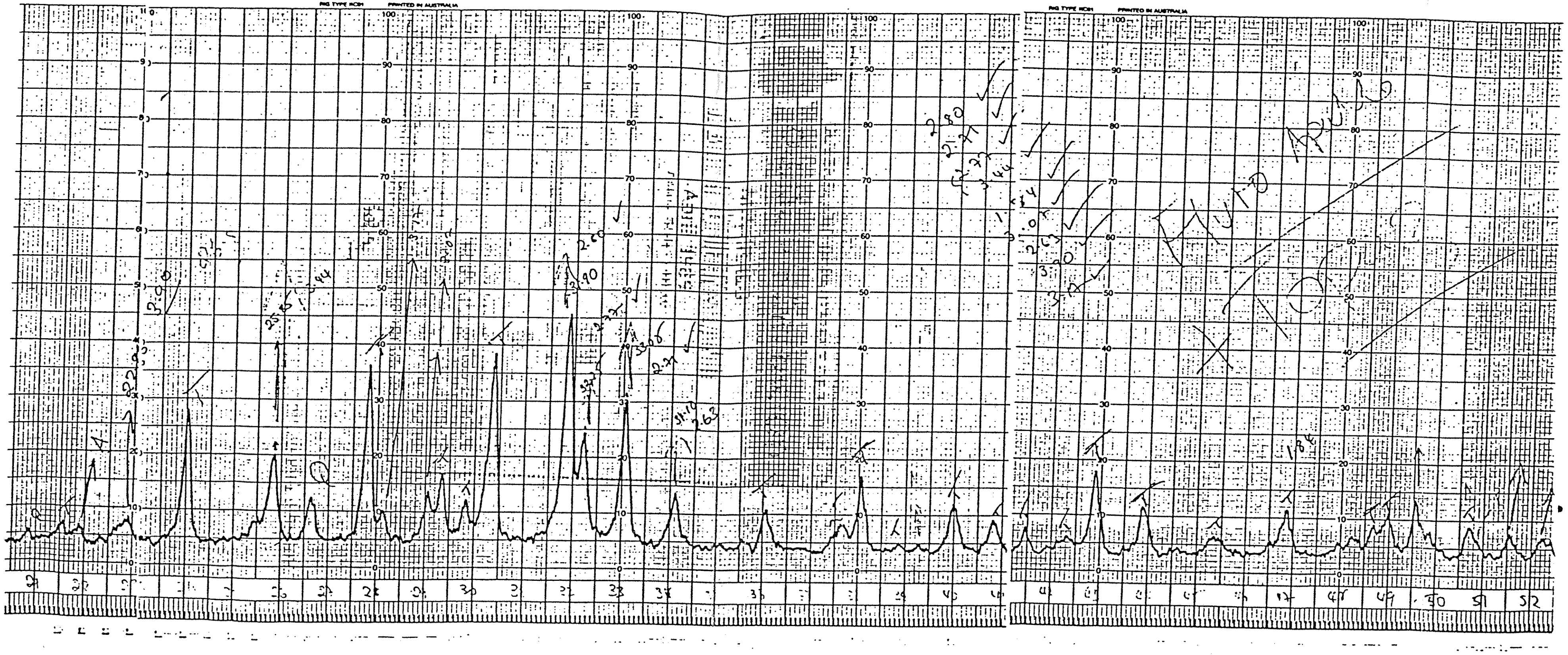

DDH3 109.3m

Topaz-flourapatite vein

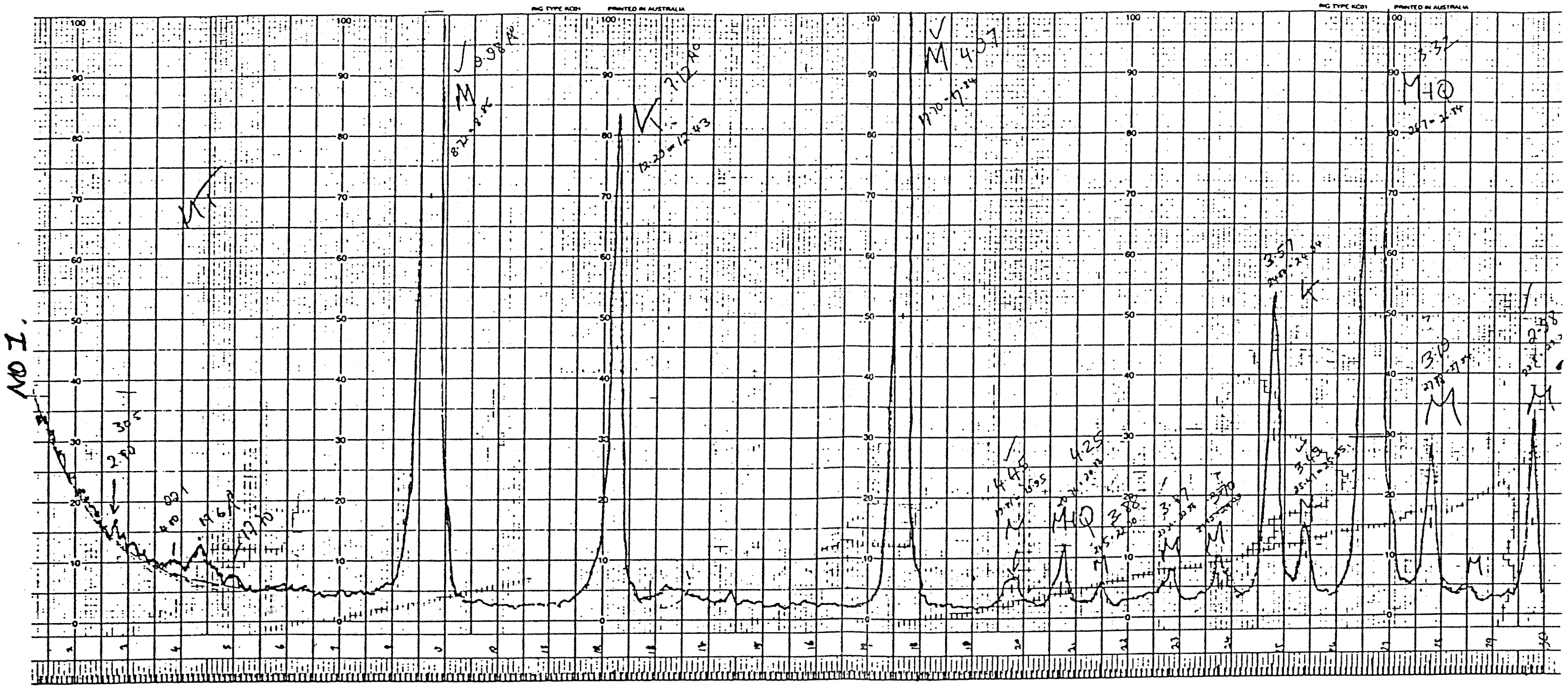

DDH3 98.7m

Highly altered crumbly clay and mica zone: muscovite with less kaolinite, and quartz.

APPENDIX 3 - DRILL LOG SUMMARIES

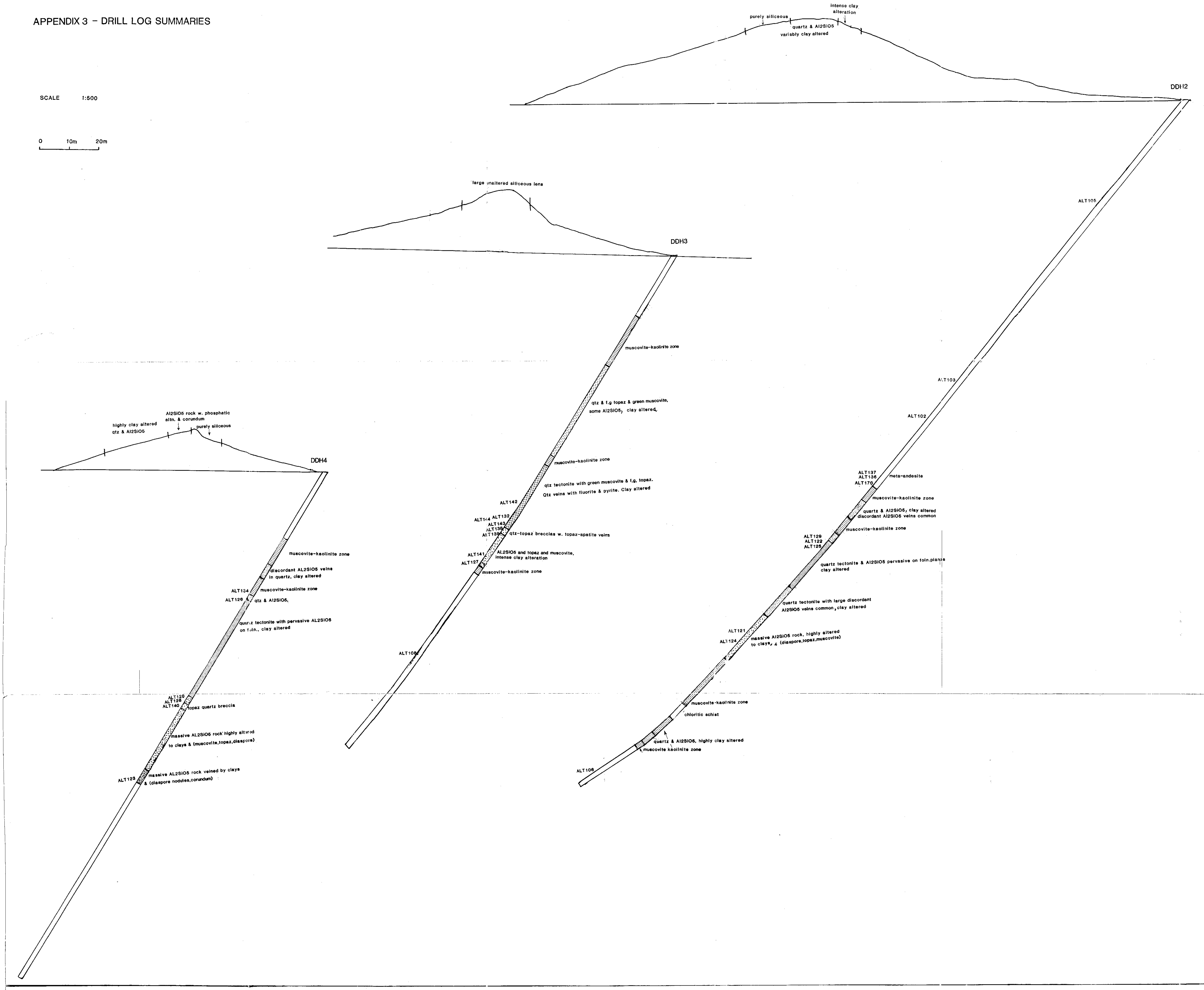

KEY

▨	Quartz tectonite
☐	Quartz tectonite – andalusite/kyanite rock (± muscovite)
▨	Andalusite/kyanite rock (± muscovite – topaz)
▤	Topaz – quartz rock
▩	Highly clay altered rock
▧	Phosphatic alteration

QUARTZITE RIDGE

ALTERATION GEOLOGY
AND
SAMPLE LOCATIONS

SCALE 1:2000

0m 40m 80m 120m

Mapped and drafted by A.L.Timmins. 1989

APPENDIX 5 - GEOCHEMICAL ANALYSES (Withnall, 1989)

Balcooma Metavolcanics

Reg. No.	13527	13531	12518	80304006	80304056	80304024	80304025	80304026	80304023	80304021	80304022	79300436	80304019
1:100 000	7759	7759	7860	7860	7860	7860	7860	7860	7860	7860	7860	7860	7860
Grid ref.	324613	318654	542203	541193	513123	539136	520102	524099	541138	550141	541138	521559	519162
Interval	Duffs Ra	Duffs Ra	E	E	E	B	B	B	B	B	B	F	F
Rock type	Biotite gneiss	Musc. gneiss	Meta-tuff	Meta-basalt	Meta-dolerite	Meta-rhyolite	Meta-rhyolite	Meta-rhyolite	Meta-rhyolite	Fol. meta-rhyolite	Meta-rhyolite	Aphyr. meta-rhyolite	Porph. meta-rhyolite
SiO_2	76.10	79.90	62.20	53.40	54.40	79.90	78.90	83.60	78.90	78.60	83.70	73.00	72.50
TiO_2	0.14	0.07	0.91	1.20	1.60	0.08	0.09	0.07	0.09	0.39	0.08	0.39	0.40
Al_2O_3	12.30	11.60	14.00	15.60	15.50	11.40	11.40	9.20	11.70	12.80	9.00	12.80	12.80
Fe_2O_3	1.00	0.10	1.72	3.30	2.80	0.30	0.30	0.10	0.80	0.80	0.40	1.60	1.40
FeO	0.80	0.10	5.05	6.90	8.70	0.40	0.70	0.40	0.40	0.30	0.30	3.00	2.20
MnO	<0.10	<0.10	0.13	0.10	0.20	<0.10	<0.10	<0.10	<0.10	<0.10	<0.10	0.10	0.10
MgO	0.10	<0.10	3.40	6.60	4.50	<0.10	0.20	<0.10	0.20	0.50	<0.10	0.20	<0.10
CaO	0.50	0.10	6.30	5.50	7.80	0.80	2.00	0.60	0.10	0.60	1.10	1.60	2.30
Na_2O	3.90	0.40	4.35	5.00	2.60	4.10	3.30	3.50	2.60	2.00	2.40	3.40	3.70
K_2O	4.40	6.60	0.25	0.10	0.50	1.70	2.20	1.50	4.30	3.40	2.00	2.80	2.30
P_2O_5	0.01	<0.01	0.17	0.20	0.41	<0.01	<0.01	<0.01	<0.01	<0.01	<0.01	0.04	0.05
CO_2			0.02	0.10		0.50						0.70	1.10
H_2O+	0.30	0.60	0.94	1.20	0.40	0.60	0.70	0.50	0.70	0.80	0.50	0.40	0.60
H_2O-	<0.10	<0.10	0.18	0.10	<0.10	0.10	<0.10	<0.10	<0.10	<0.10	<0.10	<0.10	<0.10
Total	99.55	99.46	99.62	99.30	99.41	99.87	99.78	99.46	99.78	100.18	99.47	100.03	99.45
Ba	1130	1270	120	38	140	615	920	450	960	470	780	510	410
Rb	85	150	5	<5	15	75	80	60	175	120	90	65	55
Sr	55	60	310	165	270	100	130	50	50	35	75	45	65
Pb	5	5	25	85	5	20	25	30	10	20	10	5	40
Th	10	10	8	<5	<5	10	10	10	10	15	5	10	10
Zr	185	85	150	95	120	100	95	85	100	105	75	300	300
Nb	55	10	-	10	10	10	10	<5	10	15	10	25	20
Y	55	25	22	20	30	25	40	25	30	45	35	50	65
La	87	26	-	17	18	41	36	25	25	29	28	39	39
Ce	150	42	-	18	44	72	66	52	48	47	52	76	80
V	5	<5	150	230	170	5	<5	<5	5	<5	<5	<5	15
Cr	<10	<10	60	110	70	<10	<10	<10	<10	<10	<10	<10	<10
Ni	<10	<10	60	20	<10	<10	<10	<10	<10	<10	<10	<10	<10
Cu	<5	<5	15	260	5	<5	<5	<5	10	<5	<5	<5	<5
Zn	30	10	-	745	195	60	75	55	65	90	60	230	310
Ga	18	13	-	-	-	10	10	7	14	15	6	14	14
Ti/Zr	4.5	4.9	36.0	76.0	80.0	4.8	5.7	4.9	5.4	22.3	6.4	7.8	8.0
Y/Nb	1.0	2.5	-	2.0	3.0	2.5	4.0	-	3.0	3.0	3.5	2.0	3.3
Zr/Nb	3.4	8.5	-	9.5	12.0	10.0	9.5	-	10.0	7.0	7.5	12.0	15.0
Zr/Y	3.4	3.4	6.8	4.8	4.0	4.0	2.4	3.4	3.3	2.3	2.1	6.0	4.6
Mg Number	20.5	-	54.1	57.8**	44.9**	-	37.6	-	54.7	81.9	-	10.4	-
Differentiation Index	95.2	95.9	56.7	43.8	35.3	94.1	88.4	95.9	95.3	89.7	93.1	83.5	83.3
S-I Index	1.02	1.45	0.74	0.85	0.81	1.13	0.99	1.09	1.28	1.59	1.11	1.11	1.00
Normative* Mineralogy													
Quartz	35.7	52.9	17.8	-	10.1	48.6	47.0	56.9	47.4	52.4	60.6	37.7	37.3
Orthoclase	26.3	39.6	– 1.5	0.6	3.0	10.2	13.2	9.0	25.7	20.3	12.0	16.8	14.0
Albite	33.3	3.4	37.4	43.2	22.2	35.2	28.2	30.0	22.2	17.0	20.6	29.1	32.1
Anorthite	2.4	0.5	18.2	20.2	29.4	4.0	9.9	3.0	0.5	3.0	5.5	7.8	11.4
Diopside	-	-	10.2	5.2	5.8	-	0.14	-	-	-	-	-	-
Hypersthene	0.5	-	10.3	21.2	23.0	0.2	1.2	0.35	0.5	1.3	-	4.3	2.5
Olivine	-	-	-	4.6	-	-	-	-	-	-	-	-	-
Magnetite	1.5	-	2.5	1.9	2.1	0.44	0.44	0.15	0.71	-	0.41	2.3	2.1
Hematite	-	0.10	-	-	-	-	[illegible]	-	0.32	0.80	0.12	-	-
Ilmenite	0.27	-	1.75	2.3	3.1	0.15	0.17	0.13	0.17	0.42	0.15	0.75	0.78
Rutile	-	0.07	-	-	-	-	-	-	-	0.17	-	-	-
Apatite	0.02	-	0.41	0.48	0.98	-	-	-	-	-	-	0.1	0.12
Corundum	0.22	3.7	-	-	-	1.4	-	0.73	2.6	4.8	0.89	1.36	0.15
Plag An	6.8	12.8	32.8	31.9	56.9	10.3	25.9	9.2	2.2	15.0	21.2	21.1	26.2

* Normative mineralogy calculated on a volatile-free basis

** Mg Number and normative calculated using Fe_2O_3/FeO of 0.15

Analyst - Queensland Government Chemical Laboratory.
Registered numbers prefixed by 8030 or 7930 are stored at the BMR; others are in the Department of Mines rock collection.

Ringwood Park Microgranite

Reg. No.	80304057	80304061
Field No	C7/62/2	C9/14/10
1:100 000	7860	7860
Grid ref	584261	595173
Unit	Ringwood Park Microgranite	Ringwood Park Microgranite
Rock type	micro-granodiorite	micro-granodiorite
SiO_2	74.90	79.50
TiO_2	0.25	0.07
Al_2O_3	13.20	12.60
Fe_2O_3	1.10	0.20
FeO	0.80	0.40
MnO	<0.10	<0.10
MgO	0.30	<0.10
CaO	1.80	1.30
Na_2O	4.70	4.60
K_2O	1.50	0.80
P_2O_5	0.04	<0.01
CO_2		
$H2O^+$	0.90	0.30
$H2O^-$	<0.10	<0.10
Total	99.49	99.66
Ba	965	265
Rb	35	25
Sr	170	200
Pb	5	<5
Th	10	15
Zr	215	110
Nb	15	15
Y	45	50
La	36	26
Ce	80	60
V	15	20
Cr	-10	<10
Ni	-10	<10
Cu	-5	<5
Zn	25	25
Ga	15	14
Mg Number	43.6	-
Differentiation Index	87.7	91.2
S-I Index	1.04	1.17
Normative corundum	0.67	1.81

APPENDIX 6 - SAMPLE LISTS

(P) = polished thin section used in microprobe analyses
(X) = unidentified vein sampled and analysed by XRF

Field No.	ALT TS No.	Minerals/rock type		JCU cat. No.
1		qtz biotite schist		
2		clay alt. andal in qtz mylonite		
3	119	" "		29731
4	156	ky vein in qtz with muscovite		29732
5		as above, with folded qtz veins		
6	163	coarse vein ky in qtz mylonite	(P)	29733
7		coarse ky rock with muscovite		
8		qtz mica pyritic schist		
9		highly alt. ky rock		
10	168	brittle fault breccia		29734
11		pure qtz tect + large casts pyrite		
12		float		
13		float		
14		corundum rock,+ musc and pyroph alt		
15		muscovite pyroph rock, crumbly		
16		pyroph rich rocks, v. soft.		
17		highly clay alt. Al2SiO5 rock		
18		contact Al2SiO5 clay alt.+ qtz tect.		
19	118	qtz topaz breccia		29735
20		as 18		
21	162	highly clay alt. AL2SiO5 rock, breccia	(P)	29736
22		" "		
23		m.g. ky rock.		
24		qtz tect contact to qtz topaz breccia		
25		qtz tectonite, unaltered		
26		highly clay altered qtz andal rock		
27A		alt. andal/musc/topaz clay contact		
27B		with unalt. qtz lens		
27C	167	qtz tect + musc topaz veins		29737

28A	116	highly clay altered andalusite rock		29738
	113	" "		29739
	150	has andalusite vein		29740
28B	166	v. alt qtz /andal/topaz/clay rock		29741
	165	" "		29742
28C	159	corundum andalusite rock	(P)	29743
28D	147	banded andal/diaspore rock		29744
	148	with phosphates	(P)	29745
	160	no phosphates		29746
28E		white alt qtz rock		
28F		v. alt qtz/andal rock and alt qtz vein		
28G		see B		
28H		see A		
28I	158	diaspore, corund, andal rock	(P)	29747
28J	117	andal, phosphate rock		29748
	115	" "		29749
	146	andal,phos,diaspore,apatite		29750
	170	with late andalusite vein		29751
29	112	qtz topaz breccia		29752
30		weathered country rock		
31 I.	154	ky/and + corund, apatite veins (P)		29753
31 II	155	as above, more musc alt.		29754
31 III.	149	ky, + musc,topaz, diaspore,clay		29755
31 IV.	157	" "		29756
32	161	qtz + Al2SiO5 fine network	(P)	29757
33		coarse vein of Al2SiO5 in above		
34	151	ky rock with qtz fragments		29758
35		qtz chlorite sericite schist		
36A	169	qtz mylonite with Al2SiO5 alt to clays		29759
36C		coarse Al2SiO5 veins in qtz tect + musc		
36D	153	alt coarse ky and diaspore nodules + topaz		29760
36E		" "		
36F	145	white m.g. kyanite rock,andal, diaspore		29761
	152			29762
39	164	ky + corundum breccia + musc		29763

Drillcore location	**ALT TS No.**		**JCU cat No.**
DDH2 48.5m	105	qtz/actinol/albite/chlorite schist	29764
DDH2 137	102	qtz/chlorite/epidote schist	29765

DDH2	121.6	103		qtz schist, calcareous schist	29766
DDH2	166.5	137		qtz/albite/chlorite+musc alt	29767
DDH2	166.6	136		" "	29768
DDH2	169.5	171		pyritic qtz/musc tr chlor schist	29769
DDH2	190.3	130	(P)	3cm wide kyanite vein in qtz	29770
DDH2	190.4	135		coarse kyanite in qtz vein	29771
DDH2	191.9	129		qtz+kyanite alt. topaz/musc+clays	29772
DDH2	194.2	125		qtz+andal, pyrite, clay alt.	29773
DDH2	193.3	122	(X)	qtz+andal, andal vein-clay alt.	29774
DDH2	232.9	121		v. clay alt.,topaz/musc, diaspore	29775
DDH2	234.6	124		v. clay alt.,musc/topaz, diaspore	29776
DDH2	305.5	106		qtz/biotite schist	29777
DDH4	46.0	134		coarse ky encloses qtz fragments	29778
DDH4	47.0	131		ky veins in qtz, rep'd by clay	29779
DDH4	50.9	126		qtz+ky, f.g. topaz, clay alt.	29780
DDH4	91.7	128		qtz+topaz breccia, apatite, musc.	
DDH4	91.7	120	(P)	v.clay alt.,relict andal patches	
DDH4	91.9	140		qtz+topaz breccia+rebrecc, apatite	
DDH4	122	123		andal+diaspore nodules, clay alt.	
DDH4	123	101		qtz/albite/chlorite/sericite schist	
DDH3	99.0	142		qtz+topaz,pyrite,flourite,apatite	
DDH3	102.1	144		qtz+musc, topaz,andal,pyrite	
DDH3	107.0	143		qtz tect, topaz,pyrite.	
DDH3	109.3	138		qtz+topaz, apatite-qtz veins	
DDH3	109.3	139	(X)	Qtz+topaz, topaz-apatite vein	
DDH3	122.4	141		v. clay alt, mostly qtz+pyrite	
DDH3	124.2	127		sheared qtz+topaz, apatite,musc.	
DDH3	103.6	132		qtz+musc, topaz, crenulated	
DDH3	159.5	109		f.g qrtzite/musc/chlor/epidote/ser	
DDH3	161.0	108		f.g. qtzite/ser/chlor/calcite, veins	

STABILITY RELATIONSHIPS IN THE SYSTEM Al_2O_3-SiO_2-H_2O WITH APPLICATION TO HYDROTHERMAL ALTERATION ENVIROMENTS

Anna Timmins BSc.
1989

Submitted in partial fulfillment of the requirements for the degree of Bachelor of Science with Honours in the Department of Geology, of the James Cook University of North Queensland.

ABSTRACT

Construction of phase stability diagrams of the Al_2O_3-SiO_2-H_2O (A-S-H) system are useful in aiding interpretation of the paragenesis and conditions of formation of aluminous assemblages, such as advanced argillic alteration suites in solfarctic and porphyry systems.

Experimental determination of equilibria in the A-S-H system are used to quantify phase diagrams. Results of early workers have been misleading and inaccurate due to non-recognition of metastable phases and undemonstrated reversibility.

Phase diagram topologies and reaction directions are derived from geologic knowledge of incompatabilities to produce qualitative diagrams produced from first principles. Mineral associations are assumed to be in local equilibrium and the phase rule is modified to P=C-M to allow consideration of hydrothermal alteration enviroments.

Phase relationships are controlled dominantly by T , $aSiO_2$ and aH_2O. Reactions between minerals within the system are those of dehydroxylation / rehydroxylation and silicification / desilicification. Pressure effects on topologies are minimal.

Hydrolyitic processes causing extreme base leaching result in aluminous assemblages. In these environments sulphur and halogen anions will form associated minerals such as alunite. The physical parameters of alteration processes such as degree of buffering by solids, fluid flow rate and external control of fluid composition will effect reactions and reaction rates.

The paragenesis of a case study, the Foxtrap Pyrophyllite deposit, can be interpreted with aid of $aSiO_2$ vs 1/T and μHK_{-1} vs μH_2O diagrams. Earlier interpretations by Papezik and Keats (1976,1978),

are shown by Bryndzia (1988), to be topologically insensible in this context and a sequence consistent with phase stabilities suggested.

CONTENTS

INTRODUCTION

Stabilities of minerals defined in terms of the variables temperature, pressure, bulk chemical composition of solid phases and solution composition provide a framework which can be used to examine alteration enviroments. The stability relations of minerals in the system Al_2O_3-SiO_2-H_2O are important to a variety of mineral assemblages associated with ore formation and hydrothermal alteration.

Alteration styles resulting in aluminous assemblages are found in rocks altered by late magmatic processes, hydrothermal alteration and weathering (Hemley et al, 1980). The system will be reviewed here with respect to its use in interpretation of hydrothermal alteration assemblages.

Such aluminous alteration assemblages formed by hydrothermal processes are found associated with porphry copper and solfartic ore deposits in particular. Examples include: Roseki, Japan (Kamitani, 1977); Equity, British Columbia (Wodjak and Sinclair, 1984); ElSalvador, Chile (Gustafon and Hunt, 1975).

The Al_2O_3-SiO_2-H_2O system has been studied extensively in the literature resulting in a large body of experimental thermodynamic data. This data has been used to study stability relationships by various authors in different ways. A review of diagram construction and their interpretation is of value in the useful application of such diagrams to understanding mineral paragenesis in aluminous alteration assemblages.

CONSTRUCTING PHASE STABILITY RELATIONSHIP DIAGRAMS

Phase diagrams can be generated quantitatively from existing thermodynamic data to calculate equilibria for pertinant reactions from first principles, or by qualitatively assesing all available data including geologic observations, experimental and compositional restrictions.

Calculations of equilibria between minerals and fluids from first principles require accurate thermochemical data for the phases involved. Availability of accurate basic data has been a problem for this method. However experimental determination of phase equilibria provides a basis for derivation of this data. (Rose and Burt, 1979).

Problems with experimental determinations of equilibria:

A comprehensive summary and critique of thermodynamic data available for the system was prepared by Helgeson et al.(1978).
Early experimental studies dealt largely with the determination of the PH_2O and temperature stability limits of the hydrous phases. However most of the early work represents fields of mineral synthesis in excess of stable equilibrium values. The method of determining the equilibrium point has been conventionally either an x-ray estimate of the change in the mineral ratios in the run product or a technique involving the gain or loss of weight of a single mineral crystal in the product (Hemely et al. 1980).

One of the problems with experimental data is that of phase characterisation of both the experimental and those occuring in nature. Problems arise with grainsize and degree of crystallinity , presence and activities of other components in solid solution, substitutional of order-disorder, mixed layering of clay minerals, sorption of anions and cations, etc. (Rose & Burt, 1979).

For example $Al^{3+} + H^{+}$ for Si^{4+} in pyrophyllite results in expanded basal spacings, due largely to the formation of OH on the basal surface and with increased thermal stability due to the formation of H bonds between O's in adjacent silica sheets. This is detected in pyrophyllite synthesised in gels, but analyses of natural pyrophyllite also suggest limited substitution of this type (Rosenburg, 1974).

Possible mixed layer pyrophyllite/smectites are also shown to exist and possibly be found in nature (Erbel, 1979). Brindley and Wardel (1970) identified two layer monoclinic and one layer triclinic forms.

Formation of metastable phases or recognition of such has also been problem in the attainment of equilibria in laboratory experiments. Variations in the delta $G^{0}{}_{298}$, of pyrophyllite have been identified as due to the formation of metastable x-andalusite (Timoshkova, 1978).

Experimental determinations of equilibria:

Earliest attempts only served to determine maximum temperature at which mineral phases may stably exist at 1 atm. Developement of the metastable phases boehemite, hydralsite and gibbsite obscured equilibrium reactions.

Roy and Osborne (1954), and Kennedy (1964) established equilibrium for diaspore to corundum; metastable phase formation of boehemite and hydralsite recognised by Kennedy (1964) plagued these studies. A previously unidentified mineral of assumed same composition as andalusite found by Rostrum and Osbourne (1954), and confirmed by Aramaki and Roy (1963), was later refered to as x-andalusite by Timoshkiva (1978) and others who futher studied the phase. In these early studies nucleation and sluggish reaction rates were a problem and in most cases equilibrium was not attained and reactions were not reversed.

Matsushima et al. (1967) futher contributed to the developement of phase diagrams by futher defining the PY = KY + Q and PY + C = KY, and A/SI boundary, however runs were not of sufficient lengh to attain equilibrium (Haas and Holdaway, 1973).

Kerrick (1968) experimented with the reaction PY to A using X-ray and single crystal techniques and Haas (1972) used the single crystal epitaxis growth method for DI to C reaction. The single crystal method was found to be superior because intense grinding to produce the reactants for the charge induced strain within the crystals leading to the developement of metastable phases and impeding x-ray identification (Haas and Holdaway 1973, Velde and Kornprobst 1969, Althaus 1969).

Day (1976) in a topological analyses of the Al_2O_3-SiO_2-H_2O system concludes that there is a disturbing lack of data which may be used to define sucessfully the mineralogical reactions that were operative in nature and that gibbsite and boehemite are metastable phases. In his revised pressure temperature diagram these phases are omitted (on the basis of both field and experimental considerations) but he presents a working model with PY, KA, A, C, KY, Q, W, & D that is topologically sensible with respect to both geological observations, experimental and thermodynamic data .

Log (Al^{3+}) and (H_4SiO_4) plots at varying pH (weakly to strongly acidic) and low temperatures (25 to 300°C) for bauxite, kaolin, pyropyllite/diaspore deposits were constructed from available data by Tsuzuki (1976) and Tsuzuki and Mizutani (1974) and used to interpret dissolution of feldspars in producing zoning sequences through fluid evolution.

Walther and Helgeson (1977) comptuted the thermodynamic properties of aqueous silica, and the solubilities of SiO_2 polymorphs to 5Kb and 600°C which were used together with corresponding calculations for ionic species (Helgeson and Kirkman 1974, 1976 , Walther and

and in most cases equilibrium was not attained and reactions were not reversed.

Matsushima et al. (1967) futher contributed to the developement of phase diagrams by futher defining the PY = KY + Q and PY + C = KY, and A/SI boundary, however runs were not of sufficient lengh to attain equilibrium (Haas and Holdaway, 1973).

Kerrick (1968) experimented with the reaction PY to A using X-ray and single crystal techniques and Haas (1972) used the single crystal epitaxis growth method for DI to C reaction. The single crystal method was found to be superior because intense grinding to produce the reactants for the charge induced strain within the crystals leading to the developement of metastable phases and impeding x-ray identification (Haas and Holdaway 1973, Velde and Kornprobst 1969, Althaus 1969).

Day (1976) in a topological analyses of the Al_2O_3-SiO_2-H_2O system concludes that there is a disturbing lack of data which may be used to define sucessfully the mineralogical reactions that were operative in nature and that gibbsite and boehemite are metastable phases. In his revised pressure temperature diagram these phases are omitted (on the basis of both field and experimental considerations) but he presents a working model with PY, KA, A, C, KY, Q, W, & D that is topologically sensible with respect to both geological observations, experimental and thermodynamic data .

Log (Al^{3+}) and (H_4SiO_4) plots at varying pH (weakly to strongly acidic) and low temperatures (25 to 300°C) for bauxite, kaolin, pyropyllite/diaspore deposits were constructed from available data by Tsuzuki (1976) and Tsuzuki and Mizutani (1974) and used to interpret dissolution of feldspars in producing zoning sequences through fluid evolution.

Walther and Helgeson (1977) comptuted the thermodynamic properties of aqueous silica, and the solubilities of SiO_2 polymorphs to 5Kb and 600°C which were used together with corresponding calculations for ionic species (Helgeson and Kirkman 1974, 1976 , Walther and

Helgeson 1977) and thermodynamic data for minerals (Helgeson, Delaney and Nesbitt 1978) to generate equilibrium constants and activity diagrams for hydrothermal/metamorphic systems at high pressures and temperatures

Models of silica speciation in aqueous solution are discussed by Walther and Helgeson (1977) and a temperature versus log $aSiO_2$ (aq) equilibrium diagram constructed ($YSiO_2$ (aq) is considered as a function of CO2 concentration and temperature and pressure). The computed stability fields for the minerals in the A-S-H system at 1Kb and 25-600 C are very close to those derived experimentally. Comparison of experimental and calculated concentration of aqueous silica in equilibrium with various mineral assemblages at high pressures and temperatures suggest that the equations and parameters derived from the solubility data also afford close approximations of the thermodynamic behaviour of aqueous silica in undersaturated solutions with respect to α-quartz.

Hemley <u>et al</u> (1980) investigated mineral stability relations in the A-S-H system via aqueous silica dependant equilibria. Aqueous silica concentration is monitered as the variable rather than the reaction products gain or loss of reactants (as in X-ray and crystal growth methods). Minerals dissolve nonstoichiometrically to produce an aqueous phase in which the Si/Al ratio is higher than in the dissolving solid. A residual material enriched in Al is produced and a two phase mineral assemblage results. These silica dissolution reactions are for the most part readily reversible and can be applied to the delineation of fields of mineral stability. Al is considered immobile and silica is believed to exist as the hydrated aqueous species $SiO_2.2H_2O$

The minimum $alkali^+/H^+$ values corresponding to assemblages produced in the system A-S-H with a mica present are those of K-mica decomposition to kaolinite ,pyrophyllite or andalusite. Lower values correspond to the loss of K-mica from the system. The mica and montmorillonite curves then define a set of end member conditions for relations within the A-S-H system.

Hurst and Kunkle (1985) refined the stability field of kaolinite futher by experimentation of kaolinite de- and rehydroxylation reactions. results yielded three P,T time curves and two important reaction reversals (yielding three isobaric points in the A-S-H system following Hemley <u>et al</u>, 1980). Phase identifaction was through x-ray diffraction techniques and electron diffraction from TEM.

Investigations in the system K_2O-Al_2O_3-SiO_2-H_2O deal mainly with hydrogen metasomatism and feldspar dissolution. These reactions are well understood from a experimental viewpoint (Beane, 1982). Studies of reactions controlled by H^+/K^+ with temperature have been by Hemley and Jones (1964), Shade (1974), Montoya and Hemley (1975), Burt (1975). Ivanov (1967), Burt (1975), and Rose and Burt (1979) contributed to the developement of μH_2O and μHK_{-1} diagrams.

Qualitative phase diagrams:

An alternative approach to experimental and thermodynamic methods is to use geologic observations to constrain phase equilibria diagrams. This is useful where appropriate thermodynamic data is lacking. The resulting diagrams are schematic only and lack precise numbers on the axes but will be reasonable in terms of field geology and consistant with thermodynamic principles (Rose and Burt, 1976). The method (Burt, 1976) consists of the following steps:

(1) Choose the relevant system as defined by appropriate components (e.g. Al_2O_3, SiO_2, H_2O).
(2) List all phases that might occur in the system. (e.g. PY, Q, W., D, C, KA, KY, A, SI.)
(3) List all incompatible components of these phases as deduced from compositional restrictions, experimental datafield relations, or worst case - guesswork.
(4) Assume that all remaining reactions among phases are permitted.

Finger and Burt (1972) have devised a computer programme for calculating these reactions, which can be used to generate the phase diagram. Its topologies are already specified by the incompatibilities determined in step (3). These will be minerals that never touch each other in nature. The diagram is derived from determining the number of invariant points by manipulation of Gibbs phase rule and constructed in accordance with Shrienermakers principles.

Simple to draw chemical potential diagrams (μ-μ) drawn qualitatively from a knowledge of natural mineral assemblages (Korzinskii 1959, Burt 1971) are capable of demonstrating topological problems in experimentally derived phase diagrams, especially those involving difficult to synthesise minerals investigated over a limited temperature range (Burt, 1975).

An advantage here is that in natural environments over the span of geologic time metastable phases that are found in short run experiments do not occur. Isobaric, isothermal chemical potential diagrams must use only such data (i.e. formed at the same temperature and pressure) which will be overprinted in nature by cooling etc. and may not be easy to identify.

Solid solution in natural minerals extends their fields of stability and must be taken into consideration.When observing natural samples mineral incompatibilities rather than compatiblities should be used.

Equilibrium and 'local equilibrium' :

Intrinsic in the nature of hydrothermal alteration is the concept that the fluids are in extreme disequilibrium with the surrounding rocks, and that they fluctuate in their chemical properties over short periods of time. The close proximity of theoretically non-compatible phases in hand specimens and thin sections suggests that alteration may be a disequilibrium process. As a consequence the applicability of the phase rule and other thermodynamic principles has been questioned.

Korzhinskii (1980) showed that the assumption of 'local' or 'mosaic' equilibrium allows treatment of many metasomatic processes using modified versions of thermodynamic relationships. The essence of local equilibrium is that if a small enough volume of rock is taken it contains no incompatible phases and is substantially in thermodynamic equilibrium.

Local equilibrium may be assumed if if reaction rates between solids and fluids are rapid relative to migration of material by fluid flow or diffusion. (Thompson 1959, Elliot and Fischer 1974). One criterion for a system in local equilibrium is that no incompatible phases are in contact. Some hydrothermally altewred rocks satisfy this criterion; however many argillised aluminosilicate rocks contain incompatible phases apparently in contact.

Many water rock reactions are sluggish and are critically dependant on sufficient fluid access to attain equilibrium. In poorly permeable rocks, disequilibrium assemblages are frequently preserved or conversley stable mineralogies do not form (Hedenquist and Reed, 1984). Hemley and Jones (1964) suggest that equilibrium only exists between the solution and the fluid being formed rather than between all phases in the rock (Rose and Burt, 1979). In a highly dynamic situation such as might occur in and adjacent to a channelway, marked disequilibrium is likely to be the rule rather than the exception.

As a framework for interpretation the experimental work is pertinant, to both the nearly static and dynamic situation; that is as to whether the the process is conceived as functioning fairly close to equilibrium or proceeding towards it from a condition of extreme disequilibrium. It might also be emphasised that an open system process does not necessarily imply marked disequilibrium, for such processes might proceed slowly under conditions that are close to equilibrium (Hemley and Jones, 1964).

Phase rule application :

Korzhinskii(1936) and Thompson (1955,1959,1974) have shown that in metasomatic situations the Gibbs phase rule and the mineralogical phase rule can be modified to read P = C - M, where P is the maximum phases present in an assemblage at an arbitary choice of temperature and pressure and fluid composition, C is the total number of components in the system, and M is the number of 'mobile' components for which the concentration or chemical potential is controlled externally to the system rather than by an initial bulk composition (Vidale and Hewitt, 1973).

In a great many systems many of the components are mobile and as a result the number of phases present in the altered rock is small in some cases unity. Even if metasomatism is minor the number of phases tends to decrease from zone to zone as the vein or other source of fluid is approached (Rose and Burt, 1979) i.e. the number of components mobilised in alteration increases towards the vein (Hemley and Jones, 1964).

FACTORS CONTROLLING STABILITY FIELDS

The fundumental controls on the alteration reactions are pressure (pH_2O and P), temperature, and solution composition (Hemely and Jones, 1964). Solution composition may be described in terms of cation$^+$/H^+ ratio, pH, salinity, $aSiO_2$, Si/Al ratio, and chemical potential of volatile acid components - μHCl, μHF, μH2S. Physical parameters such as rate of fluid flow (i.e. sufficient to prevent silica saturation) and initial bulk composition will futher limit reactions.

In the system Al_2O_3-SiO_2-H_2O the reactions between mineral phases can be classified as either hydration / dehydration or silicification / desilicification reactions. The pertinant reactions are listed in table 1.

Hydration reactions are a chemical combination of H_2O with another substance. There is no selective consumption of H^+ or OH^- as opposed to hydroysis which is a decomposition reaction with water in which either H^+ or OH^- ion is selectively consumed and thereby changes the ratio in the solution (Hemley and Jones, 1964). Hydrolytic or base leaching reactions deplete the reacting phases in cations (such as K^+, Ca^{++}, Mg^{++}, Na^+) by exchange with H^+ from acidic fluids. Thus the hydrolytic decomposition of silicates is quantitatively the most significant process involved in producing a compositionally restricted system whose bulk composition is a combination of aluminium, silica and water.

TABLE 1.- Reactions in the Al_2O_3-SiO_2-H_2O system.

Desilisification reactions:

(1) pyrophyllite + H_2O = kaolinite + $2H_4SiO_4$ (aq)

(2) kaolinite + $3H_2O$ = 2 diaspore + $2H_4SiO_4$ (aq)

(3) pyrophyllite + $8H_2O$ = 2 diaspore + $4H_4SiO_4$ (aq)

(4) pyrophyllite + $5H_2O$ = andalusite + $3H_4SiO_4$ (aq)

(5) andalusite + $3H_2O$ = diaspore + H_4SiO_4 (aq)

(6) andalusite + $2H_2O$ = corrundum + H_4SiO_4 (aq)

Quartz dissolution reaction:

(7) α-quartz + $2H_2O$ = H_4SiO_4 (aq)

Dehydration reactions:

(8) kaolinite + 2 quartz = pyrophyllite + H_2O

(9) 2 kaolinite + = pyrophyllite + 2 diaspore + $2H_2O$

(10) pyrophyllite + 6 diaspore = 4 andalusite + $4H_2O$

(11) pyrophyllite = andalusite + 3 quartz + H_2O

(12) 2 diaspore = corrundum + H_2O

(After Hemley <u>et</u> <u>al</u>. 1980)

Aqueous silica species:

Investigations by numerous early workers support the hypothesis that SiO_2 is present in aqueous solution primarily as a monomer species. The reversible reaction of monomer aqueous silica with α-quartz is commonly written as equation (8).

H_4SiO_4 is taken as the conventinal representation by Hemley et al. (1980) and Hurst and Kunkle (1985). Hemley et al. (1980) suggests that the conventional H_4SiO_4 appears to provide a very reasonable set of graphical relationships from the standpoint of geological and experimental observation. Futhermore the use of $SiO_2(aq)$ in some equations, for example will, imply the reversal of hydration reactions known to go foward.

The hydration state of SiO_2 is immaterial for the purposes of thermodynamic calculation, provided that the activity of water departs negligably from unity (Hemley et al. 1980). That is the thermodynamic properties of reaction (8) may be regarded as zero and that if little or no complexing of $SiO_2(aq)$ occurs ($ySiO_2$ approximates 1) , then equilibrium constants like those plotted on the $aSiO_2$ vs. T phase relationship diagram (fig 2) determine the concentration of $SiO_2(aq)$ (Walther and Helgeson 1977).

Aluminium mobility:

Owing to the commomly believed relatively insoluble nature of aluminium in moderately acid conditions, component Al_2O_3 is conventionally considered to be conserved among solid phases during alteration (Hemley et al. 1980, Beane 1982).

In highly acidic situations there is evidence of Al mobility. The effect of Al+ has been discussed mainly in the developement of diagrams describing clay weathering profiles and weathering processes resulting in lateritic profiles. For studies on aqueous aluminium species and solubility see Tsuzuki (1976) and Tsuzuki and Mizutani (1974).

Exchange operators:

Some types of hydrothermal alteration involve only a one way transfer of constituents, from the fluid to the rock or vice versa, e.g.hydration / dehydration. This involves a gain or loss in this case of H_2O. Thus the component H_2O is the' operator' that performs the change and the tendency towards that change can be expressed in terms of its pressure, fugacity, concentration, activity or chemical potential. Precipitation of a mineral is similarly a one way process and solubility is the controlling parameter.

The concentration of the operator itself may be negligable. The operators are a kind of chemical shorthand for the species actually present and are used because they are convienient as components for balancing reactions. A nonficticous operator H_2O can be used to show that water can cause the exchange of two hydroxals for one oxide, as in the reaction

(13) $Al_2O_3 + (OH)2O\text{-}1 = 2AlOOH$

In hydrolysis reactions with chloride solutions the electrically neutral HK_{-1} can be used so that Cl as a component of halides does not need to be considered directly (and does not appear in any of the phases). For example:

(14) $KAlSi3O10(OH)2 + HK_{-1} + 3SiO_2 = 1.5Al2Si4O10(OH)2$
muscovite pyrophyllite

This procedure is developed and explained in detail by Burt (1974b, 1975), and Rose and Burt (1979).

Pressure - temperature diagrams:

As previously discussed earlier attempts to define stability fields for the $Al_2O_3\text{-}SiO_2\text{-}H_2O$ system were on P-T plots. Reactions in P-T space are given by equations (8) to (12) and illustrated in figure 1a after Hemley et al (1980). It is evident that no great

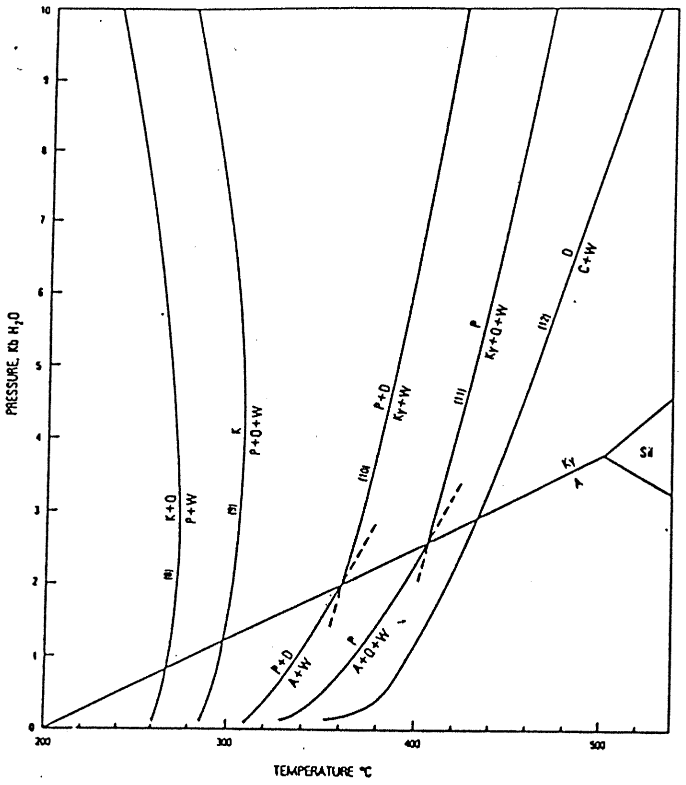

FIGURE 1A : Calculated P - T curves for the A-S-H system based on IKb stability relationships and derived thermodynamic data (Hemley et al., 1980).

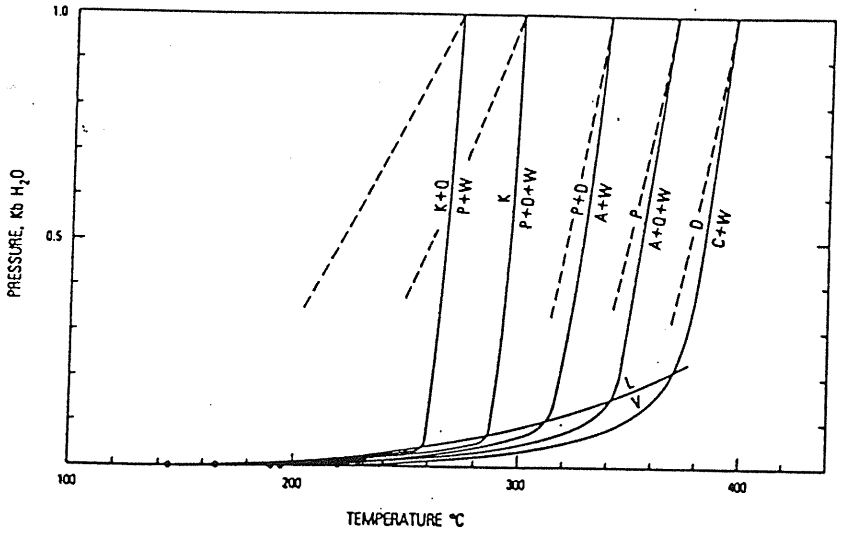

FIGURE 1B : Calculated P - T curves in the A-S-H system based on 1Kb stability relationships and derived thermodynamic data. Dashed curves are 1Kb total P at indicated pH_2O (Hemlet et al., 1980).

topological changes are pressure controlled. These thermal dehydration reactions on the P-T plot correspond to the respective isobaric invariant triple points on the $aSiO_2$-1/T diagram (fig 2) .i.e. the intersections of the aluminosilicate phase boundaries with the quartz solubility curve on figure 2. Thus the combination of reactions (1) and (7) for example yields:

(8) kaolinite + 2 quartz = pyrophyllite + $2H_2O$

Also shown on figure 1 are the experimental phase relations of andalusite, kyanite and sillimanite from Holdaway (1971) (Hemley 1980). The polymorph of the AlSi2O5 phase will be pressure and temperature dependant.

The most obvious and fundamentally important conclusion that can be drawn from this diagram is that assuming constant fluid composition then, a decrease in temperature results in an increase in hydration of the phases . Another important feature is the evident non-intersection of the reaction curves K = P + D + W with P + D = A + W and D = C + W with P + D = A . Therefore stable associations of andalusite and kaolinite or pyrophyllite and corundum are not permitted (Hemley et al. 1980). The diagram also assumes chemical incompatability of quartz with either diaspore or corundum.

Pressure will be important where a large change is involved at moderate to high temperatures since this will produce a change in silica concentration. Pressure will also restrict the extent of hydrolysis by supressing the ionization of the acid constituents relative to all other components of the system (Hemley and Jones 1964, Camutti 1984).

Ptotal > PH_2O:

Figure 1b shows in detail the low water pressure region of figure 1 on an expanded scale, including the liquid / vapour curve and the terminations of the curves at 1 bar. Imposition of 1 Kb of total pressure on the equilibria is illustrated by the dashed lines

(Hemley et al. 1980).

The reduction in the dehydration temperature of of kaolinite is seen to be quite large compared to the effect on the three other curves. This implies the possible formation of pyrophyllite at very low temperatures if intergranular rock pressure greatly exceeds pore fluid pressure. This point was discussed by Day (1976) in his extensive review of the system. Dehydration curves are depressed because there is a negative volume change for solids in these reactions. Low temperature reactions are most effected but no explanation is offered for this effect.

A futher consideration of the Ptotal>PH_2O situation is that the temperature of the andalusite - kyanite polymorph boundary is independant of PH_2O at a fixed Ptotal so that the dehydration occurs only in terms of kyanite thus decreasing the number of coexisting phases in the system.

Silica activity - temperature diagrams :

Silica activity and temperature are the most crucial controls on the system as can be seen from figures 2a & 2b. These two parameters fundamentally define the stability fields since increasing $aSiO_2(aq)$ promotes silicification reactions; and increasing temperature dehydration reactions.

Silicification and dehydration reactions associated with high temperatures and high silica activity can be considered prograde reactions and conversley the most hydrated phases are the products of retrograde reactions occuring with decreasing temperature.

As seen in the P-T diagrams in figure 2a there is no equilibrium association (i.e. intersection of stability fields) of andalusite and kaolinite or pyrophyllite and corundum. Similarly neither diaspore nor corundum intersect the quartz solubility curve and thus cannot form a stable association with that mineral. All related invariant points then are ruled out e.g. KADPW, ADCPW and KDPQW (Hemley et al. 1980).

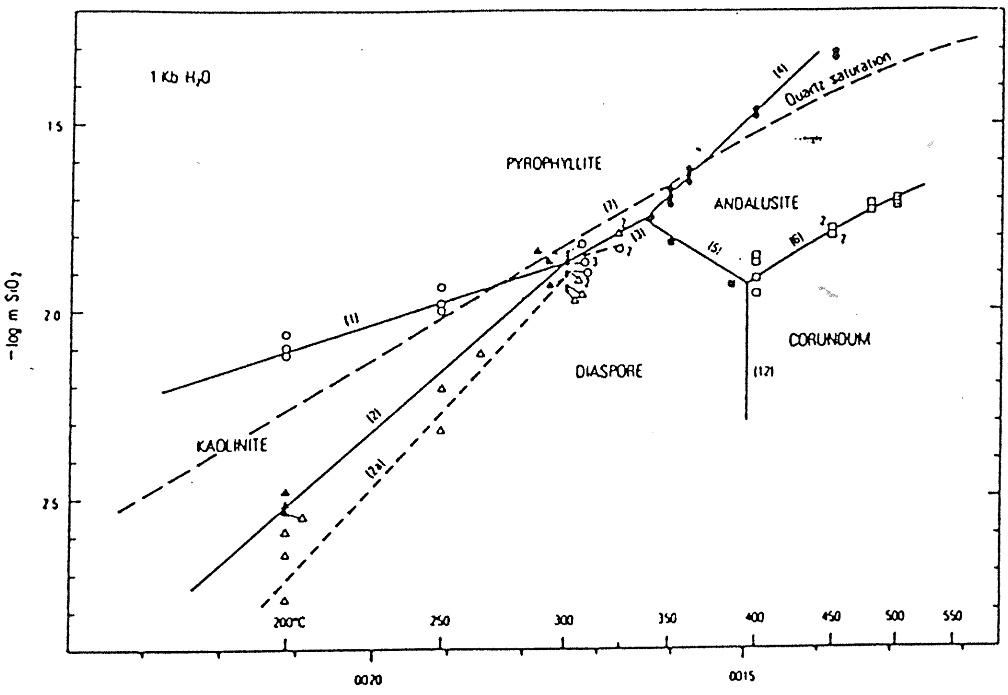

Symbols:

○, kaolinite-pyrophyllite; ●, pyrophyllite-andalusite; △, kaolinite-boehmite; ☐, andalusite-corundum; ■, andalusite-diaspore; and ▽, pyrophyllite-diaspore. ▲, kaolinite-diaspore;

FIGURE 2A : Stability relations in the A-S-H system at 1Kb H_2O as a function of $aSiO_2$ and T (Hemely et al., 1980).

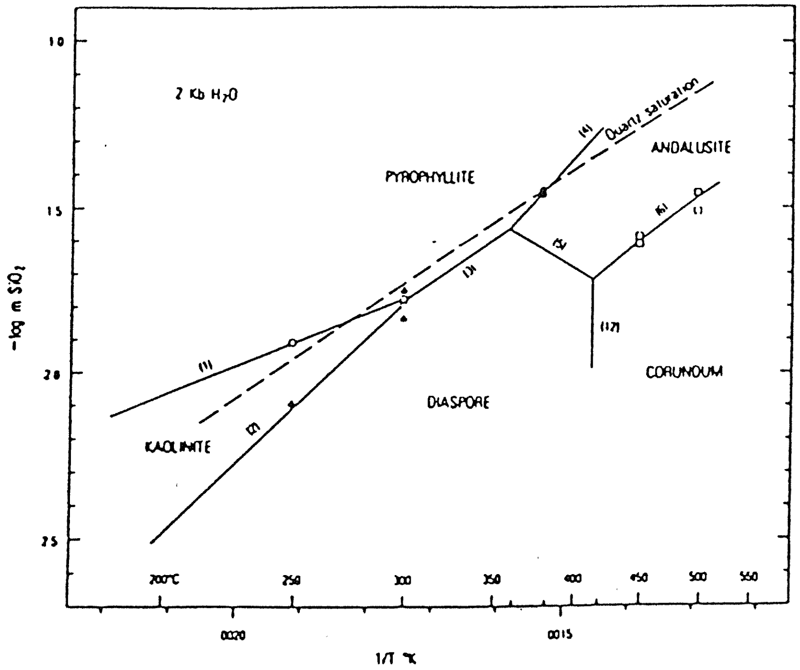

FIGURE 2A : Stability relations in the A-S-H system at 2Kb H_2O as a function of $aSiO_2$ and T (Hemley et al., 1980).

The close proximity of the quartz curve with the pyrophyllite-diaspore curve suggests their possible convergence and intersection at certain PT values to yield a pyrophyllite diaspore quartz assemblage . However inspection of the equilibrium constants for the relevant reactions - (1) and (7) - shows that the PH_2O dependancy of aqueous silica activity is the same for both reactions. Both curves then should migrate up the diagram at the same rate and never intersect. In reality the formation of metastable phases and the persistance of assemblages with an inappropriate number of phases or an excessive number of phases is encountered in both experimental and natural enviroments (Hemley et al. 1980).

Hurst and Kunkle (1985), found that if H_4SiO_4 is above kaolinites stability field and the temperature below 100°C halloysite forms rather than pyrophyllite. In addition pyrophyllite forms readily instead of kaolinite above 150°C if H_4SiO_4 is controlled by cristobalite or non crystalline silica (i.e. the solution is supersaturated with respect to silica)(Reed and Hedenquist 1984).

Composition diagrams:

Composition and compatibility diagrams based on chemical composition as in figure 3 show the assumed mineral compatibilities within the system (Burt 1975, Hemley et al 1980). At a given temperature and pressure each three phase assemblage buffers the chemical potential of H_2O, and each is described by its relevant dehydration reaction (Burt 1975, Zen 1961, Hemley et al. 1980).

Hydrolytic alteration (pH, aK^+/aH^+ and $\mu\mu\mu HK_{-1}$ / $\mu\mu\mu H_2O$):

Processes by which natural rock compositions reach the compositionally restricted system of Al_2O_3-SiO_2-H_2O are those of intense hydrolytic base leaching.

Hydrolysis reactions are conventionally represented on aK^+/aH^+ - T diagrams (see Hemley 1959, Shade 1974, and others). Hemley and

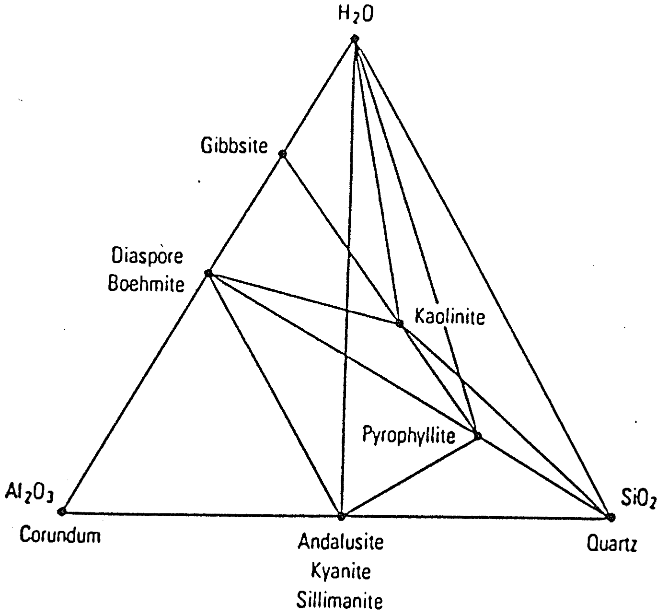

FIGURE 3 : Composition diagram and compatability triangles triangles in the A-S-H system (Hemley et al., 1980).

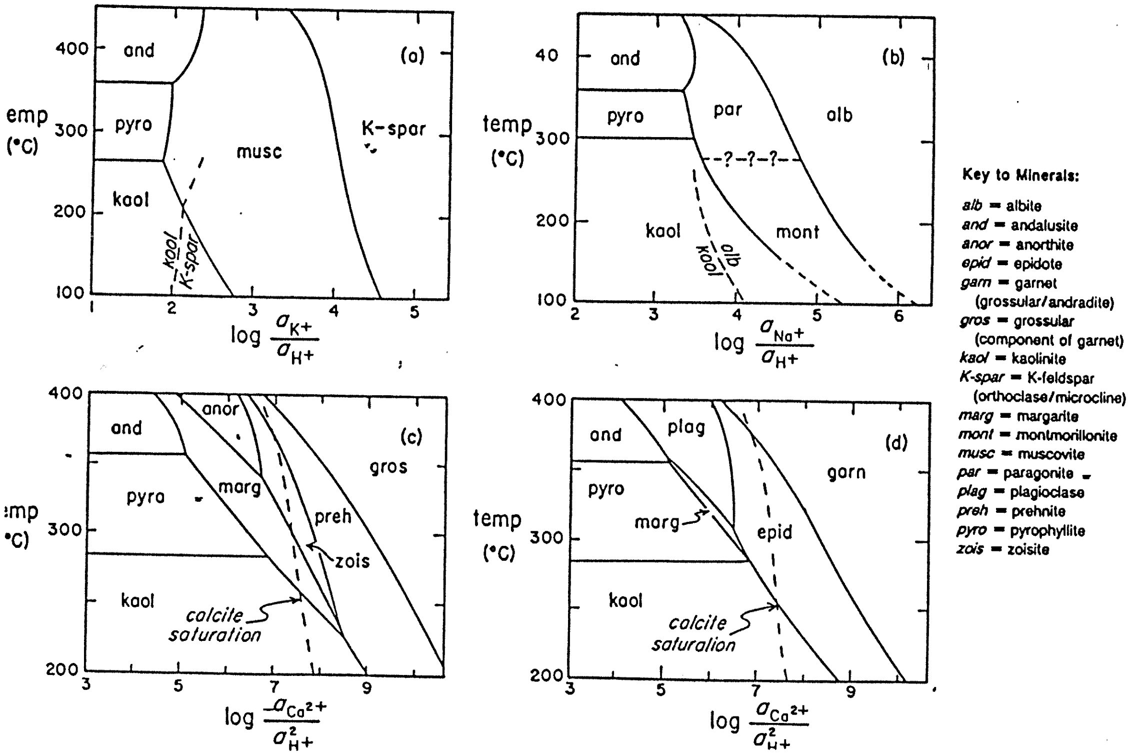

FIGURE 4 : Calculated stablity relations among minerals as function of temperature and and cation activity ratios in a coexisting aqueous phase at 500bars. All systems conserve Al_2O_3 among solids and contain excess SiO_2 and H_2O (Beane, 1982).

Jones (1964) established that activity ratios and not the absolute activity of H^+ or other ions control reactions and stability relations. Minerals in the Al_2O_3-SiO_2-H_2O system obviously then occupy the low cation to H^+ ratio portion of the diagram and decrease in hydration states with T.

Alternative representations by Burt (1975), and Ivanovov (1974) use isothermal, isobaric, chemical potential diagrams. Figure 4 shows progressive hydration of aluminosilicate phases as expected with increasing μH_2O (analogous to decreasing T). The other variable is the chemical potential of exchange operator HK_{-1} which represents increasing degrees of hydrolysis to pure aluminosilicate phases (analogous to decreasing pH). The stability fields of the aluminosilicates are not greatly effected by uHK_{-1}, once below that level corresponding to the decomposition to andalusite, pyrophyllite and kaolinite and thus corresponding to assemblages produced in the A-S-H system.

Change in pH has negligable effects on the stability relations between pyrophyllite, kaolinite, diaspore, andalusite, boehemite and gibbsite (Tsuzuki 1976). At very high acidities mineral decompositions occur by metastble reactions such as:

(14) kaolinite + $6H^+$ = pyrophyllite + $2Al^{3+}$ + $4H_2O$

The kaolinite pyrophyllite equilibrium already discussed [eqn (1)] implicitly obeys equilibrium of eqn (14) as well, and Al is obviously mobile to some degree. In a stable system within the kaolinite field Al^{3+} and quartz would form rather than pyrophyllite through reaction (14) though the acidity required is geologically unreasonable. However field (Gradusov and Zotov 1975) and laboratory observations (Hurst and Kunkle 1975) have shown that vigorous acid attack on silicate rocks tends to drive silica rapidly and metastably into solution to values above quartz saturation with opal,crystobalite or non-crystalline silica and pyrophyllite as a common product at temperatures as low as 150°C.(Reed and Hedenquist 1984, Gradusov and Zotov 1975).

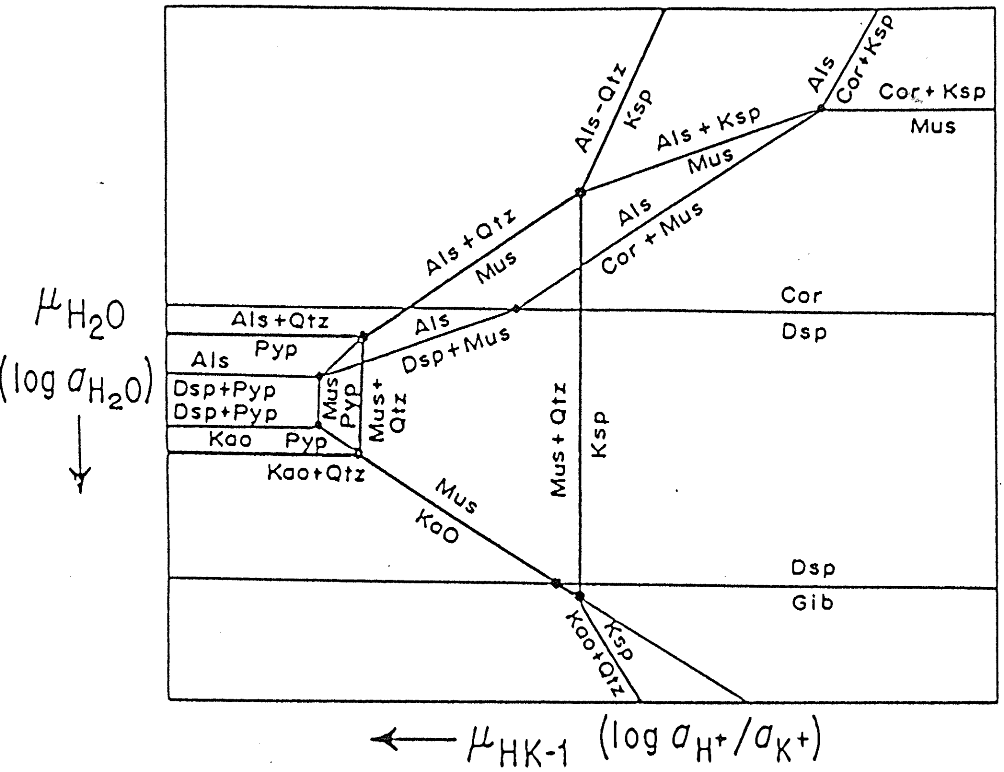

Als = aluminum silicate, Cor = corundum, Dsp = diaspore, Gib = gibbsite,

Kao = kaolinite, Ksp = K-feldspar, Mus = muscovite, Pyp = pyrophyllite, Qtz = quartz.

FIGURE 5 : Schematic stability of minerals in the K-A-S-H system at low to moderate P and T, under isothermal, isobaric conditions, as a function of μH_2O and μHK_{-1}. Heavy lines refer to quartz bearing systems (Rose and Burt, 1979).

Thus eqn (14) is represented on figure 2 by the pyrophyllite-kaolinite boundary extending to high aqueous silica values in the low temperature region below 300°C.

Additional anion components:

Acid volatiles in the fluid cause low $cation^+/H^+$ ratios and promote intense hydrolytic leaching. Therefore aluminous alteration assemblages will usually contain minerals formed by these additional anion components.

Sulphate rich fluids produce additional phases such as alunite $KAl_3(SO_4)_2(OH)_6$ and barite $BaSO_4$. Chloride and flouride rich fluids yield zunyite $Al_3SiO_2O(F,OH)_18Cl$ or topaz $Al_2SiO_4(F<OH)_2$, and boron additions promote the formation of dummortiorite $Al_7BO_3(SiO_4)O_3$ or tourmaline (Na,Ca)(Mg,Fe,Mn,Li,Al) $3Al_6(Si_6O_{18})(BO_3)_3(OH,F)_4$ (Hemley et al 1980).

Within epithermal and and porphyry style enviroments magmatically derived H_2S and halogen ionizing acids are released into circulating groundwater systems. A high fO_2 will result in oxidation of H_2S producing extremely acidic fluids (Brimhall and Ghiarso 1983, Hemley and Jones 1964, Reed and Hedenquist 1984, Hemley et al 1980).

Diagrams 6 and 7 show the stability fields of F and S bearing minerals and their relationship to associated minerals of the A-S-H system in terms of chemical potentials.

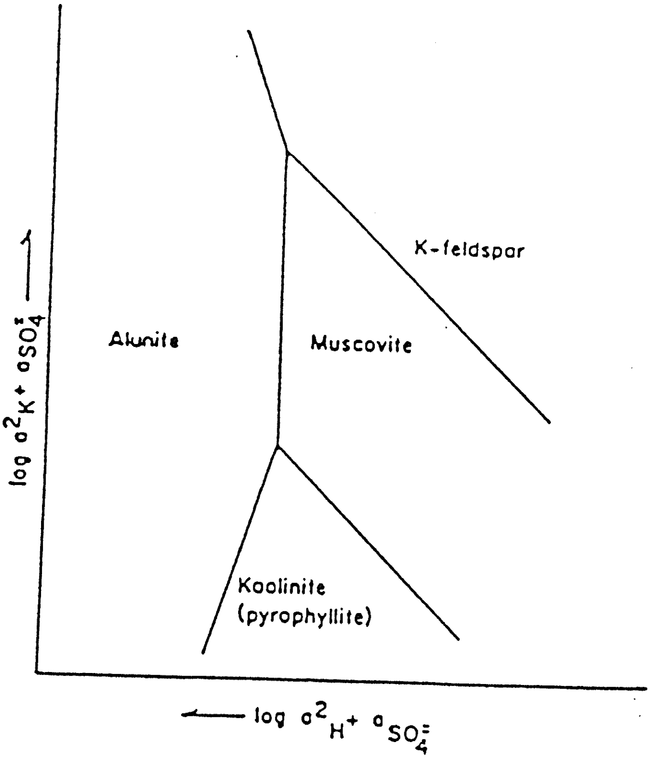

FIGURE 6 : Schematic representation of stability relations of alteration products as a function of aK_2SO_4 and aH_2SO_4 (after Hemley et al., 1969).

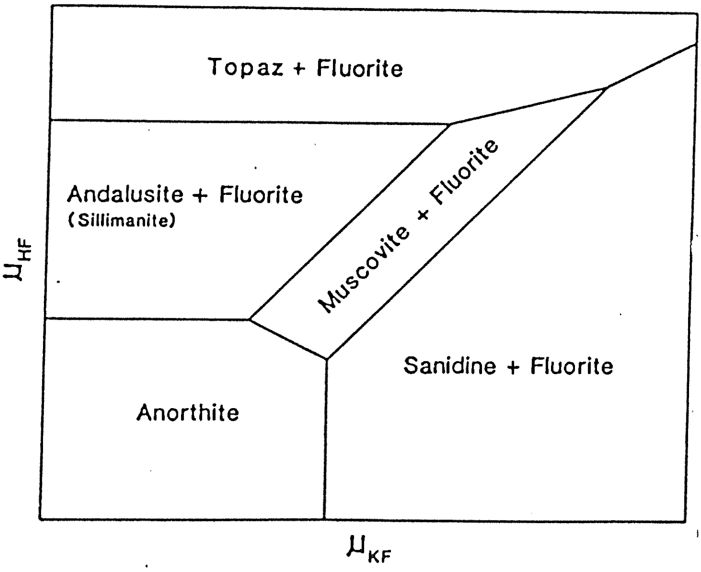

FIGURE 7 : Schematic diagram of relationships between fluorite and flouride buffering minerals as a function of μHF and μKF at an arbitary PH_2O and T. Quartz is present (Haselton et al., 1988).

APPLICATIONS FOR HYDROTHERMAL PROCESSES

Reactions that occur as a function of changes in temperature or solution composition constitute the most useful approach for geologic analysis . Temperature, $aSiO_2$, and uH_2O are the most obvious controls on mineral stabilities.

Total mineral solubility and the tendency towards incongruent dissolution both increase as temperature increases (silica is dissolved preferentially over aluminium). Changes in mineral assemblages that occur on the $aSiO_2$ - T plot when either variable is specified are well displayed.

With the exception of relations at the andalusite/diaspore boundary, prograde paths across figure 1 to produce silica leaching reactions and retrogtrade paths the reverse. This of course is a consquence of the tendency of aluminosilicates to undergo non-stochiometric dissolution, favouring loss of silica to solution.

Hemley et al (1980) propose that in isothermal enviroments the rapid flow of fluids deficent in silica will tend to shift bulk compositions of of the rock to a higher Al content. In this way an alumino hydrate may form isothermally even in the presence of quartz. This may have some bearing on the formation of known diaspore quartz associations (Berg 1937, DeRoever 1947).

The $aSiO_2$-1/T diagram:

Changes in assemblage that occur as temperature changes, but where the solution is buffered by excess solids will follow the quartz saturation curve and relevant reaction boundaries on figure 1 (This is an isobaric situation). Thus in in a prograde (rising temperature) sequence a kaolinite diaspore assemblage would continue up the boundary according to reaction (2) since SiO_2 is produced.

At the triple point then pyrophyllite and will be produced from kaolinite according to reaction (9). Silica levels increase again with migration along the reaction boundary of pyrophyllite to diaspore. At the next triple point then pyrophyllite and daispore go to andalusite by reaction (10). At this stage an excess of pyrophyllite or diaspore will be produced unless of course the original bulk composition was that of andalusite.

If excess pyrophyllite remained then the solution would migrate up the pyrophyllite andalusite boumdary until quartz saturation is reached. With futher increasing temperature migration along the quartz solubility curve would continue within the andalusite stability field.

In the case of insuffcent reaction rates relative to buffering the path followed by the fluid will migrate left or right for rapid heating or cooling respectively. Rapid cooling will produce silica supersaturation causing silica precipitation in channelways and porosities. Rapid heating causes insuffcent SiO_2 dissolution for equilibrium such that kaolinite, diaspore and andalusite are produced from other silicate minerals.

In this way it is extremely useful to use the diagram for describing evolution of the alteration fluids. Hemley et al (1980) recomend that for isothermal representation constrruction of a $aSiO_2$ vs. aH_2O diagram would be appropriate.

<u>Alteration processes:</u>

Hydrothermal alteration systems are character4ised by by high fluid flow rates with large thermal and chemical gradients between fluid and wall rock. These may also fluctuate markedly over short periods of time (Rose and Burt 1979).

transportation

The transport of the materials involved in wallrock alteration can occur either by infiltration (mass movement due to fluid flow thru the rock.) or by diffusion (transport by diffusion of chemical species through stagnant pore fluids.) or by a combination of both processes (Rose and Burt 1979).

In reality processes will generally be a combination.

fluid flow

Mineral assemblages will change in response to externally controlled solution composition changes or by rate processes within the system as discussed above. If reaction rate then exceeds the rate of solution migration internal buffering will not be complete . If this is the case then replacement is likely to occur. Where rate of migration exceeds rate of reaction then dissolution and either precipitation insitu or elsewhere will tend to prevail (Curtis 1983, Williamson 1984).

Rates of fluid flow are controlled by structure, permeability controls, temperature and pressure gradients and physical properties of the fluid. Negative volumes of reaction such as in hydrolysis and dehydration reactions will increase permeability of the wallrock. Physical processes such as hydrobrcciation will increase permeability and may increase reaction rates by increasing the surface area for fluid wallrock interaction (Helgeson 1970).

fluid composition

Gradual changes in fluid compositions would be expected as the fluids are depleted in reactants and gain in reactant products with increasing distance from the fluid source (e.g. higher silica saturation futher from the channelway and therefore a lesser intensity of desilicification reactions). Rock adjacent to the channelway starts to insulate chemically the remaining wallrock.

Sudden changes in fluid composition are caused by boiling for example. Alkali ion /H^+ ratios would be increased in the liquid phase due to the expulsion of acid volatiles from solution and condensation of the same at higher levels (or lower temperature regions) especially in high fO_2 fluids results in very low pHs.

Temperature increases in general promote faster reaction rates, however high temperatures do not favour disassociation of acid components and maximum rates for hydroysis will be at an intermeadiate temperature (Hemley 1959).

By their very nature aluminous alteration assemblages resulting from geothermal hydrolytic alteration will be the product of extremely dynamic systems in which all variables have been subject to sudden variation. Futhermore prograde and retrograde paths in the formation of the assemblage will be superimposed. In using mineral equilibria diagrams in interpretation it must be remembered that associations are not likely to be in equilibrium, and that equilibrium phases may only be those in direct contact with each other. In extreme disequilibrium minerals may only have been in equilibrium with the altering fluid.

The phase diagram then allows us to describe fluid evolution and paragenisis of the assemblage by assesing phase compatability, stability fields and macro and micro replacement and alteration textures of the assemblage itself. An example of reinterpretation of an aluminous assemblage in the light of consideration of recent phase stability diagrams in association with geologic observation is given.

CASE STUDY: THE FOXTRAP PYROPHYLLITE DEPOSIT, AVALON PENNINSULA NEWFOUNDLAND.

The pyrophyllite deposit forms a lens like body in a northerly trending belt of rhyolitic flows and pyroclastics (part of the Main Harbour Group) near the contact with a granitiod pluton (the Holroyd Batholith), both of late Precambrian age (Papezik and Keats 1976).

Most of the felsic rocks have been silicified and partly sericitized within a 1 to 2 km radius of the contact (Bryndzia 1988). The rocks near the pluton have been locally fractured and or sheared and subjected to intense hydrothermal alteration resulting in a very fine grained pyrophyllite-quartz-muscovite assemblage (with varying proportions) and small quantities of kaolinite (Papezik and Keats 1976).

These pyrophyllite rich rocks contain irregular patches of cryptocrystalline silica and sparsely distributed diaspore nodules which occur as rosettes intergrown with coarse grains of pyropyllite in a barite rich matrix with rutile occuring as an acessory phase. These were originally described by Papezik and Keats (1976). They also suggested a mechanism by which the pyropyllite /diaspore assemblage formed.

It is concluded by all workers that the fluids responsible for the pyrophyllitization of the acid volcanics were genetically related to the intrusion of the pluton.

On the basis of previously documented assemblages and the experimental results of Tsuzuki and Mizutani (1971), Papezik and Keats (1976) proposed the following alteration sequence for the Foxtrap deposit:

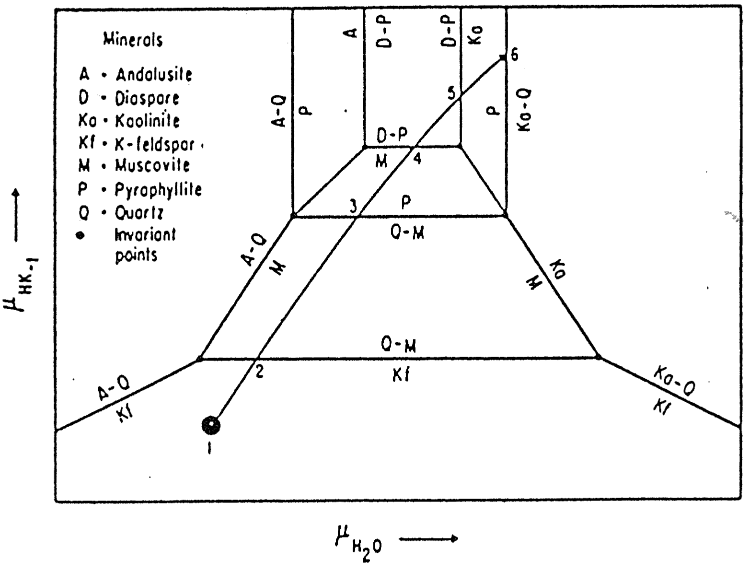

FIGURE 8 : Schemmatic isobaric, isothermal representation of mineral equilibria in the K-A-S-H system as a function of μHK_{-1} and μH_2O. Heavy lines indicate mineral stabilities in equilibrium with quartz. Light lines indicate stabilities for which unity of SiO_2 is less than unity. Point 1 represents primary igneous potassium feldspar in unaltered rhyolite. Points 2-6 represent various stages in the evolution of the hydrothermal fluid (Byrndzia, 1988).

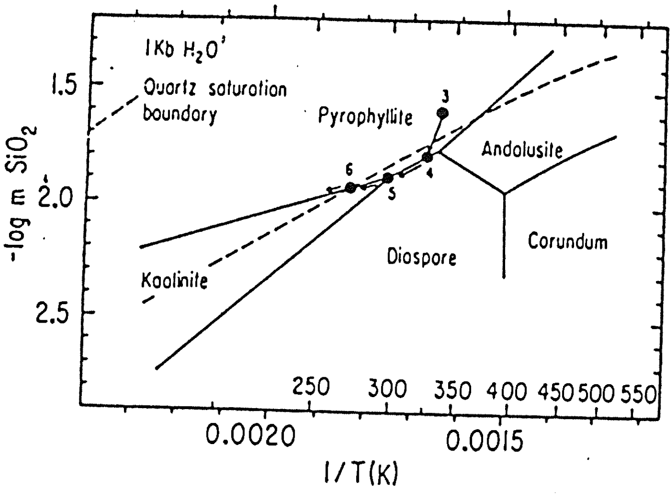

FIGURE 9 : Stability relations in the A-S-H system at 1Kb after Hemley et al.,(1980). Points 3-6 correspond qualitatively to points 3-6 on FIG 8 (Byrndzia, 1988).

(1) original alkali feldspar ......> sericite
(2) sericite ......> kaolinite
(3) kaolinite ......> pyrophyllite

Tsuzuki and Mitzutani (1971) had reported the presence of a narrow zone of kaolinite between pyrophyllite and sericite. Studying the topologies of figure 9 it can be seen that the kaolinite zone is not sensible and this highlights the ease with which metastable kaolinite may form in laboratory experiments. Papezik and Keats interpretation seems more unlikely considering that they did not observe a kaolinite zone at the foxtrap deposit, only extensive silicification and sericitization surrounding the pyrophyllite lenses.

On the basis of the μHK_{-1} vs μH_2O diagram modified after Burt (1976), and Hemley et als (1980) $aSiO_2$ vs 1/T diagram; Bryndzia (1988) suggested a new interptretation. The processes proposed for the formation of the deposit are considered to be consistant with the textural relationships and assemblages documented by Papezik and Keats. Paths depicting their proposed paragenisis are shown on figures 9 and 8.

On figure 8 then the initial sericitization of the K-feldspar occurs at point 2 as μHK_{-1} increases. With futher increase of μHK_{-1} and μH_2O muscovite is converted to pyrophyllite as in equation (14). If within the pyrophyllite stability field the fluid becomes undersaturated with respect to quartz, then diaspore would become a stable phase as is shown by segment 4-5. As expected from the diagram neither sericite nor quartz are found in association with the pyrphyllite diaspore nodule.

With a fall in temperature the kaolinite field is just intersected on figure 9. Small amounts may have formed at this point possibly from pyrophyllite and diaspore (equation (9)). Futher decreases in temperature and resaturation of the fluid with quartz (see point 6) causes precipitation of cryptocrystaline silica in association with kaolinite and pyrophyllite. Kaolinite forms then from pyrophyllite as in equation (1).

The Foxtrap deposit then resulted from initial hydrolysis of felsic rocks by high temperature magmatically derived fluids to cause initial sericitization. This continued to complete K^+ leaching in the highly permeable shear zones resulting in a bulk composition close to that of pyrophyllite.

Falling temperature in the later stages were characterised by increasing degrees of hydration. At some stage in its evolution the fluid became undersaturated with respect to quartz and this enabled diaspore to coexist with pyrophyllite.

Kaolinite may have formed metastably with pyrophyllite and persisted until the fluid was again on the quartz saturation curve at which time the assemblage pyrophyllite-quartz-kaolinite became stable. As indicated figure 9 the alteration seqence proposed by Byrndzia would span the approximate temperature range of 340-275°C at 1Kb, a reasonable pressure estimate for a shallow level intrusion.

CONCLUSION

Hydrolytic base leaching by strongly acidic fluids such as occur in acid sulphate epithermal or porphry style systems can produce aluminosilicate bulk rock compositions as end member products. Within this compositionally restricted field major controls on on phase stability relationships are temperature, activity of aqueous silica and activity of water.

Reactions within the A-S-H system are those of silicification / desilicification and hydration / dehydration. Thus the construction of experimentally derived T vs $aSiO_2$ and $aSiO_2$ vs aH_2O phase equilibria diagrams will constitute a useful approach for application to geologic anayses of natural assemblages.

Hydrothermal alteration assemblages will be unlikely to represent equilibrium states. However diagrams like that constructed by Hemley et al (1980) are extremely useful in providing a thermodynamic framework, from which the paragenisis of the mineral assemblage can be described when considered together with geologic observation of textural relationships between minerals.

APPENDIX 1.

Mineral formulae:

kaolinite	$Al_2Si_2O_5(OH)_5$
pyrophyllite	$Al_2Si_2O_{10}(OH)_2$
andalusite,kyanite,sillimanite	$Al_2Si_2O_5$
diaspore	$AlO(OH)$
corrundum	Al_2O_3
gibbsite	$Al(OH)_3$
dickite	$Al_2Si_2O_5$
boehmite	$AlO(OH)$
halloysite	$Al_4Si_4(OH)_8O_{10}.8H_2O$
hydralsite	$2Al_2O_3.2SiO_2.H_2O$

REFERENCES

ALTHAUS, E., 1969, The system Al_2O_3-SiO_2-H_2O experimental investigations and their significance for the petrogenisis of metamorphic rocks; part 3, Petrogenic interpretations of the stability relations of Al2SiO5 polymorphs: Neues. Jahrb. Mineralogie Ahb., v. 111, pp144-161.

ARAMAKI, S. A., and ROY, R. A., 1963, A new polymorph of AlSiO5 and futher studies in the system Al_2O_3-SiO_2-H_2O: Am. Mineralogist., v.48, pp111-121.

BEANE, R. E., 1982, Hydrothermal alteration in silicate rocks : Southwestern North America, in Advances in the geology of porphyry deposits, Southwestern North America, ed. Titley, S. R.,:The Univeristy of Arizona Press, pp117-131.

BERG, E. L., 1937, An occurance of diaspore in quartzite: Am. Mineralogist., v.22, pp997-999.

BRIMHALL, G. H., and GHIORSO, M. S., 1983, Origin and ore forming consequences of the advanced argillic alteration process in hypogene environments by magmatic gas contamination of meteoric fluids: Econ. Geol., v.78, pp73-90.

BRINDLEY, G. W., and WARDELL, R., 1970, Monoclinic and triclinic forms of pyrophyllite and pyrophyllite anhydride: AM. Mineralogist., v.55, pp1259-1272.

BRYNDZIA, L. T., 1988, The origin of diaspore and pyrophyllite in the Foxtrap pyrophyllite deposit, Avalon Penninsula, Newfoundland: A reinterpretation: Econ. Geol., v. 83, pp450-453.

BURT, D. M., 1971, Some phase equilibria in the system Ca-Fe-Si-C-O:

Carnegie Institute Washington Yearbook 70, pp178-184.

BURT, D. M., 1974, Concepts of acidity and basicity in petrology-the exchange operator approach: Geol. Soc. Am., Program with Abstracts, v.6, pp674-676.

BURT, D. M., 1975, Hydrolysis equilibria in the system K_2O-Al_2O_3-SiO_2-H_2O-Cl_2O_{-1}: comments on topology: Econ. Geol v.71, pp665-671.

CURTIS, C. D., 1983, Link between aluminium mobility and the destruction of secondary porosity: A.A.P.G., v.67 (3), pp380-393.

DAY, H. W., 1976, A working model of some equilibria in the alumina-silica-water: Am. J. Sci., v.276, pp1254-1271.

ERBEL, D., 1979, Synthesis of pyrophyllite polytypes and mixed layers: Am. Mineralogist, v.64, pp1091-1096.

FINGER, L. W., and BURT, D. M., 1972, REACTION, a Fortran IV computer program to balance chemical reactions: Carnegie Inst. Washington Yearbook v.71, pp616-620.

GRADVSOV, B. P., and ZOTOV, A. V., 1975, Low temperature pyrophyllite in surface deposits around acid springs on Kunashir Island: Doklady Akad. Nauk. USSR, v.224 (6), pp1406-1409.

HAAS, H., and HOLDAWAY, M. J., 1973, Equilibria in the system Al_2O_3-SiO_2-H_2O innvollving the stability limits of pyrophyllite and thermodynamic data of pyrophyllite: Am. J. Sci., v.273, pp449-463.

HASELTON, H. T., CYGAN, G. L., and D'ANGELO, M. D., 1988, Chemistry of aqueous solutions co-existing with flouride buffers in the system K_2O-Al_2O_3-SiO_2-H_2O-F2O-1 (1Kbar, 400-700 C): Econ. Geol., v.83, pp163-173.

HELGESON, H. C., 1970, Reaction rates in hydrothermal flow systems: Econ. Geol. v.65, pp299-303.

--------------, and KIRKMAN, D. H., 1974, 1976, Theoretical predication of the thermodynamic behaviour of aqueous electrolytes at high temperatures and pressures: Parts I and II - Am. J. Sci., v.224, pp1089-1261; Part III - Am. J. Sci., v. 276, pp97-240.

HELGESON, H. C., NESBITT, H. W., and DELANEY, J., 1975, Summary and critique of the thermodynamic properties of rock forming minerals: AM. J. Sci., v. 278A, 225pp.

HEMLEY, J. J., MONTOYA, J. W., MARINENKO, J. W., LUCE, R. W., 1980, Equilibria in the system Al_2O_3-SiO_2-H_2O and some implications for alteration/minerization processes: Econ. Geol., v.75, pp210-228.

HEMLEY, J. J., and JONES, W. R., 1964, Chemical aspects of hydrothermal alteration with emphasis on hydrogen metasomatism: Econ. Geol., v.59. pp538-569.

HEMLEY, J. J., 1959, Some mineralogical equilibria in the system K_2O-Al_2O_3-SiO_2-H_2O: Am. J. Sci., v.257, pp241-270.

HOLDAWAY, M. J., 1971, Stability of andalusite and the aluminium silicate phase diagram: Am. J. Sci., v.271, pp97-131.

HURST, V. J., and KUNKLE, A. C., 1985, Dehydroxylation, rehydroxylation, and stability of kaolinite: Clay and Clay Min., v.33 (1), pp1-14.

IVANOV, I. P., 1967, Studies of mineral equilibria in the H_2O-K_2O-SiO_2-Al_2O_3 systems by the multisystems method: Doklady Akad. Nauk. USSR, v.176 (6), pp1403-1406.

KENNEDY, G. C., 1959, Phase relations in the system Al_2O_3-H_2O at high temperatures and pressures: Am. J. Sci., v. 257, pp563-573.

KERRICK, D. M., 1968, Experiments on the upper stability limit of pyrophyllite at 1.8 kilobars water pressure: Am. J. Sci., v.266, pp204-214.

KORZHINSKI, D. S., 1959, Physiochemical basis of the anayses of the paragenisis of minerals: New York, Consultants Bureau p142.

MATSHUSHIMA, S., KENNEDY, G. C., AKELLA, J., and HAYGARTH, J., 1967, A study of equilibrium relations in the systems Al_2O_3-SiO_2H_2O and Al_2O_3-H_2O: Pub. 486, Inst. Geophys. Planet. Phys., University of California, Los Angeles.

MONTOYA, J. W., and HEMLEY, J. J., 1975, Activity relations and stabilities in alkali feldspar and mica alteration reactions: Econ. Geol., v.70, pp577-594.

PAPEZIK, V. S., and KEATS, H. F., 1976, Diaspore in a pyropfyllite deposit on the Avlon Penninsula, Newfoundland: Canadian Mineralogist, v.14, pp442-449.

REID, F., HEDENQUIST, J., 1981, Epithermal gold, models for exploration: Short course notes, Earth Resources Foundation, Univerity of Sydney.

ROSE,A. W., and BURT, D. M., 1979, Hydrothermal Alteration in Geochemistry of hydrothermal ore deposits, 2nd ed., Ed. Barnes, H. L.,: Wiley-Interscience, New York/Chichester/Brisbane/Toronto.

ROSENBERG, P. E., 1974, Pyrophyllite solid solutions in the systems Al_2O_3-SiO_2-H_2O: AM. Mineralogist, v.59, pp254-260.

ROY, R., and OSBORN, E. F., 1954, The system Al_2O_3-SiO_2-H_2O: AM. Mineralogist, v.39, pp853-885.

SHADE, J. W., 1974, Hydrolysis reactions in the SiO_2 excess portion of the system K_2O-Al_2O_3-SiO_2-H_2O in chloride fluids at magmatic conditions: Econ. Geol., v.69, pp218-228.

THOMPSON, J. B., 1959, Local equilibrium in metasomatic processes in Albeson, P. H., ed., Researches in geochemistry vl.: John Wiley and Sons, New York.

---------------, 1959, The thermodynamic basis for the mineral facies concept: Am. J.Sci., v.253, pp65-103.

TIMOSHKOVA,L. P., 1978,The relationship between the Gibbs energies of pyrophyllite and x-andalusite from data on the solubility of pyrophyllite in water: Internat. Geol. Rev., v.20 (2), pp236-238.

TSUZUKI, Y., 1976, Solubility diagrams for explaining zone sequences in bauxite, kaolin and pyrophyllite-diaspore deposits: Clay and Clay Mins. v.24, pp297-302.

TSUZUKI, Y., and MIZUTANI, S., 1971, A study of rock alteration processes based on kinetics of hydrothermal experiment: Contr. Mineralogy Petrology, v.30, pp15-33.

VELDE, B., and KORNPROBST, J., 1969, The stability of the hydrated aluminium silicates: Contr. Mineralogy Petrology, v. 21, pp63-74.

VIDALE, R. J., and HEWITT, D. A., 1973, Mobile components in the formation of calc-silicate bands: Am. Mineralogist. v.58, pp991-997.

WALTHER, J. V., and HELGESON, H. C., 1978. Calculation of the thermodynamic properties of aqueous silica and the so;ubility of quartz and its polymorphs at high temperatures and pressures: Am. J. Sci., v. 277, pp1315-1351.

WILLIAMS, S., 1984, Argillic Alteration: an overview: unpub., B.Sc. Hons literature review, James Cook University of North Queensland.

WISE, S. W., 1975, The origin of the assemblage silica + Al-silicate + rutile + Al-phosphate: Fortschr. Miner., v.52, special issue IMA papers, pp151-159.

ZEN, E-AN, 1961, Mineralogy and petrology of the system Al_2O_3-SiO_2-H_2O in some pyrophyllite deposits of North Carolina: Am. Mineralogist v. 46, pp52-66.